Design of Hybrid Renewable Energy Power Source with Energy Management Control System (Case Study in the Village of Fogera Wereda, Northern Ethiopia)

Sintayehu Alemnew Hailu

A Thesis Submitted to

The Department of Electrical Power and Control Engineering

School of Electrical Engineering and Computing

Presented in Partial Fulfillment of the Requirement for the Master of Science Degree in Electrical Power and Control Engineering (Power Engineering)

Office of Graduate Studies

Adama Science and Technology University

Adama, Ethiopia

July-2020

Design of Hybrid Renewable Energy Power Source with Energy Management Control System (Case Study in The Village of Fogera Wereda, Northern Ethiopia)

Sintayehu Alemnew Hailu

Advisor: Dr.-Ing. Getachew Biru
Co-Advisor: Prof. Gang Gyoo Jin

A Thesis Submitted to
The Department of Electrical Power and Control Engineering
School of Electrical Engineering and Computing

Presented in Partial Fulfillment of the Requirement for the Master of Science Degree in Electrical Power and Control Engineering (Power Engineering)

Office of Graduate Studies
Adama Science and Technology University

Adama, Ethiopia
July-2020

APPROVAL OF BOARD OF EXAMINERS

We, the undersigned, members of the Board of Examiners of the final open defense by Sintayehu Alemnew Hailu have read and evaluated his thesis entitled "Design of Hybrid Renewable Energy Power Source with Energy Management Control System (Case Study in The Village of Fogera Wereda, Northern Ethiopia)" and examined the candidate. This is, therefore, to certify that the thesis has been accepted in partial fulfillment of the requirement of the Degree of Masters in Power Engineering.

________________	________________	________________
Student	Signature	Date
________________	________________	________________
Advisor	Signature	Date
________________	________________	________________
External Examiner	Signature	Date
________________	________________	________________
Internal Examiner	Signature	Date
________________	________________	________________
Chairperson	Signature	Date
________________	________________	________________
Head of Department	Signature	Date
________________	________________	________________
School Dean	Signature	Date
________________	________________	________________
Postgraduate Dean	Signature	Date

DECLARATION

I hereby declare that this MSc thesis is my original work and has not been presented for a degree in any other university, and all sources of material used for this thesis have been duly acknowledged.

Name: Sintayehu Alemnew Hailu

Signature:________________

This MSc thesis has been submitted for examination with my approval as a thesis advisor.

Name: Dr.-Ing. Getachew Biru

Signature: _______________

Date of submission: July 22, 2020

ADVISOR APPROVAL SHEET

To: Department of Electrical Power and Control Engineering (EPCE)

This is to certify that the thesis entitled "Design of Hybrid Renewable Energy Power Source with Energy Management Control System (Case Study in The Village of Fogera Wereda, Northern Ethiopia)" submitted in partial fulfillment of the requirements of the Master of Science Degree in Electrical Power and Control Engineering, postgraduate in Power Engineering, and has been carried out by Sintayehu Alemnew Hailu Id No. PGR/18176/11 under my supervision. Therefore, I recommend that the student has fulfilled the requirements and hereby he can submit the thesis to the department.

Dr.-Ing. Getachew Biru	_______________	July 22, 2020
Name of Advisor	Signature	Date

ACKNOWLEDGMENT

First and dearest I would like to thank my supervisor Dr.-Ing. Getachew Biru for his supervision, friendly attitude, and sharing of many good ideas. Regardless of his often-high workload, he always makes time to answer questions as well as giving encouraging advice. You are highly appreciated!

I am also very grateful to my co-advisor Prof. Gang Gyoo Jin for lots of advice and helping in preparing the thesis documentation, but also for good ideas and discussions regarding everything from implementations of the system in Simulink in general.

Finally, I would moreover like to thank Dr. Molla Biweta, Dr. Tefera Terefe, and Mr. Minyamer Gelawe (MSc.) for their patience, helpful attitude, and sharing of their work regarding the implementation of the Simulink modeling.

I would like to thank my whole family. Especially words cannot express how grateful I am to my brother and friends for their love, encouragement, and all of the sacrifices that they have made on my behalf.

TABLE OF CONTENTS

LIST OF TABLES

LIST OF FIGURES

LIST OF ACRONYMS

Abbreviations	Description
BP	Bio-mass Power
FLC	Fuzzy Logic Controller
IC	Installed Capacity
LD	Load demand
MATLAB	Matrix Laboratory
MhP	Micro-Hydro power
NASA	National Aeronautics and space Administration
NMA	National Metrology Agency
PD	Demand power
PI	Proportional Integral
PID	Proportional Integral Derivative
PL	Peak Load
PV	Photovoltaic
SP	Solar power
E.C	Ethiopian calendar

LIST OF SYMBOLS

Symbols	Description
W_S	Mean sun rise hour angle
Δ	Solar declination angle for average day in the month
Φ	Latitude of the selected site
Ho	Average value of extra-terrestrial solar radiation on horizontal surface for each month
S	Monthly average of bright sun shine hours per day
So	Average of the maximum daily
N	Day of the year
Pu	Per unit
Kt	Charnels index
Ns	Number of solar panels connected in series
Np	Number of solar panels connected in parallel
Isc	Solar constant which has a value of $1367 w/m^2$

ABSTRACT

Ethiopia is a developing country, where the majority of the population lives in rural areas without access to electricity. The country is endowed with sufficient renewable energy resources. These resources are mainly micro hydropower, biomass, and sun which can be used individually or in hybrid form. The application of hybrid renewable energy system has become an important alternative solution for rural electrification program. This study deals with the design and simulation of hybrid power generation system and the energy management system to be used in rural village in Ethiopia. The overall power management strategy for coordinating and/or controlling the different energy sources is also presented in the thesis work. The site consists of 426 households with a total electric demand of 120 kW. To satisfy this demand, 50%, 30% and 20% is to be contributed from hydro, solar, and Biomass respectively. To use the power economically fuzzy logic controller is used. The controller monitors the demand and the available sources and then switches to the appropriate power supply according to the protocol developed. Simulations have been carried out to verify the system dynamic performance using a practical load profile and weather data. The result shows that the overall power management strategy is effective and the load demand is balanced. This is done by the artificial intelligence system effectively.

Key words*: - Hybrid, MATLAB/Simulink, Bio-mass, Micro-hydro and Solar*.

CHAPTER 1

1. INTRODUCTION

1.1. Background

Energy is essential to our society to ensure quality of life and to support all other elements of our economy. Energy is a crucial human need that is very necessary for carrying out day to day activities. And also linked directly to the economic, environmental and social development of any country. Among the very many important forms of energy available to any country, electrical energy is one important energy form that has contributed substantially to rapid economic growth and industrialization. The desirability and usefulness of electrical energy to the world cannot be overstrained. Electrical energy is useful in industrial, commercial and residential establishments. Electrical energy is useful in all manufacturing, telecommunications, residential (lighting, heating, cooling, entertainment) and commercial activities [1].

The access to electricity has proven to be a key factor necessary for socioeconomic development, both for the publics and infrastructure of a country. It is a source for development and industrialization in the current modern times. With electricity, lines being confined to large cities and towns, developing countries lag far behind in many sectors when compared to industrialized countries. Ethiopia, despite being the one of Eastern African country, has a very poor electricity penetration rate. Electricity is available for 41% of the population and only 17% of the households are connected to the central grid; even the above coverage is confined to major towns and cities [2].

The shortage and depletion of source of power and fuels demanded an urgent need for alternative sources of energy. This is also an immediate response to reduce the effect of global warming phenomenon. From the previous literature, the environmentally friendly power generation technologies really play a role in the future source and supply of energy. Electrical energy can be derived from diverse sources such as hydro (Electrical energy from water sources), nuclear, wind, solar (Energy from the sun) and the thermal sources [1]. Indeed, the renewable energy technologies such as hydroelectricity, tidal/water power, solar power, wind power, geothermal, and biofuel and biomass will definitely shape the future of the world’s energy supply. These alternative sources of energy benefitted the energy market in terms of supply security, reduced carbon emission, improved power quality, reliability and employment opportunity to the local people.

Ethiopia is endowed with sufficient renewable energy resources which can be used as standalone electric energy supply systems for electrifying remote areas of the country. These resources are mainly small-scale Hydropower, biomass, wind, and solar which can be used individually or in combination of one another. However, traditional biomass energy is the dominant sources of energy in the rural area for about 83% of the total population of Ethiopia [2].

Village electrification is a crucial step for improving the socio-economic conditions of rural areas and overall development of the country. A number of benefits can be achieved in accessibility of electricity. Presence of electricity can help to reduce poverty since it creates job employment opportunities for the villagers and promotes a better standard of life and helps economic development by fulfilling the education, health, water supply for drinking and irrigation needs of the rural population [3].

Ethiopia has a huge renewable energy (micro-hydropower, solar, geothermal, biomass and wind energy) potential that has not yet been assessed for rural electrification. If rural communities are supplied with modern electricity from renewable energy resources, the energy consumption of the country increases and then the livelihood of its population will be improved and simultaneously the environment will be saved from pollution. Worldwide attentions is given to renewable energy technologies because they are pollution free, take low gestation period and environmentally friendly.

1.2. Statement of the Problem

Even though Ethiopia is rich in renewable energy resources, majority of the population which live in rural areas depend on biomass energy for cooking food and lighting. Due to many reasons most of the villages of the country are not getting electrical energy currently. To connect the rural areas to the grid, high costs and adequate power for the whole country is required. On the other hand, there are many bottle neck challenges related with using the traditional biomass energy, such as, the continued depletion of forest resources for firewood has resulted in environmental problems, increasing scarcity and cost of household fuels, particularly firewood increased stress on women and children who usually are supposed to collect fuel, and the cost of petroleum imports has brought worsening impact on Ethiopia’s trade balance and foreign exchange availability. For lighting systems in rural areas, kerosene is used which produces smokes and emits pollutants that brings health problem, Health centers and schools have no access also to electricity.

Fig. 1. 1: Lack of electricity accesses and its consequences in rural village

1.3. Motivation

The majority of Ethiopians are living in rural areas with very traditional way of living styles. The areas have been using Kerosene for lighting, diesel for milling and pumping, traditional biomass as source of energy for cooking. However, the current increase in oil price and the negative effects of fossil fuels on the environment motivates to search for other alternative (preferably renewable) sources of energy. The second motivation comes from the fact that most research works in Ethiopia which have been conducted till now on the hybrid systems are merely feasibility studies with little focus on Energy management control system. In addition, the intelligent control system was used to make an intelligent decision to use the energy resources in more effective way.

1.4. Objectives of the Study

1.4.1. General Objective

The main objective of this thesis is to design of hybrid renewable energy source with its energy management system for Fogera wereda.

1.4.2. Specific Objectives

The specific objectives include:

- To estimate the renewable energy resource of the area; micro hydro, solar radiation and Bio-mass potential.

- To determine the power and energy demand of the village living in the selected areas, by considering the basic needs of the people.
- To design Hybrid Solar, Micro-Hydro and Bio-mass based Generating System.
- To design and simulate the energy management system using Fuzzy Logic Controller.

1.5. Research Questions

In general, the research and analysis has been guided by addressing and answering the following questions:

1. Are there enough solar, Micro-hydro and Bio-mass potential in the study area?
2. How much power is needed to electrify the selected village?
3. Is it possible to design hybrid solar/Micro-hydro/Bio-mass system for the selected village?
4. How the energy usage is managed and controlled using the modern controllers?

1.6. Scope of the Study

The scope of this research was to asses renewable energy potentials of the study site, Design and Evaluate the performance of artificial intelligence Based Hybrid Renewable Power Generation for Fogera Wereda based on the load assessment of the selected site.

1.7. Significance of the Study

The energy consumption of people of any country determines the development of that country. If so, generating electrical energy and supplying that electrical energy to all Ethiopian is the duty of electrical engineers so as to improve the living standard of the people who are living specially in the rural areas. In addition to that it is possible also to reduce the pollution of the environment and cost of electricity.

1.8. Limitations of the Study

During working research papers there is always a limitation: the first limitation is lack of cooperation to get necessary and relevant information and recorded data especially on the amount of rice husk from the workers in the selected site. The second limitation is because of the scope of the study it is not possible to model each component of the proposed hybrid system in MATLAB/Simulink to generate the actual signal for the controller rather random signal generator is used.

1.9. Outline of the Study

This thesis consists of five chapters. The first chapter discussed about the general introduction, and chapter two explained the general concept of the proposed green energy production components namely the Photovoltaic, Micro hydro and Biomass, and literature review. Chapter three explained about the potential assessment of the three energy resources in the selected site, primary and secondary data gathering, data analysis, system modeling and designing each components capacity.Chapter four discussed about the simulation results of the hybrid components and the Fuzzy logic controller and MATLAB function program in MATLAB/Simulink 2016a. Chapter five explained about conclusions, recommendation and future works.

CHAPTER 2

2. THEORETICAL BACKGROUND AND LITERATURE REVIEW

2.1. Literature Review

Several researches have been conducted in hybrid off-grid power generation all over the world and in Ethiopia. Different scholars used different Technology option and approaches to evaluate the various configurations of renewable energy resources, such as solar energy, Bio-mass, wind energy, small hydropower and their hybrid configurations. A number of studies results have been published some of the thesis paper are reviewed in the following paragraph.

The author in [4] conducted the hybridization of PV/FC energy system also has been developed. The work assumes as if the main power for the hybrid system comes from the photovoltaic (PV) panels, while the fuel cell (FC) and secondary batteries are used as a backup unit. In the work HOMER (Hybrid Optimization Model for Electric Renewable) is used as optimization software. In this system the authors specified one sensitivity variable with two values; which are the intercept coefficient in FC and the marginal fuel consumption of the FC. And the result shows that the Net Present Cost (NPC) and the Cost of Energy (COE) have increased due to the rise in fuel consumption in the FC. But, the work refrains from carrying out the issue of dynamic modeling.

A paper in [5], described that solar power is a viable and sustainable way to ensure electricity supply. Although the system with a diesel backup generator was the most reliable, it was also the most expensive, and it was decided that the optimal solution for the complex was the system without backup. However, due to great seasonal variations in irradiation, a system based solely on solar power is bound to be either over-dimensioned for the dry season with high irradiation resulting in high amounts of excess electricity or under-dimensioned for the rainy season with high amount of unmet load in this period. One of the arguments for choosing the system without backup, was the possibility of including a biomass-based generator in the system. This possibility was investigated by the author in her specialization project, where it was concluded that including a biomass generator in a hybrid system compared to increasing the PV-battery system in order to achieve a higher reliability in the rainy season is the optimal solution regarding both technical and economic aspects.

In the similar manner the authors in [6] proposed a model of a hybrid system comprising of solar and wind technology for small locality and the hybrid system is designed with the help of HOMER software. Also, it comprises the simulation data of each component used in project work and as well as the cost of the project during working and during step up. Finally, it concludes that rural electrification. Presents different load patterns in relation to that of urban loads in terms of the daily variation expected and the yearly variation: rural patterns are smoother. But the control mechanism of the renewable energy resources is not discussed in detail, also urban load pattern is not analyzed in detail in this paper.

The closely related work in [7] were investigated a model for simulating Solar-Wind-Battery-Diesel system using fuzzy logic for telecom commercial ventures with Effective power organization regulator predestined by fuzzy logic controller (FLC) to screen the force from all load stipulate and possessions consistently as well as to manage entire hybrid energy scheme. Fundamental target of this article is to provide continues power for telecommunication loads from off-grid solar-Wind-Diesel hybrid power system with proficient energy storage system. The reliability is good but in this paper environmental pollution due to the diesel generator is not considered.

The hybrid model in [8] were analyzed the case of a remote residential area in Malaysia and used HOMER to analyses the economic viability of a hybrid system. The study uses a hypothetical case of 40 households with a peak demand of 2 kW. The peak demand is 80kW and the base demand of around 30 kW is considered in the analysis. Although such high rural demand can be typical for Malaysian conditions, it is certainly not true for others. The study also does not consider any productive use of electricity.

The author in [9], designed standalone solar, wind and Biomass hybrid power system to meet the load demand of the village at Sagar Island using genetic algorism. The decision variables he considered for this optimization processes are numbers of pv-panels, numbers of wind turbines and capacity of biomass generator. The monthly average solar radiation and wind speed of the study area are converted in to hourly solar irradiance and hub height speed; here minimum values are considered for optimization process. This writer also tries to compares per unit energy cost and co_2emission of Biomass generator and diesel generator.

Finally, research results indicate hybrid power system considering Biomass has minimum per unit energy cost and less CO_2 emission as compared to diesel generator consisting hybrid power system.

A paper [10] investigated on Fuzzy Logic Controller based hybrid renewable power generation for Barsoma (Oromia, Ethiopia).by assessing both solar and biomass capacity of Barsoma woreda he proposed a system to generate electricity. Bio-mass is one of the hybrid components where the waste of Coffee husk was the main source of bio-fuel for the dual-generator, environmental pollution from by-product of coffee will be decreased. Finally, in his paper Fuzzy Logic controller Based solar/Micro-hydro/Bio-mass Hybrid Renewable power generating system was designed to solve the scarcity of electricity and coffee husk environmental pollution of study Woreda.

The author in [11] described to explored techno economic analysis of electrifying werder district (Somali region) with hybrid renewable energy. The software HOMER was used in this study to evaluate the technical and economic feasibility of various hybrid energy alternatives to this village. The economic analysis compares the level zed cost of electricity generation for the three option; wind/PV/diesel generator, diesel generator only system and national grid extension. The level zed cost focusing on the elements causing differences such as fuel price, PV modules, with battery or generator rather than the elements that are similar across the technology choices. The finding indicate that photovoltaic/wind/diesel generator hybrid system was feasible systems based on some important parameters such as high renewable penetration, less annual diesel consumption, less carbon dioxide emission, less unmet load, less capacity shortage and cost of energy, but still diesel is considered which it has to be ignored for the sake of the environment and fuel cost.

A paper in [12], investigated the feasibility of stand-alone hybrid energy system to meet out electric load requirements of JK Lakshmi pat university, Jaipur. And according to this paper in order to maintain a continuity of electricity supply, a single energy source is not a good option. So, it considered a hybrid system with wind turbine, solar Photovoltaic and diesel generator with integration of battery bank. The techno-economic analysis for the proposed hybrid system model has been performed using HOMER software. But variation of the load for month and a year are considered as only 10% and 20% respectively and intelligence decision making software is not used for load and supply power variations.

The author in [13], a modelling of PV solar cell and module, using MATLAB simulation. The paper concludes the proposed simple model of the PV solar module is enough, accurate and shall be used for development and simulation for a stand-alone power system, and when the influence of the temperature and solar irradiation are considered the solar irradiation influence was bigger than temperature influence especially when we focus on the decrease of solar irradiation. The impact on the output power was much heavier. But among the different types of PV solar modules only one PV module type is analyzed no other types of modules.

The closely related work in [14], described a wind/solar/diesel hybrid power for irrigation system is modelled and simulated in MATLAB software and from this it concluded fuzzy logic-controlled hybrid power for irrigation system can effectively supply the intended power demand in different cases. Accordingly, the possible power source can be solar energy alone, wind turbine alone, hybrid of wind and PV or diesel generator. This is performed on MATLAB/Simulink thus fuzzy rule is written to make the intelligence decision, but in this paper environmental pollution due to the diesel generator is not considered. and running cost are not considered.

A paper in [15], discussed about the alternative of supplying electricity from solar-wind hybrid system to a remotely located community of 200 families isolated from the national grid in Ethiopia through HOMER software. The results were compared from the list of feasible renewable power sources sorted based on net present cot and found that hybrid solar and wind system is only the promising technology for power generation to these communities.

The author in [16], described design hybrid power system for rural Eastern Amhara Region of Ethiopia using HOMER software. He assessed potentials of solar/wind/Hydro using appropriate models and power demand of the study site then he designs hybrid power system for the villages as per the load assessment. The writer also tries to optimize the designed system and also, he looks at sensitivity cases. Generally, a combined PV/wind/hydro power plant could be a reliable solution for remote rural communities in the study area. Even though, it could not be provided 100% autonomy and the cheapest solution since using renewable as the main energy sources it would be a trustworthy solution with numerous of environmental and economic benefits than running diesel generators and grid extension. The reliability is good but battery cost is not economical.

A paper in [17] presented a case study of rural area in Ethiopia entitled “Modelling and Simulating of a Micro Hydro-Wind hybrid power generation system for rural area of Ethiopia” by using HOMER software. His objective was to develop a hybrid system cost competitive to supply energy for remote villages for a model community of 660 households with one primary school two churches one mosque and one health centre. He discussed two option ,Wind/Micro hydro hybrid and Standalone Micro hydro system by comparing the cost of energy to identify cost competitive for the remote village compared to extending the existing grid to the area since the break-even grid extension is 23.6km which is less an the extension of the grid, so grid extension can be an option. According to him, the COE most favourable Wind/Micro hydro hybrid system is $0.112/kWh. Moreover, COE of standalone Micro-hydro system is $0.035/kWh. He concluded micro hydro system is the most economical and can only satisfy the energy demand of the village and technically feasible option. However, if he includes solar resources in the hybrid configuration, his hybrid system may be cost effective regarding to his title.

The author in [18], conducted Performance examination of Solar, Wind& biomass Hybrid Energy source. The operations have been finished by HOMER programming utilizing the constant field information of sunlight-based radiation, wind velocity and biomass of that specific range. There is no doubt about the reliability of the system, but Generator used in the Bio-mass is a dual fuel engine in case there will be shortage of input biomass still contributing its impact on environmental and air pollution.

2.2. Basic Understanding of Renewable Energy

Most widely applied technologies for electricity production in rural areas are photovoltaic (PV), wind energy, Micro-hydro-power, Bio-gas and Bio-mass combustion power technologies. Since the focus of this thesis is on solar, Micro-hydro and Bio-mass combustion resources, the three alternative resources are briefly introduced in the following sections.

2.2.1. Solar System

The potential solar energy that could be used by humans differs from the amount of solar energy present near the surface of the planet because factors such as geography, time variation, cloud cover, and the land available to humans limit the amount of solar energy that we can acquire [24]. Solar energy is derived from the sun through the form of solar radiation. Without sun no wind, without sun no water and no biomass. That is why sun is considered as the mother/father of all renewable energy sources.

2.2.1.1. Photovoltaic Operation (PV)

Photovoltaic is an empowering technology that allows us to do very new things, as well as, do old things better. It allows us to look completely new modes of supplying electricity to different markets around the world and out of the world (in outer space). It also allows us to do what we already do (generate electricity, which is distributed over the transmission grid), but to do it in a sustainable, pollution free, equitable fashion. Why is PV equitable? It is because nearly everyone has access to sunlight. When photons of light fall on the cell, they transfer their energy to the charge carriers [21]. The electric filed across the junction separates photo- generated positive charge carriers (holes) from their negative counterpart (electrons). In this way, an electrical current is extracted once the circuit is closed on an external load.

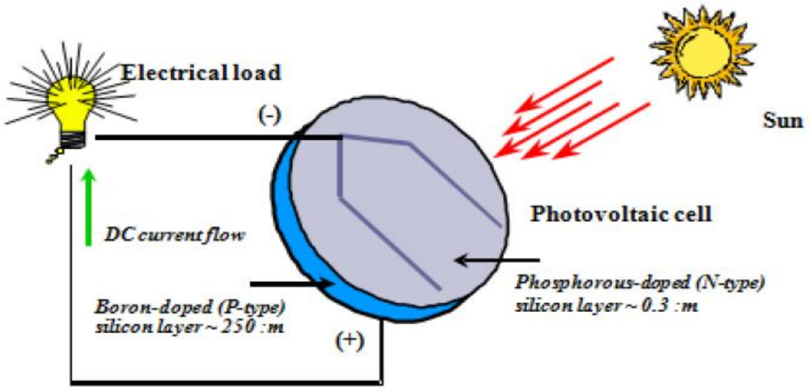

Fig. 2.1: Solar cell working principle [25]

In Fig. 2.1 illustrated when the sunlight hits the semiconductor surface, an electron springs up and is attracted towards the N type semiconductor material. This will cause more negatives in the n-type and more positives in the P-type semiconductors, generating a higher flow of electricity. This is known as Photovoltaic effect [21].

2.2.1.2. PV Cells, Modules and Arrays

A PV module consists of many PV cells wired in parallel to increase current and in series to produce a higher voltage [19],[21]. The module is encapsulated with tempered glass or some other transparent material on the front surface, and with protective and waterproof material on the back surface. Since the amount of an electrical power output from a single cell is small, multiple cells are connected in series or parallel and/or series-parallel.

a) Series Wiring: Series wiring is when the voltage of a solar is increased by wiring the positive of one solar module to the negative of another module. This is similar to installing batteries in a flashlight [19].

b) Parallel Wiring: Parallel wiring increases the current (amps) output of a solar array while keeping the voltage the same. Parallel wiring is when the positives of multiple modules are connected together and all the negatives for the same modules are connected together [19].

c) Series Parallel Combination: Solar panels can be connected in series parallel combination to increase both the voltage and current output producing a higher wattage array. PV cells are the fundamental building blocks of PV systems. The power generated by a PV cell is only not enough to power small devices such as electronic calculators. Each silicon solar cell produces about 0.5 volts. To meet higher loads the PV cells must be connected in series and/or in parallel depending on the magnitude of the voltage and current required. Typically, 36 to 48 cells are connected in series to form a module which is capable of producing enough voltage to charge 12-volt batteries and run pumps and/or motors [19].

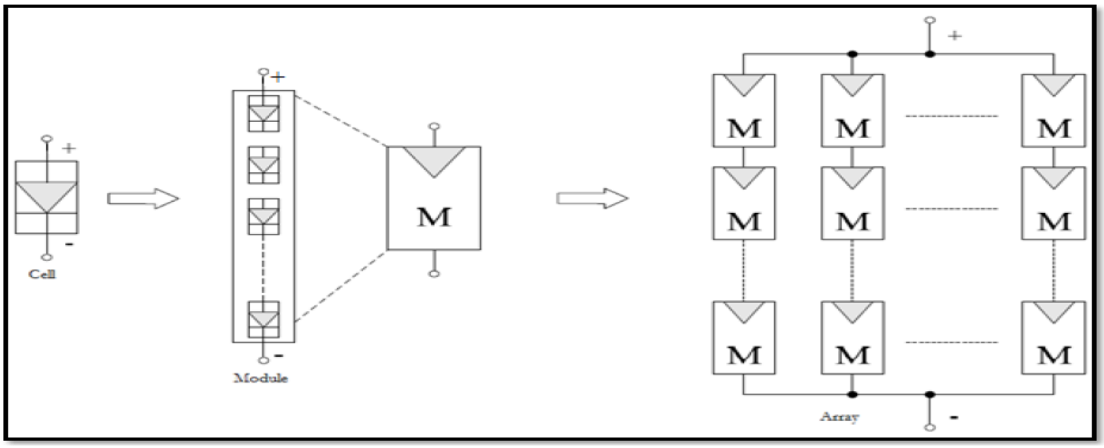

Fig. 2. 2: Schematic configuration of cells, modules and arrays [20]

Modules are the basic building blocks of systems. For more voltage or current modules are connected in series or in parallel respectively to form a panel and then panels can be assembled into a group to form a complete PV array. Fig. 2.2 shows the schematic configuration of cells, modules and arrays [20].

2.2.1.3. Photovoltaic Technology

Many crystalline or thin film PV modules power a solar PV system. Individual PV cells are interconnected to form a PV module. This takes the form of a panel for easy installation. PV cells are made of light-sensitive semiconductor materials that use photons to dislodge electrons to drive and electric current [7]. There are two broad categories of technology used for PV cells, namely, crystalline silicon, as shown in Fig 2.3. This accounts for the majority of PV cell production and thin film, which is newer and growing in popularity. The “family tree” in Fig. 2.3 gives an overview of these technologies available today.

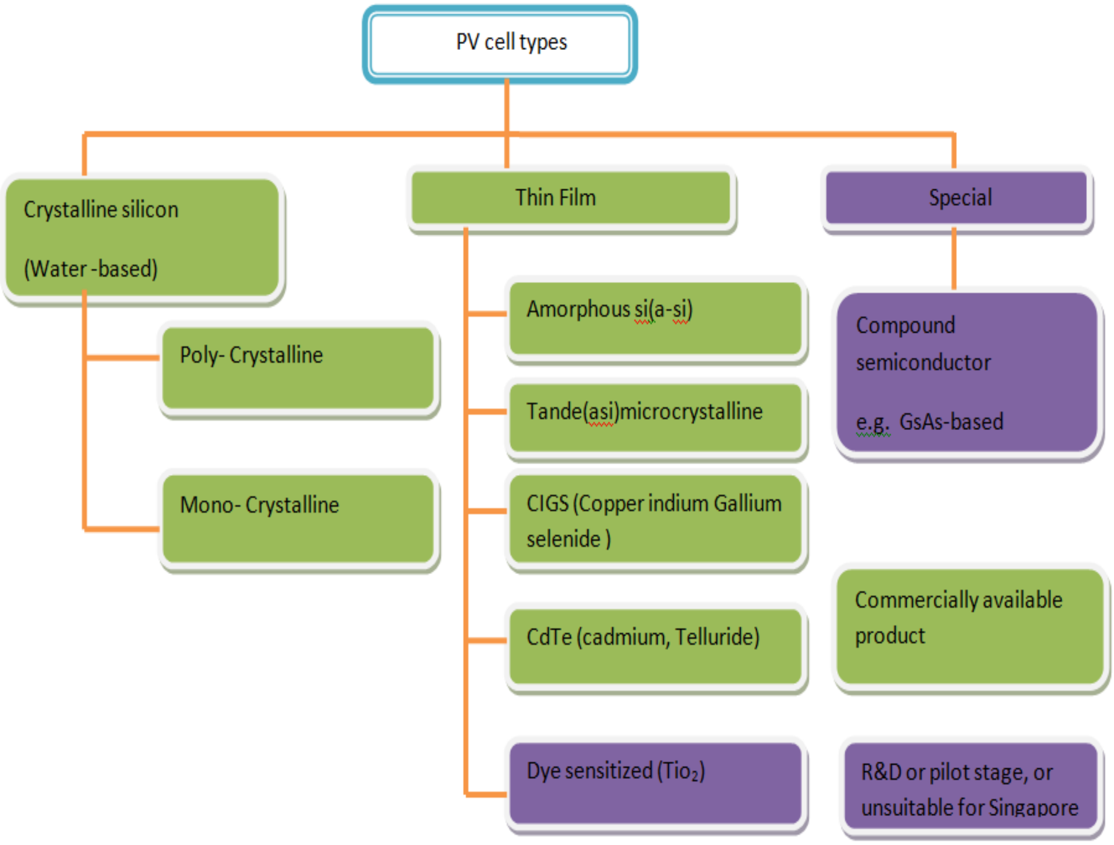

Fig. 2. 3: PV technology family trees [26]

2.2.1.4. Crystalline Silicon and Thin-film Technologies

Crystalline cells are made from ultra-pure silicon raw material such as those used in semiconductor chips. They use silicon wafer that are typically 150-200 microns (one fifth of a millimeter) thick. Thin film made by depositing layers of semiconductor material barely 0.3 to 2 micrometers thick onto glass or stainless-steel substrates. As the semiconductor layers are so thin, the costs of raw material are much lower than the capital equipment and processing costs. Depending on the manufacturing process, the modules can be of three types [7].

a) Mono-crystalline Silicon. b) Polycrystalline Silicon. c) Amorphous Silicon

a) *Mono-Crystalline Silicon*

Most photovoltaic cells are of single-crystal types. To manufacture the cell, silicon is purified, melted, and crystallized into ingots. The ingots are sliced into thin wafers to make individual cells [27]. The cells have a uniform color, usually blue or black. The disadvantage of these cells is that a complicated manufacturing process is required to produce, which results in slightly higher costs than those of other technologies,

b) Polycrystalline Silicon.

Polycrystalline cells are manufactured and operated in a similar manner. The difference is that lower cost silicon is used. This usually results in slightly lower efficiency, but polycrystalline cell manufacturers assert that the cost benefits outweigh the efficiency losses. The surface of polycrystalline cells has a random pattern of crystal borders instead of the solid color of single crystal cells [27].

c) Amorphous Silicon

The previous two types of silicon used for photovoltaic cells have a distinct crystal structure. Amorphous silicon has no such structure. Amorphous silicon is sometimes abbreviated "aSi" and is also called thin film silicon. Amorphous silicon units are made by depositing very thin layers of vaporized silicon in a vacuum onto a support of glass, plastic, or metal. Since they can be made in sizes up to several square yards, they are made up in long rectangular "strip cells." These are connected in series to make up "modules. Their disadvantage is the low efficiency, which is on the order of 6%. Nowadays, the panels made from amorphous silicon solar cells come in a variety of shapes, such as roof tiles, which can replace normal brick tiles in a solar roof. In addition to the above types, a number of other promising materials, such as cadmium telluride (CdTe) and copper indium selenide (CuInSe2) are used today for PV cells [27].

Table 2. 1: Technology and module efficiency of PV [26]

Technology	Module
Mono-crystalline silicon	12.5-15%
Poly-crystaline	11-14%
Copper indium gallium, selendine (GIGS)	10-13%
Cadmium Telluride (CdTe)	9-12%
Amphrous silicon(a-si)	5-7%

For crystalline silicon PV modules, the module efficiency is lowered compared to the sum of the component cell efficiency due to the presence of gaps between the cells and the border around the circuit i.e., wasted space that does not generate any power hence lower total efficiency.

2.2.1.5. Power Converter

The inverter must be able to handle the expected power level, but must also be compatible with the voltage of the supply and demand side. Power inverters are sized after the maximal power they need to provide. It is also important to consider the efficiency of the inverter. The highest efficiency is usually reached when the inverter operates at 50 % of its rated power. The inverter size should be 25-30% bigger than the total watts of the loads [46].

2.2.1.6. Pros and Cons of PV System

Advantages of Solar PV System [19]

- The energy resource is free, renewable, and everlasting everywhere it counter balances greenhouse gas and pollutant emissions.
- It produces energy during the day time when demand peaks, which is when power is typically most expensive to produce.
- After the initial setup, the facilities can operate with diminutive maintenance.
- Operating costs are extremely low compared to other power technologies.
- It is highly reliable and generates electricity at the actual point of use.
- PV systems are easily expandable, allowing for initial set-up even with a small budget and the addition of more modules in the future, when convenient.

Disadvantages of Solar PV System [19]

- Most types of PV power generation system require large areas of land to achieve average efficiency. The silicon used is also very expensive.
- Solar energy is currently thought to cost about twice as much as traditional sources (coal, oil etc).
- The problem of nocturnal down times means PV system can only ever generate during the daytime due to the intermittent and variable manner in which the solar energy arrives at the earth's surface.

- At present, the high cost of PV modules and equipment is the primary limiting factor for the technology.

2.2.2. Micro-Hydro Power Generation System

Hydropower engineering refers to the technology involved in converting the pressure energy and kinetic energy of water into more easily used electrical energy. The prime mover in the case of hydropower is a water wheel or hydraulic turbine which transforms the energy of the water into mechanical energy. Mechanical energy will be converted to electrical energy by using electrical generator [28]. A micro-hydropower system is a small system in the range of 5-100 kW. The simplest micro hydropower plant is based on a run-of-river design, which means it does not have water storage capability. It will produce power only when water is running or it might have relatively small water storage capability. Micro-hydropower is an interesting prospect for providing electricity for rural communities [40].

2.2.2.1. Principles of MhP

Power generation from water depends upon a combination of head and flow. Both must be available to produce electricity. Water is diverted from a stream into a pipeline, where it is directed downhill and through the turbine (flow). The vertical drop (head) creates pressure at the bottom end of the pipeline [28][40]. The pressurized water emerging from the end of the pipe creates the force that drives the turbine. The turbine in turn drives the generator where electrical power is produced. More flow or more head produces more electricity. Electrical power output will always be slightly less than waterpower input due to turbine and system inefficiencies.

Water pressure or Head created by the difference in elevation between the water intake and the turbine. Head can be expressed as vertical distance (feet or meters), or as pressure, such as pounds per square inch (psi) [40]. Net head is the pressure available at the turbine when water is flowing, which will always be less than the pressure when the water flow is turned off (static head), due to the friction between the water and the pipe. Pipeline diameter also has an effect on net head.

Flow is quantity of water available, and is expressed as ‘volume per unit of time’, such as gallons per minute (gpm), cubic meters per second (m^3/s), or liters per second (L/S). Design flow is the maximum flow for which the hydro system is designed. It will likely be less than the maximum flow of the stream (especially during the rainy season), more than the minimum flow, and a compromise between potential electrical output and system cost [28][41]. Sites where the gross head is less than 15m would normally be classed as “low head”. From 10-50m would typically be called “medium head”. Above 50m would be classed as “high head”.

2.2.2.2. Power from MhP

To determine the power potential of water in a stream it is necessary to know the flow quantity of water available from the stream and the available head. The quantity of water available for power generation is the amount of water (in m^3 or liters) which can be diverted through an intake into the pipeline (penstock) in a certain amount of time [41]. This is normally expressed in cubic meters per second (m^3/s) or in liters per second (l/s). Head is the vertical difference in level (in meters) through which the water falls down. The theoretical power (p) available from a given head of water is in exact proportion to the head and the quantity of water available [41].

The Micro-Hydropower Plants can be classified based on type of Operational feature, by demand of Electrical power, by installed capacity, available head at the inlet, discharge through the vanes and specific speed**.**

2.2.2.3. Classification of Hydropower by Operational Feature

Based on the construction of hydropower it classified as

a) Impoundment: Typical large hydropower plants head the construction of dams used to store more volume of water to provide sufficient head behind the dam. The stored water in the reservoir is required to get large amount of output power by improving the head and constant flow the through the turbine. In addition, the reservoir is used to store water for dry season [29].

b) Run-of-River: Run-of-river developments. A dam with a short penstock (supply pipe) directs the water to the turbines, using the natural flow of the river with very little alteration to the terrain stream channel at the site and little impoundment of the water [30].

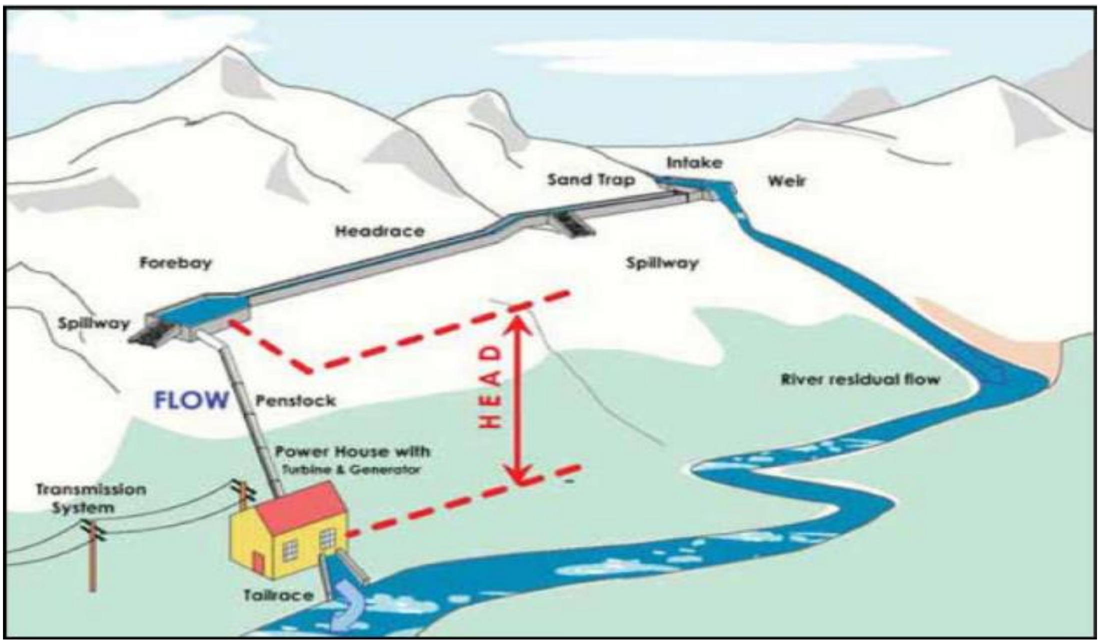

Fig. 2. 4: Run-off- river hydro power plant [30]

C) Pumped Storage

Water is pumped from a lower reservoir to a higher reservoir using inexpensive dump power during periods of low energy demand. The water is then run down through the turbines to produce power to meet peak demand [42]. Pumped storage is a dual action water flow system. During off peak hours water is pumped up to the higher reservoir from the lower one using reversible pumping turbine. The stored potential energy of water is released back to the lower reservoir to spine the turbine to generate power during peak hours [31][42].

D) Diversion and Canal Developments

The water is diverted from the natural channel into s canal or a leg penstock, thus changing the flow of the water in the stream for a considerable distance [42].

2.2.2.4. Classification of Hydro Power Based on The Demand for Electrical Power

I. Based-Load Developments. When the energy from a hydropower plant is used to meet all or part of the sustained and essentially constant portion of the electrical load or firm power requirements, it is called a base-load plant. Energy available essentially at all times is referred to firm power [42]**.**

II. Peak-Load Developments. Peak demands for electric power occur daily, weekly, and seasonally, plants in which the electrical production capacity is relatively high and the volume of water discharged through the units can be changed readily are used to meet peak demands. Storage or poundage of the water supply necessary [42].

2.2.2.5. Classification of Hydro Power by Installed Capacity

Classification of hydropower according to installed capacity is different from different scholars. Hydro systems can be regarded as a renewable energy source resulting from the natural hydrological cycle, it is by some considered sustainable due to the lack of impoundment of water and assumed negligible environmental impact [57]. The technology was initially used in Himalayan villages in the form of water wheels to provide motive power to run devices like grinders [42]. Table 2.2 shows the classification of the hydropower system based on the generated power output.

Table 2. 2: Classification of hydropower by size [57]

S/N	Classification	Rated Power	Consumer
1	Large- hydro	>100 MW	usually feeding into a large electricity grid
2	Medium hydro	15 - 100 MW	usually feeding a grid
3	Small-hydro	1 - 15 MW	usually feeding into a grid
4	Mini-hydro	100 kW - 1MW	either stand-alone schemes or more often feeding into the grid
5	Micro-hydro	5kW -100 kW	usually provided power for a small community or rural industry in remote areas away from the grid
	Pico-hydro	< 5kW	

2.2.2.6. Classification of Hydro Power by Head

Hydraulic head is a key site-specific factor affecting the turbines type selection, equipment, and construction costs of an SHP. Hence, a set of representative reference models should develop for different head ranges and corresponding turbine types:

- Low head (2-25m): axial flow (AF) Kaplan/propeller, cross-flow, Francis
- Medium head (25-70m): conventional Kaplan/propeller, Francis
- High head (>70 m): Francis, Turgo, Pelton

It is noted that the suggested water head ranges are not rigid but are merely a means of categorizing sites, and the turbine selection also depends on flow ranges and other factors at the individual sites [20].

2.2.2.7. Basic Components of MhP System

The basic components of MhP system classified into civil works components and electromechanical components (power house components) .

2.2.2.8. Civil Work Components

The civil components described in this section are those major components such as the intake, sand trap, spillway, headrace canal, settling basin, fore-bay tank, penstock pipes, and tailrace.

Intake (water diversion): the highest point of a hydro system where water is diverted from the stream to the penstock that feeds the turbine. Side intake and bottom intakes are the common.

Headrace Canal: is conveyance system that conveys designed discharge from one point to another. Generally, canal systems are used in all micro hydropower schemes whereas pipe systems are used for specific difficult terrain. A canal can be unlined or lined (stone masonry or concrete). The typical canal cross sections used in micro hydropower schemes can be rectangular or trapezoidal or triangular or semi-circular in shape.

Settling Basin: the civil component that settles sediments down in the basin for periodical flushing. Since sediment is detrimental to civil and mechanical structures and elements, the specific size of specified percentage sediment has to be trapped, settled, stored and flushed. This can only be achieved by reducing turbulence of the sediment carrying water. The turbulence can be reduced by constructing settling basins along the conveyance system. Since the settling basins are straight and have bigger flow areas, the transit velocity and turbulence are significantly reduced allowing the desired sediments to settle. The sediment thus settled has to be properly flushed back to the natural rivers.

Spillway: is a structure that diverted excess water safely to river. Spillways need to be designed to remove the excess water due to floods, in order to minimize the adverse effects to the other components of the MHS spillways are often constructed in settling basin and the fore-bay, from which the excess water is safely diverted to the water source.

Fore-bay Tank: civil component that steady flow into the turbine through the penstock. For-bay also acts as the last settling basin and allows the last particles to settle down before the water enters the penstock. Fore-bay can also be a reservoir to store water depending on its size. A sluice will make it possible to close the entrance to the penstock. In front of the penstock at rash rack need to be installed to prevent large particles to enter the penstock.

Penstock Pipe: the pipe, which conveys water under pressure from the fore-bay tank to the turbine. It is not only moving water to the turbine, but is also the enclosure that creates head pressure as the vertical drop increase.

2.2.2.9. Electro Mechanical Components (Powerhouse Components)

Powerhouse consists of electro-mechanical equipment's such as turbines, generator and drive systems. Turbine is a machine that converts energy in the form of falling water (water pressure) into mechanical shaft power, which can be used to drive electric generator. The selection of the best turbine for particular hydro site depends on the site characteristics. All turbines have a power speed characteristic. This means they will operate most efficiently at a particular speed, head and flow combination. Thus, the required speed of the generator coupled to the turbine also influences the selection. Another important point is whether the turbine is expected to generate power at part flow condition or not. The design speed of a turbine is mainly determined by head under which it operates.

2.2.2.10. Turbine Classification

As water falls from the upper position to the lower one through the penstock or tunnel, its potential energy is converted into electrical energy with a prime mover referred as hydraulic turbine. Hydraulic turbine consists of vanes, blade, or buckets due to the action of water pressure and velocity [32]. The rotary action of the turbine in turn spines a shaft that is integrated with an electrical generator that converts the torque energy of the shaft in electrical energy. Even though there are many classifications of turbines, they can be broadly classified into two types either impulse or reaction turbine. This classification criteria are based on the impact of the water energy with respect to hydraulic turbine. Impulse turbine converts the kinetic energy jet of water on air into torque energy when the jet hits the turbine runner. On the other hand, reaction turbine is totally immersed into the water [32]. Reaction turbine develops power from the combined effects of pressure and kinetic energy of the moving water. The angular and linear momentum of the water is transferred into shaft power in reaction turbine. Turbine can be classified as high-head, medium head and low-head machines. But this is relevant to the size of the machine. Low for head for large turbine can be high head for a small turbine. The classifications of hydro turbine are shown in Table 2.3.

Table 2.3: Classifications of hydro turbine according to head, flow and power [32]

Classification	Turbine Name	Head(m)	Power output(kw)
Impulse	Pelton	50-100	50-15000
	Turgo	30-200	20-5000
	Cross-flow	2-50	0.1-600
Reaction	Kaplan and Propeller	3-40	50-500
	Francis radial flow	40-200	500-15000
	Francis mixed flow	10-40	100-5000

2.2.2.11. Electrical Generators

A generator is the main unit which converts mechanical energy associated with water into electrical energy. Two types of generators (synchronous and asynchronous) can be used. Depending upon the size of a machine, types of a load to be fed, other energy sources later to be integrated, a generator is to be chosenin hydro power plants, this combination of generator and turbine is called generating unit [32]. AC generators are typically used with systems producing above 3 kW. AC voltage is also easily changed using transformers, which can improve efficiency with long transmission lines. Depending on our requirements, we can choose either single-phase or three-phase AC generators in a variety of voltages [33].

2.2.2.12. Drive Systems

The main purpose of the drive systems is to transmit the power from turbine to the generator at a stable voltage and frequency at a required speed. The drive systems consist of generator shaft, turbine shaft, bearings, couplings, gearboxes and belts and pulleys. The different types of drive systems common in MhS are direct drive, ‘V’ or wedge belts and pulleys, timing belt and sprocket pulley and gearbox drive systems. A direct drive system is one in which the turbine shaft is connected directly to the generator shaft. In contrast, ‘V’ or wedge belts and pulleys are the most commonly used type of drive systems in MhS. However, in very small systems (less than 3 kW) where efficiency is critical, timing belt and sprocket pulley are commonly used [33].

a) Controls

Alternating current is directly used by loads directly from the generator and excess electricity is burned off in dump loads (usually resistance heaters). Governors and other controls help that and AC generator constantly rotates at constant angular speed. Most commonly, micro hydro system is controlled by managing the load in the generator [34]. All MhS will have to have switchgear in order to separate the power flow when necessary and also to control the electrical power flow.

b) Turbine Selection Criteria

The type, geometry and dimensions of the turbine will be fundamentally conditioned by the characteristic of each given site. These important criteria are described as follows:

c) Net Head

The first criterion to take into account in the selection of the turbine is the net head. It is primarily the head measurement that determines the selection of a suitable turbine [35]. The selection is particularly critical in low-head schemes, where large discharges must be handled.

d) Range of Flow Volume and Discharges Through the Turbine

A single value of the flow has only very little significance. It is necessary to know the flow regime of a site. The rated flow and net head determine the set of turbine types applicable to the site and the flow environment.

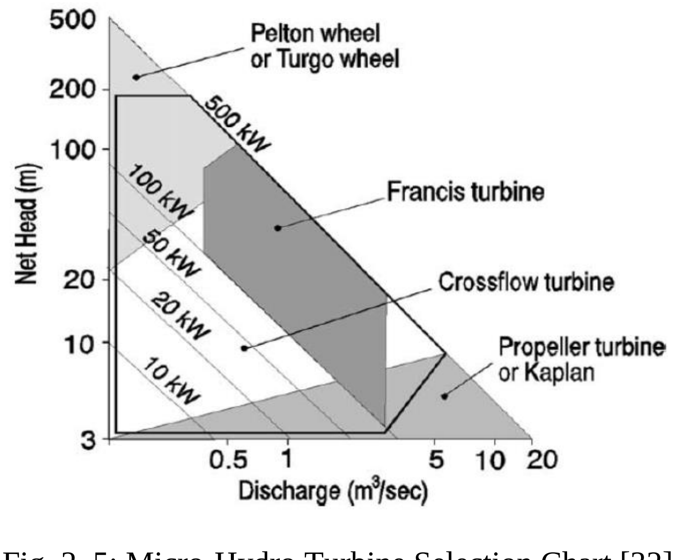

Fig. 2. 5: Micro-Hydro Turbine Selection Chart [32]

To determine the correct turbine type one solution is to use graphical tools which show the suitability of different turbine designs in relation to head, flow volume and power output [32]. The approximate range of head, flow and power applicable to different turbine types are summarized in Fig. 2.5 (up to 500 kW). This approximate depends on the precise design of each manufacturer.

From Fig. 2.5: propeller turbine is appropriate for the low heads and high flow rates. Cross-flow turbine is appropriate for flows up to 5m^3/s, net head varying from 3m to 200m and can give output power up to 500kW. Francis turbine is appropriate for flow rates from 0.5m^3/s to 4m^3/s, net head from 3m to 100m and can generate power output from 100 kW to 500 kW. Pelton wheel is appropriate for flows up to 1m^3/s, net head varying from 20 m to 500 m and can generate power from 20 to 500 kW [32]. All types of the turbines type overlapped on the desired operational region appropriate for the specific job. Now it will be necessary to compute installed power and electricity output against costs before taking a final decision about which type to use. It should be remembered that the "envelopes" vary from manufacturer to manufacturer and they should be considered only as a guide.

2.2.2.13. Specific Speed (N_s)

One of the important parameters of a turbine is the specific speed. Specific speed of a turbine can be defined as the speed of an ideal, geometrically similar turbine, which yields one unit of discharge for one unit of head [36][37]. The specific speed is also a very reliable criterion for the selection of an appropriate turbine. Given a flow and head for a specific hydro site, and the rpm (revolution per minute) requirement of the generator it becomes easy to calculate the specific speed. The turbine type can be estimated by comparing the calculated net head and specific speed with those given in Table 2.4. The specific speed constitutes a reliable criterion for the selection of the turbine. If we wish to produce electricity in a scheme with H_n (m) net head, using a P (kW) turbine directly coupled to a standard N (rpm) generator we should begin by computing the specific speed according to equation:

$$N_{s=N} \frac{\sqrt{P}}{H_n^{\;1.25}} \,. \qquad (2.1)$$

where, N_s is turbine specific speed, N is running speed of the turbine (RPM), H_n is net head (m) and P is the power to be generated (kW).

After computing the specific speed, it is possible to choose which turbine type to use or to decide whether to use a speed increaser like belts and gears.

Table 2. 4: Range of Specific speed [36]

Turbine Type	Specific speed range
Pelton one nozzle	$5<N_s<25$
Pelton two nozzles	$7<N_s<35$
Pelton four nozzles	$10< N_s <50$
Cross -flow	$20< N_s <200$
Francis	$50< N_s <350$
Kaplan and propel	$200< N_s <1550$

To obtain constant frequency from a generator driven by a water turbine, it must run at a constant speed and drive the generator through a fixed gear-ratio. The speed of the water turbine is controlled by a governor which opens or closes a valve or gate to hold the speed constant as the load changes. Both mechanical and electrical hydraulic governors are used to control the flow of water through the turbine by adjusting the gate position [37].

2.2.2.14. Generator Selection

Micro-hydro generators are low speed machines of salient pole type, having a large number of poles, a large diameter and a short rotor. Synchronous generator is used in most MHP systems because it has the ability to establish its own operating voltage and maintain frequency while it is operating in a remote location.

Table 2. 5: Selection of generator type [39]

Size of scheme	UP to 10 kW	10 to15 kW	More than 15 kW
Generator	Synchronous/induction	Synchronous/Induction	Synchronous
Phase	Single or Three phase	Three phases	Three phases

2.2.3. Bio-Mass System

The term biomass encompasses a large variety of materials, including wood from various resources, agricultural residues, and animal and human waste. Biomass is a renewable energy source because the energy it contains comes from the sun through the process of photosynthesis. One of the major waste products of the Rice processing is the Rice husk [14]. Biomass is any organic matter wood, crops, seaweed, animal wastes that can be used as an energy source. Biomass is probably our oldest source of energy after the sun. For thousands of years, people have burned wood to heat their homes and cook their food.

Biomass gets its energy from the sun. All organic matter contains stored energy from the sun. During a process called photosynthesis, sunlight gives plants the energy they need to convert water and carbon dioxide into oxygen and sugars. These sugars, called carbohydrates, supply plants and the animals that eat plants with energy [56]. Foods rich in carbohydrates are a good source of energy for the human body. Biomass is a renewable energy source because its supplies are not limited. We can always grow trees and crops, and waste will always exist.

This research, therefore, has investigated the performance of a fixed bed gasifier using various agricultural residues as the feedstock. The atmospheric gasifier was operated in downdraft mode. The agricultural residues considered in this research include groundnut shells, coffee husks, rice husks, bagasse, and maize cobs.

2.2.3.1. Gasification Process of Bio-Mass (Rice Husk)

Thermal conversion processes for biomass involve some or all of the following processes:

Pyrolysis: Biomass + Heat …………………Charcoal, oil, and gas
Gasification: Biomass + Limited oxygen -……………….…. Fuel gas
Combustion: Biomass + Stoichiometric' oxygen -……………. Hot combustion products

biomass gasification is a process in which solid biomass fuels are broken down by the use of heat in an oxygen-starved environment to produce a combustible gas [56]. Biomass fuels conducive to gasification include dry materials such as wood, charcoal, rice husks, and coconut shells. Biomass gasification, in the sense used here, should be distinguished from biogas production, which uses wet organic feedstocks such as animal dung or stillage and works by means of microbiological action to generate methane gas.

Biomass gasification is the thermal chemical conversion of biomass into a combustible gaseous product (producer gas) by the supply of a gasification agent which can be air, oxygen or steam [57]. Biomass gasification has the potential of contributing to the growing energy needs of the world particularly as a renewable energy technology Biomass gasification is the thermal chemical conversion of biomass into a combustible gaseous product (producer gas) by the supply of a gasification agent which can be air, oxygen or steam. Biomass gasification has the potential of contributing to the growing energy needs of the world particularly as a renewable energy technology.

Gasification process thermally converts carbon-containing material into gas that can be combusted or used in chemical applications. Gasification as technology is much newer and less used than combustion but is becoming more and more common due to its benefits over direct incineration [56][58]. Much more effective use of low-grade fuels and biomass and reduced emissions are only a few incentives to gasification. The rate of the gasification reaction mainly depends on the reactivity of the fuel, gasifying medium and temperature and pressure of the process. Different reactions are favored by different conditions in the gasifier reactor.

2.2.3.2. Gasification Phenomena

The phenomena occurring in the gasifier can be theoretically divided into different thermal stages occurring in different temperatures (Basu 2006, p63). There are no clear boundaries between the stages and they can overlap in a large particle (Basu 2010, p120). Fig 2.6 represents the main steps of gasification and the resulting products. 1. Drying >150^{o}C 2. Devolatilization/Pyrolysis 150-700^{o}C 3. Combustion 700-1500^{o}C 4. Gasification 800-1100^{o}C When a fuel particle is heated, moisture starts to vaporize. If the moisture content is high, this part requires more energy and reduces the temperature inside the gasifier and the product gas heating value. That is why some pre drying is necessary to lower the moisture content of the fuel, especially with biomass. (Basu 2010, p120) Pyrolysis is a complex process including multiple chemical and physical reactions producing light gases (H_2, CH_4, CO, CO_2, H_2O), tar and char. (de Souza-Santos, 2010, p25) Pyrolysis raises the carbon concentration of the char. (Rezaiyan & Cheremisinoff 2005, p17) Combustion reactions occur in the presence of oxygen and they provide thermal energy. Gasification reactions occur between carbon of the char and steam, carbon dioxide and the resulting gases. They are slower than combustion reactions and are commonly endothermic.

Gasification is a process, where a liquid or solid fuel is converted into gaseous form. Normally this product gas consists mostly of H_2 and CO (also CO_2, H_2O, CH_4 and various heavy hydrocarbons). In gasification, a solid or liquid fuel, such as biomass or coal, reacts in temperatures over 800^{o}C with a gasifying medium – air, oxygen, steam or a mixture of these – that includes a restricted amount of oxygen (equivalence ratio (ER) < 1). When oxygen reserve is limited, combustion becomes incomplete and slower gasification reactions have time to proceed. (Basu 2006, p59; Rezaiyan & Cheremisinoff 2005, p5) Fig represents a simple gasification process.

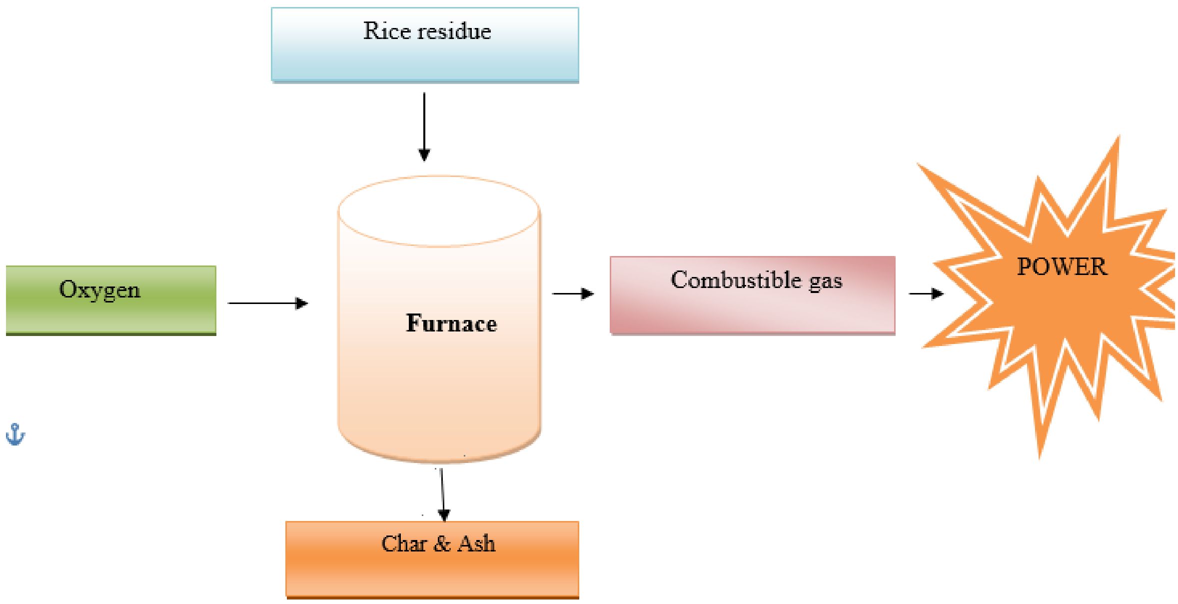

Fig. 2. 6: Simplified gasification process

2.2.3.3. Benefits of Gasification

Gasification enables the use of cheap, potentially CO_2-neutral or low-grade fuels that are usually available locally, and long-distance transportation can be avoided. By converting them into combustible gas, these fuels can be exploited with much better efficiency than with direct incineration [58]. Emissions of sulfur and nitrogen oxides and particulates are significantly lower with gasification than combustion.

2.2.3.4. Fluidized Bed

The operation of both up and downdraught gasifiers is influenced by the morphological, physical and chemical properties of the fuel. Problems commonly encountered are: lack of bunker flow, slagging and extreme pressure drop over the gasifier [56]. A design approach aiming at the removal of the above difficulties resulted in the fluidized bed gasifier illustrated schematically in Fig. 2.7. Air is blown through a bed of solid particles at a sufficient velocity to keep these in a state of suspension. The bed is originally externally heated and the feedstock is introduced as soon as a sufficiently high temperature is reached. The fuel particles are introduced at the bottom of the reactor, very quickly mixed with the bed material and almost instantaneously heated up to the bed temperature [56][58]. As a result of this treatment the fuel is pyrolyzed very fast, resulting in a component mix with a relatively large amount of gaseous materials.

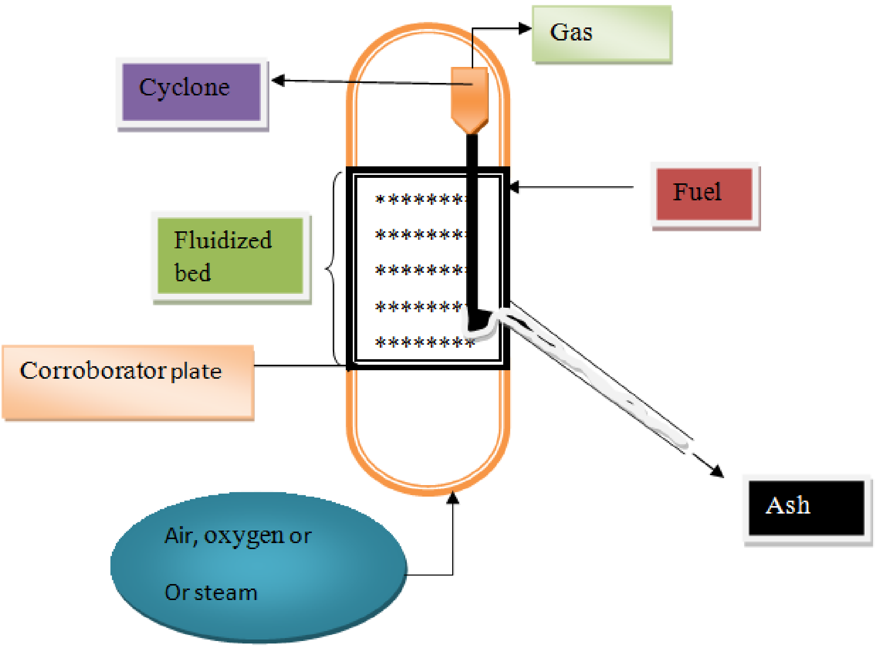

Fig. 2. 7: Diagram of fluidized bed gasified

Further, gasification and tar-conversion reactions occur in the gas phase. Most systems are equipped with an internal cyclone in order to minimize char blowout as much as possible. Ash particles are also carried over the top of the reactor and have to be removed from the gas stream if the gas is used in engine applications [56]. The major advantages of fluidized bed gasifiers, as reported by Van der Aarsen (1984) stem from their feedstock flexibility resulting from easy control of temperature, which can be kept below the melting or fusion point of the ash (rice husks), and their ability to deal with fluffy and fine grained materials (sawdust etc.) without the need of pre-processing.

2.2.3.5. Dual-fuel mode of operation

Producer gas obtained from gasifiers has been successfully employed as IC engine fuel, both in dual-fuel mode, using diesel as pilot fuel, and in single-fuel mode. In dual fuel operation, commercially available diesel engines are directly used, with the inlet manifold connected to the gasifier outlet through at-joint so as to aspirate a gas-air mixture in place of pure air. The gas-air ratio is regulated of ten manually by controlling the valves on the gas and air lines connecting to the manifold. Diesel is sprayed in to the cylinder to initiate combustion of the lean mixture of producer gas and air .This mode of operation results replacement of diesel up to a maximum of 80%, *i.e.*, pilot diesel quantity required can be reduced to 20% of what an engine running on diesel alone would consume[56]. But it still needs a fossil fuel to run the engine. The main advantage of this technology is that when the gasifier is down for some reason, the engine can continue to operate using diesel fuel alone, since the engine system has not been modified.

2.2.3.6. Gasification Reactions

The chemistry of biomass gasification is complex. Biomass gasification proceeds primarily via a two-step process, pyrolysis followed by gasification. Pyrolysis is the decomposition of the biomass feedstock by heat. The remaining non-volatile material, containing high carbon content is referred to as char [56]. Combustion, occurring in the oxidation zone, is described by the following chemical equations:

$$C + O_2 \rightarrow CO_2 + 393.8 \text{ kJ/mol}$$

$$C + \tfrac{1}{2}O_2 \rightarrow CO + 123.1 \text{ kJ/mol}$$

$$C + 2H_2 \rightarrow CH$$

These three reactions are exothermic and provide, by auto-thermal gasification, the heat necessary for the endothermic reactions in the drying, pyrolysis and reduction zones. The water vapor introduced with the air and production by the drying and pyrolysis of the biomass reacts with the hot carbon according to the following heterogeneous reversible water gas reaction:

$$C + H_2O + 118.5 \text{ kJ/mol} \leftrightarrow CO + H_2$$

The most important reactions are the water gas reaction and the following backward reaction:

$$C + CO_2 + 159.9 \text{ kJ/mol} \rightarrow 2CO$$

These heterogeneous endothermic reactions increase the gas volume of CO and H_2 at higher temperatures and lower pressures (a high pressure suppresses the gas volume) [56]. Besides these reactions several other reduction reactions take place of which the most important ones are the water shift reaction and the mechanization reaction respectively shown below:

$$CO_2 + H_2 + 40.9 \text{ kJ/mol} \rightarrow CO + H_2O$$

$$C + 2H_2 \rightarrow CH_4 + 87.5 \text{ kJ/mol}$$

The exhaust heat from the engine systems have great attraction for agricultural applications like drying of farm products and wet Rice husk. Since the production of gas is uneven and fluctuates with time it is necessary to have a storage of gas. This can provide every uniform quality gas. Because of the low energy content of producer gas (5 MJ/m^3) which is about 10-15% that of natural gas, special burners are needed. A gasifier fuel can be classified as good or Bad according to the following parameters. The full physical schematic diagram of any Bio-mass gasifier can be drowned as in the following diagram.

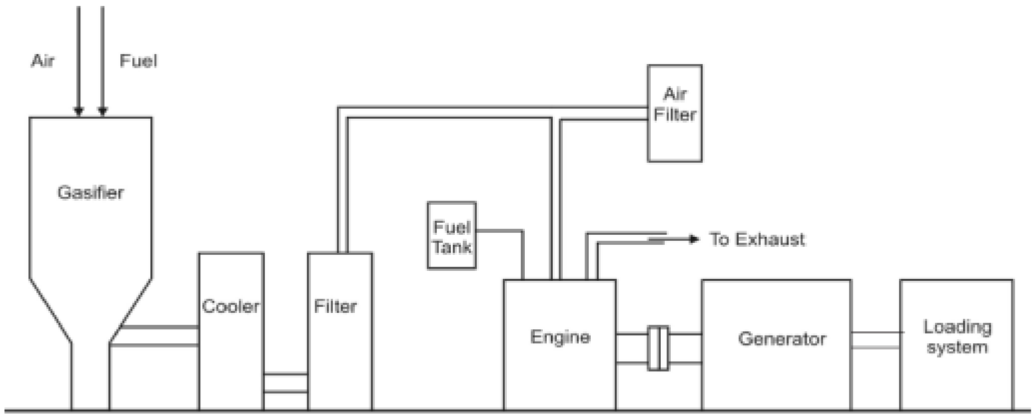

Fig. 2. 8: Schematic diagram of Biomass power plant

Energy content and bulk density of fuel: - The higher the energy content and bulk density of fuel the similar is the gasifier volume since for one charge one can get power for longer time. Bulk density is also an indicator of residence time in the gasifier ultimately determining the conversion efficiency of the gasification process.

Moisture content: - In most fuels, there is very little the type of fuel, its origin treatment, determines choice in moisture content since it. It is desirable to use fuel with low moisture content because heat loss due to its evaporation before gasification is considerable and the heat budget of the gasification reaction is impaired. Besides impairing the gasifier heat, budget high moisture content also puts load on cooling and filtering equipment by increasing the pressure drop across these units because of condensing liquid. Thus, in order to reduce the moisture content of fuel some pretreatment of fuel is required. Generally, desirable moister contents for fuel should be less than 20.

Dust content: - All gasifier fuels produce dust. This dust is a nuisance since it can clog the internal combustion engine and hence has to be removed. The gasifier design should be such that it should not produce more than 2-6g/$m^3$of dust. The higher the dust produced more load is put on filters necessitating their frequent flushing and increased maintenance.

Cooling and Cleaning of Gas: - The temperature of gas coming out of generator is normally between 300-500^{o}C.This gas has to be cooled in order to raise its energy density. Most coolers are gas to air heat exchangers where the cooling is done by free convection of air on the outside surface of heat exchanger. Thus, ideally the gas going to an internal combustion engine should be cooled to nearly ambient temperature. The Producer gas is then cleaned and cooled as it passes the cyclone and scrubber and delivered to the dual fuel engine as a clean gas through the main gas valve (MGV) while the diesel is supplied through the diesel tank.

Ash Handling: - The mineral content in the fuel that remains in oxidized form after complete combustion is usually called ash. The ash content of a fuel and the ash composition have a major impact on trouble free operation of gasifier. Handling the ash is also very important and many times appears to be one of the technical barriers for biomass gasification. In this paper, the ash from the process can be used for fertilizer and road construction.

2.3. The Proposed Hybrid System

The proposed hybrid consists of a solar, micro-hydro and bio-mass renewable combination. The capability of the electric generation hybrid systems is to satisfy the power demand on the climatic data, and location of the area, and vastness of the households. Such conditions will define different operation modes of the system. The controller is used to use the power efficiently and to serve the power demand of customer. The controller looks first at the load and switches the appropriate source to meet the demand from the customer side.

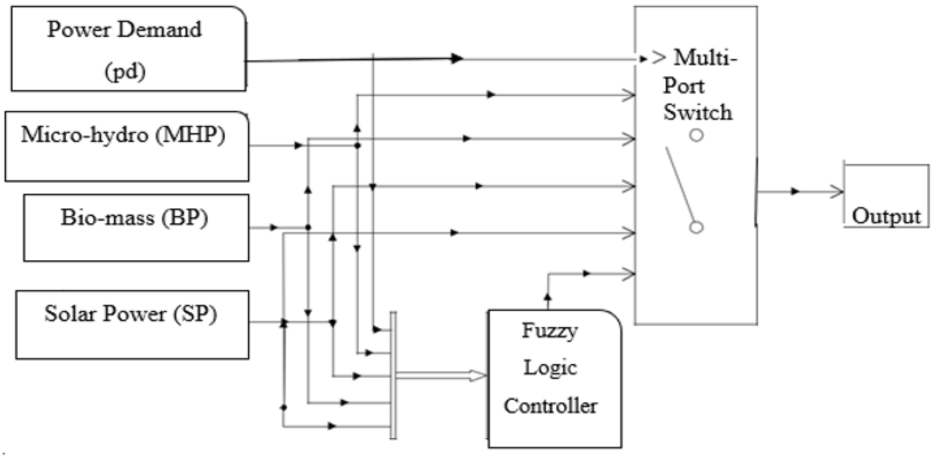

Fig. 2. 9: Block diagram of proposed hybrid system

Basically, these operation modes are determined by the energy balance between the total generation and the total demand. A comprehensive controller is essential to efficiently manage the operation of the generation subsystems accordingly. That is depending on the amount of the load the controller makes the intelligent decision to switch the multi-port switch to the required load demand output.

CHAPTER 3

3. METHODOLOGY

3.1. Introduction

This chapter includes data collection and analysis of the hybrid system. The data used in the design of the hybrid components are collected directly from the site and from Ethiopian Metrology agency, and for perfectness of the analysis these data are compared with the NASA data obtained using the latitude and longitude of the site.

3.2. Methods

In order to attain the above general and specific objectives of the study, the following methods and techniques will be followed.

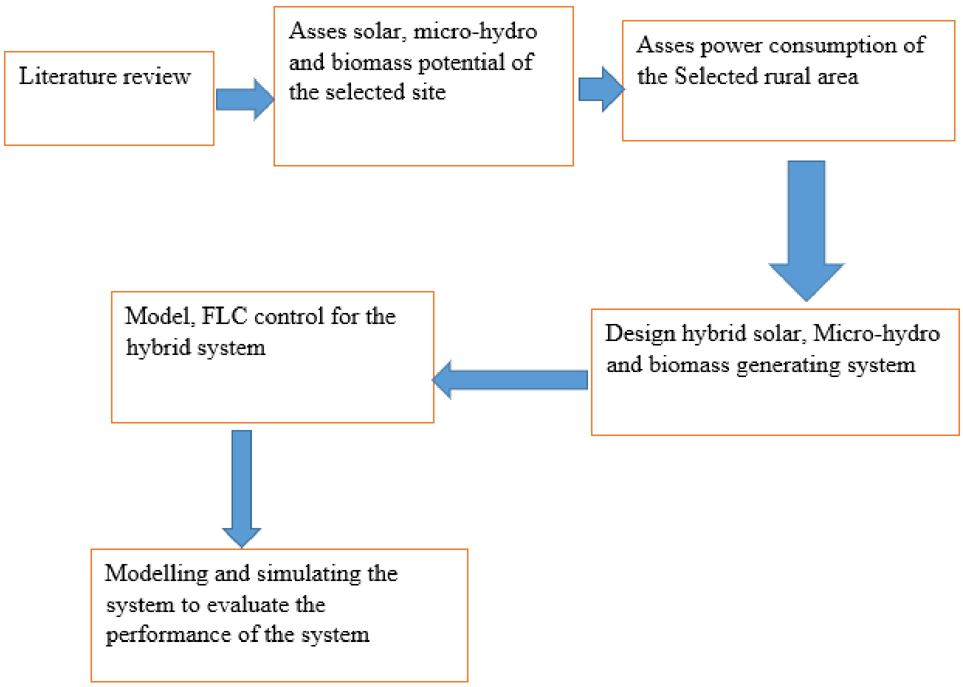

Fig. 3. 1: Block diagram of the methodology

3.3. Description of the Study Site

Fogera is one of the woredas in the Amhara Region of northwest Ethiopia. It is one of the 106 Woredas of the Amhara Regional State and found in South Gondar Zone. Benti village is located in Fogera Woreda on average at 34 km away from Wereta town that is 73 km from Debub Gondar town having latitude of 11.916 N and longitude of 37.7 E with an elevation of 1828 m. The residents are farmers who are engaged in rice plantation and other farming activities using irrigation on Gumara River. The residents are the descendants of Amhara clan and their total number of households are 426 and 4 people on average in each household. The village is very far from main grid and scattered, so it is difficult to electrify through grid system. The only viable option to electrify this village is through off grid system using available resources.

Fig. 3. 2: Google map of Fogera town

3.4. Data Gathering

The data used in the design of the hybrid components are collected directly from the site and from Ethiopian Metrology agency and for perfectness of the analysis these data are compared with the NASA data obtained using the latitude and longitude of the site. The Micro hydro and solar data which are collected from Ethiopia Ministry of Water and Energy and the Ethiopian metrology agency and NASA are considered as secondary data inputs.

3.4.1. Energy Demand

The first step in designing power system is determining the total power consumption of the study area. The size and cost of hybrid system components are highly influenced by the size of electrical loads. The load determination of the village was performed for 426 household numbers with average of four family members per household; that depicts a population number of 1704 (source: city administration). Load estimation was done by identifying the type, daily hours of operation; quantity of the appliances and their ratings. Accordingly, the electricity consumption was estimated using the general formula:

Energy consumption(kWh)= (number of appliances used*power rating of each appliance(W)*hours of operation/100. (3.1)

Energy demands of the population (426) in the village is estimated based on the following need assumptions: lighting (100% of population), 4 water pumping motors for irrigation, Radio (70% of population), TV (70% of population), house hold Refrigerator (25% of population), Stove (10% of population), Injera Mitad (7% of population) elementary school and refrigerator in the health clinic. The load profile for the respective village was taken from administrative offices of the Fogera Wereda and Benti Kebele and observing previous trends of similar villages recently electrified.

Table 3. 1: Total energy consumption of Benti village.

Time	Total load (kWh)					
	Energy Household (kWh)	Public loads (pump) (kWh)	Energy in church (kWh)	Energy in clinic (kWh)	Energy in school (kWh)	Total load Energy
0:0-1:0	10.65	-	0.026	0.126	-	10.802
1:0-2:0	10.65	-	-	0.1	-	10.75
2:0-3:0	10.65	-	-	0.1	-	10.75
3:0-4:0	10.65	-	-	0.1	-	10.75
4:0-5:0	16.188	-	-	0.1	-	16.288
5:0-6:0	105.222	-	0.134	0.1	-	106.122
6:0-7:0	108.63	-	0.134	0.1	-	108.864
7:0-8:0	44.73	-	-	0.1	-	44.83
8:0-9:0	44.73	9.5	-	1.115	-	55.345
9:0-10:0	44.73	9.5	-	1.415	-	55.645
10:0-11:0	44.73	-	-	0.4	1.2	46.33
11:0-12:0	44.73	-	-	0.1	0.300	45.13
12:0-13:0	108.63	-	-	0.1	-	108.73
13:0-14:0	44.73	-	-	0.1	-	44.83
14:0-15:0	44.73	9.5	-	1.115	0.3	55.645
15:0-16:0	44.73	9.5	-	1.415	0.3	55.945
16:0-17:0	44.73	-	-	0.4	0.9	46.03
17:0-18:0	44.73	-	0.080	0.1	-	44.91
18:0-19:0	136.32	-	0.184	0.204	0.182	136.89
19:0-20:0	72.42	-	0.160	0.204	0.234	73.018
20:0-21:0	72.42	-	0.026	0.152	0.104	72.702
21:0-22:0	57.51	-	-	0.152	0.052	57.714
22:0-23:0	21.726	-	-	0.126	0.052	21.904
23:0-24:0	10.65	-	-	0.126	-	10.776
Total load Energy	1199.616	38	0.744	8.085	3.624	1250.069

The total electric energy consumption of households, commercial loads (health center, church, school), and public loads were 1199.616 kWh, 12.453 kWh, 38 kWh respectively. Total electric energy consumption of the Benti was 1250.069 kWh. Fig 3.3 shows the total load profile of the village. The peak load from 19:00, 20:00, 21:00 hours due to the expected significant lighting load in the households. The minimum load is indicated from 22:00 - 06:00 because energy consumption during night is very low.

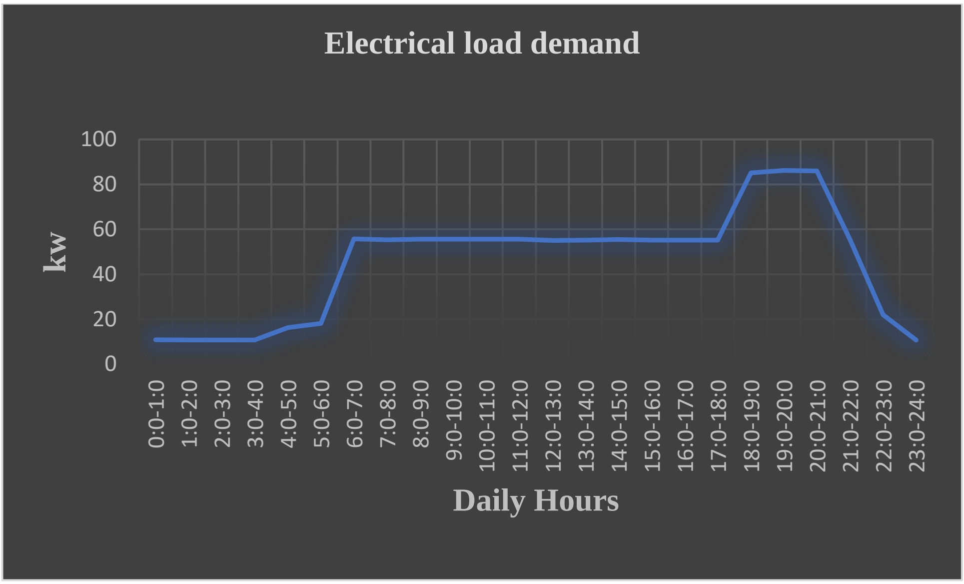

Fig. 3. 3: Load profile of Benti village

The total energy consumption of the selected sites of the village per day is about 1250.069 kWh, and from this the annual energy consumption is $1250.0.69\ \text{kWh} \times 365$ which is 456,275.185kWh (456.275 MWh). Average load demand (LD) per hour is 52.1 kW, and the peak load (PL) is calculated by dividing the average load demand by the load factor (LF), and taking 0.6 load factor.

$$\text{Peak load} = \frac{\text{load demand}}{\text{load factor}}, \quad \text{PL} = \frac{\text{LD}}{\text{LF}} = \frac{52.1\,\text{kW}}{0.6} = 86.8 \qquad (3.2)$$

$\text{Installed capcity} = \text{Peak load} + \text{Loss}$, and assuming loss of 7% of peak load (PL) which gives 6.076 kW, thus installed capacity is 86.6 kW + 6.076 kW = 92. 876 kW. Therefore, the total electric energy demand of the village is 92.876 kW.

3.4.1.1. Forecasting of Load Demand after 10 Years

The total electric energy consumption of households currently is 1199.616 kWh as given in Table 3.1. Per household's consumption (U) = annual energy consumption (A) ÷ numbers of households (N).

$$U_{2030} = 437.85\,\mathrm{MWh} \div 426 = 1027.84\,\mathrm{kWh}$$

$$\log G = 1.28 + C_1 + ... - K_1 \times K_2.....K_N\, 0.155 \log u \qquad (3.3)$$

where, G= annual percentage growth in per household consumption, U is annual kWh usage per household, C_1.... etc. are constants for household's growth (2.3%) and others. $K_{1,}$, K_2........ K_N are constant assumed unity.

$$\log G = 1.28 + C_1 - 0.15 \log u, C_1 = 0.05 \times PR, C_1 = 0.115$$
$$\log G = 1.28 + C_1 - 0.15 \log 1027.84,$$
$$\log G = 1.28 + 0.115 - 0.45178$$
$$\log G = 0.9432, G = 10^{0.9432} = 8.77$$

Annual kWh usage per households in the year 2030 is

$$U_{2030} = U_{2030} \times (1 + \frac{G}{100})^{10} \div (1 + \frac{PR}{100})^{10} \qquad (3.4)$$

$$U_{2030} = 1027.84 \times (1 + \frac{8.77}{100})^{10} \div (1 + \frac{2.3}{100})^{10} = 1897.8\,\mathrm{kWh}.$$

Number of house hold (HS) for 2030

$$HS_{2030} \times (1 + \frac{PR}{100})^{10} = 426 \times (1 + \frac{2.3}{100})^{10} = 535\text{Households}$$

Energy consumption per household for 2030=1897.8 kWh x 535 = 1015.3 MWh

$$\text{Peak load demand} = \frac{\text{Annual energy consumption}}{\text{total time of the year}} = \frac{1015.3}{365} = 115.9\,\mathrm{kW} \qquad (3.5)$$

Table 3. 2: Forecasting public and commercial loads

Type of load	Commercial loads			Public loads	
	Clinic	School	Church	Flour mill	Pump
Existing condition	1	1	1	1	1
kW	0.336	0.15	0.031	1.25	0.333

Total kW	2.1				
10 years plan	1	1	1	1	2
kW	0.66	0.65	0.25	2	0.666
Total kW	4.1				

The load demand of commercial and public loads of Benti village of next 10 years is shown in Table 3.2.

As per the plan for the year 2020 – 2030 G.C of Benti village, the total electrical demand of commercial and public loads was assumed to be 4.1 kW working 10 hours per day. The total energy consumption therefore was 4 kWh. This indicates the commercial and industrial loads will grow very fast because of the growth of Schools, Health centers, Irrigation, rice production and others. Therefore, the total Electrical Energy demand of Benti Village for the year 2030 G.C will be 120 kW.

3.4.2. Solar Radiation Assessment

In this work the number of sunshine hours data is recorded every day using the sunshine hour recorder for four consecutive years (2014-2018) G.c. The collected solar radiation data is analyzed. Regression constants in the first order Angstrom-Prescott type correlations for the selected site are calculated using regression analysis. To do this analytical estimation the monthly average daily global solar radiation, altitude, latitude, declination angle of the day, the average day in the month and the sunshine hour data are used as the input data.

Linear Angstrom-Prescott regression equation related monthly average daily radiation to clear day radiation in a given location and average fraction of possible sunshine hour data which is given by the following equation.

$$\frac{H}{H_o} = a + b(\frac{S}{S_o}) \qquad (3.6)$$

where H, is monthly average daily global solar radiation, H_O is monthly average daily extraterrestrial solar radiation, S and So are Angstrom's correlation parameter, S is monthly average daily hours of sunshine from sunshine recorder, So is monthly average of the maximum possible hours of sunshine, Ho is determined based on the Solar Constant, average day of the month and the declination angle.

$$H_o = \frac{86400}{\Pi} * I_{sc}\{1 + 0.033\cos\frac{360n}{365}\{\frac{2\Pi W_s}{360}(\sin\phi\sin\sigma) + (\cos\sigma\cos\phi\sin W_s)\}J/m^2 \quad (3.7)$$

Since there are 3600 seconds in an hour and 86400/3600 =24, the following equation gives the monthly average daily extraterrestrial solar radiation in Wh/m^2.

$$H_o = \frac{24}{\Pi} * I_{sc}\{1 + 0.033\cos\frac{360n}{365}\{\frac{2\Pi W_s}{360}(\sin\phi\sin\sigma) + (\cos\sigma\cos\phi\sin W_s)\} \quad (3.8)$$

where I_{sc} is the solar constant which has a value of $1367W/m^2$, W_s is the mean sun rise hour angle for the given month, n is the number of days of the year starting from first January

$$S_o = \frac{2}{15}W_s \quad (3.9)$$

$$W_s = \cos{-1}(\tan\delta\tan\phi) \quad (3.10)$$

where; W_s is the mean sunrise hour angle, δ is the solar declination angle for the average day in the month, ϕ is the latitude of the selected site, the solar declination angle (δ) throughout the year can be well approximated by sine function and is given by the following equation,

$$\delta = 23.45\sin[360(\frac{284+n}{365})] \quad (3.11)$$

where; n is the day of the year. The value of n for any day of the month can be determined. The accuracy of the estimated values of the regression coefficients 'a' and 'b' are expected to improve by adding the effect of elevation, sunshine duration, and latitude together. Thus, the regression coefficients 'a' and 'b' in terms of the latitude, elevation and percentage of possible sunshine for any location around the world are correlated by Goliathan with equation below.

$$a = -0.309 + 0.539\cos\phi - 0.0693h + 0.29(\frac{n}{N}) \quad (3.12)$$

$$b = 1.527 - 1.027\cos\phi + 0.0926h - 0.359(\frac{n}{N}) \quad (3.13)$$

where h is altitude of a site in kilometers 34 km, δ is declination angle for the average day in the month calculated from the above Equation (3.8), Φ is Latitude of the site 11.9167 N and 37.7 E for the specific study site, and W_s Sunset hour angle calculated from the above Equation (3.7).

Table 3. 3: Recommended average days for months and declination angle

Month	n for the day of the month, D	Date	Day of the year(n)	δ (degrees)
January	D	17	17	-20.92
February	31+D	16	47	-13.03
March	59+D	16	75	-2.44
April	90+D	15	105	9.42
May	120+D	15	135	18.81
June	151+D	11	162	23.15
July	181+D	17	198	21.22
August	212+D	16	228	13.53
September	243+D	15	258	2.24
October	273+D	15	288	-9.63
November	304+D	14	318	-18.95
December	334+D	10	344	-23.1

Table 3. 4: average solar radiation in $kWh/m^2/day$ of Benti

Date of Month		Δ (degree)	Ws (degree)	S (hr)	So (hr)	S/So	Ho ($kWh/m^2/d$)	a	b	H ($kWh/m^2/day$)
Jan-17	17	-20.92	86.56	6.92	11.54	0.599	9.013	0.246	0.53	5.85
Feb-16	47	-13.03	87.93	7.125	11.72	0.607	9.685	0.248	0.5	6.14
Mar-16	75	-2.44	90.6	8.09	12	0.552	10.293	0.304	0.42	5.80
Apr-15	105	9.42	91.48	6.65	12.19	0.545	10.522	0.231	0.53	5.63
May-15	135	18.81	93.09	6.185	12.41	0.498	10.372	0.217	0.55	5.53
Jun-11	162	23.15	93.84	4.975	12.51	0.397	10.21	0.187	0.58	4.36
Jul-17	198	21.22	93.84	3.66	12.51	0.292	10.232	0.144	0.62	4.4
Aug-16	228	13.53	92.17	3.56	12.28	0.289	10.393	0.143	0.62	4.0

Sep-15	258	2.24	89.65	5.06	11.95	0.423	10.319	0.182	0.624	4.801
Oct-15	288	-9.63	88.51	6.78	11.8	0.574	9.824	0.226	0.57	5.534
Nov-14	318	-18.95	86.9	7.26	11.58	0.626	9.141	0.254	0.5	5.282
Dec-10	344	-23.1	83.85	8.04	11.54	0.606	8.765	0.314	0.41	6.14
Average								**0.22**	**0.54**	**5.11**

The regression coefficients 'a' and 'b' in terms of the latitude, elevation and percentage of possible sunshine for any location around the world are correlated. The average daily global solar radiation varies from around 4.0 (kWh/m^2/day) in rainy month of August to just 6.14 (kWh/m^2/day) in the dry months.

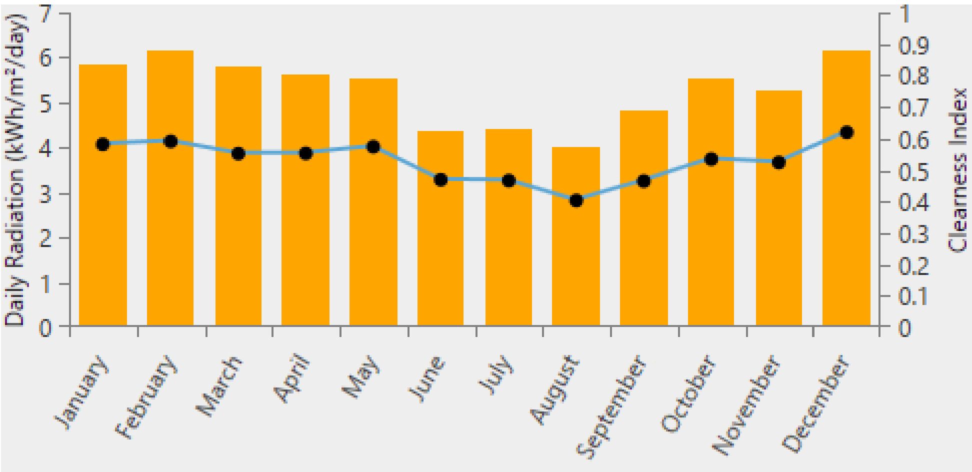

Fig. 3. 4: Average global solar radiation

3.4.2.1. Data Compression of Global Solar Radiation of NMA and NASA

The Table 3.4 and Fig. 3.5 shown below compares the post processed data taken from the NMSA Debrtabor branch and NASA.

Table 3. 5: Data compression of global solar radiation of NMSA and NASA

Months	Jan	Feb	Mar	Apr	May	Jun	Jul	Aug	Sep	Oct	Nov	Dec	Avg
NMSA	5.85	6.14	5 .8	6.63	5.53	4.36	4.4	4.0	4.801	5.534	5.282	6.14	5.2889
NASA	5.91	6.18	5.9	6.72	5.62	4.53	4.9	4.14	5.13	5.61	5.35	5.98	5.4975
Change	0.06	0.04	0.1	0.09	0.09	0.17	0.5	0.14	0.329	0.076	0.068	0.16	0.2086

The average global solar radation of NMA Deber Tabor branch was 5.29 kWh/m^2/d, average global solar radationof NASA was 5.4 kWh/m^2/d and average change (difference) betewen the calculated and NASA data was 0.2086 kWh/m^2/d.

Calculated (NMSA) NASA

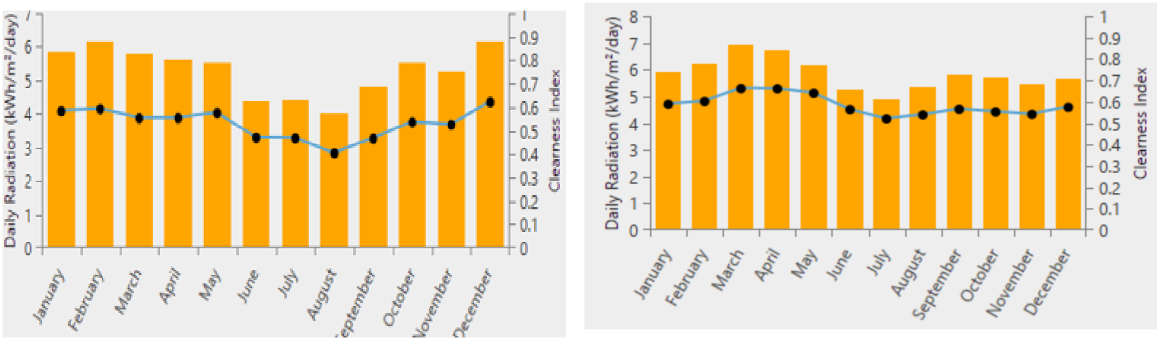

Fig. 3. 5: Data comparison of NMA and NASA

From the above tables and figures it is possible to understand the data taken from NMA was valid and there was enough solar radiation to electrify the village Benti from solar system.

3.4.3. Micro Hydro Resource Assessment

The daily average flow rate of Gumara River for the hydro resource data of 10 years was taken from FDRE Ethiopian Ministry of water, Irrigation and energy. However, HOMER accept monthly average stream flow. So, daily average flow is changed into monthly average. The site gross head is 14 m.

Fig. 3. 6: Gumara river [Photo is taken by phone]

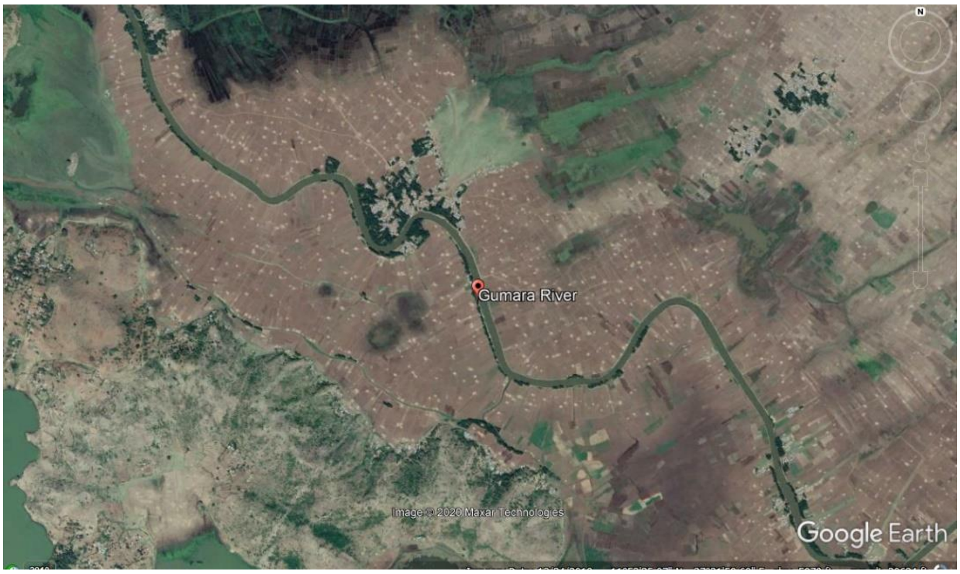

Fig. 3. 7: Google map of Gumara river

The monthly average stream flow and its pictorial representation is given in Table 3.6 below.

Table 3. 6: Monthly flow rate of Gumara

Month	Flow rate of Gumara (m^3/s)
Jan	5.619
Feb	3.793
Mar	3.046
Apr	2.139
May	2.593
June	17.248
July	87.048
Aug	157.669
Sep	90.521
Oct	35.995
Nov	15.81
Dec	8.475
Average	35.82966

Fogera wereda is one of the wereda's found in Debub Godar Zone which is very reach in rivers. Gumara river is one of the rivers found in Fogera Wereda with 2.139 m^3/s flow rate and 14 head in m. The numbers indicates that the hydro potential in Gondar Zone is suitable for Micro-hydro power generating system to electrify the rural village Benti of Fogera Wereda.

3.4.3.1. Hydrological Data Analysis

The purpose of the hydrology study is to ensure that the turbine is of the correct size for the water flow, and has the correct variable flow characteristics, so that the investment is not wasted for over or under capacity. The sizing of the channel, penstock, etc. is also determined by the hydrology study. For the case of Gumara, there is no gauging station. Especially for the design of all the components of MHP (micro-hydro power), water flow rate data should be available. The minimum and maximum monthly average flow rate of Gumra river is 2.139m^3/s and 157.669m^3/s.

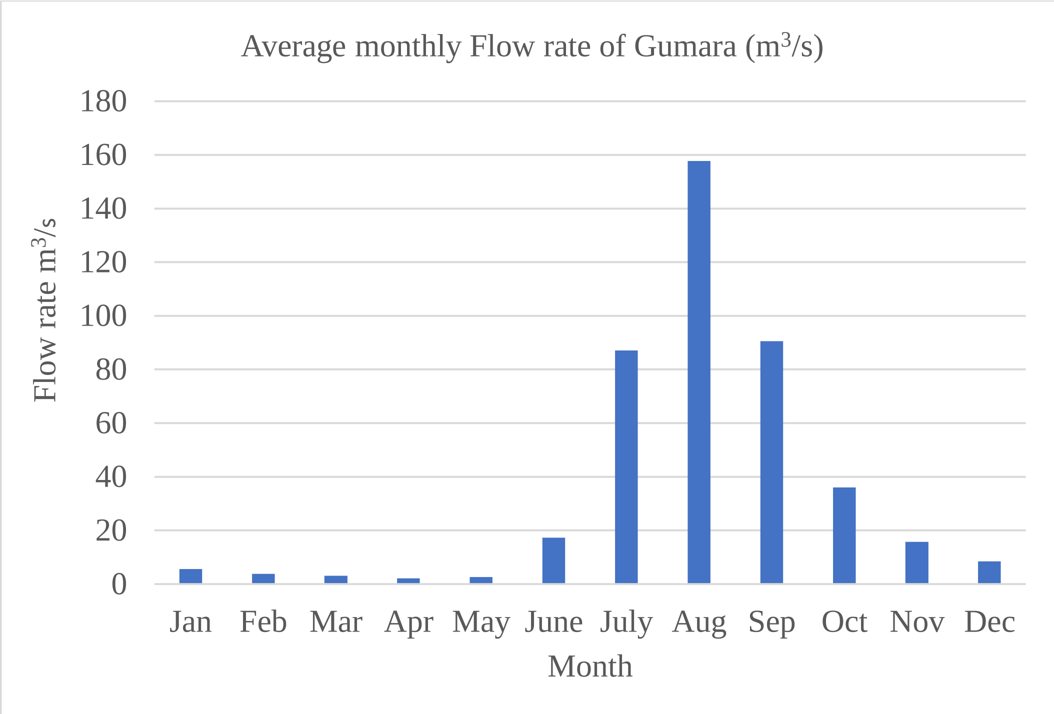

Fig. 3. 8: Average flow rate of Gumara river

As it is seen from the Fig. 3.8, the average flow rate of Gumara river from December-May is less than 10 m^3/s, whereas the average flow of this river from Augest More than 150 m^3/s.

Table 3. 7: Ten years monthly stream flow data of Gumara river based on E.C.

	Jan	Feb	Mar	Apr	May	Jun	Jul	Aug	Sep	Oct	Nov	Dec
1990	2.39	0.91	0.61	0.40	0.54	1.31	52.81	180.36	109.28	19.82	4.14	1.93
1991	1.01	0.53	0.38	0.44	0.81	14.22	83.22	168.09	76.81	23.43	4.76	4.79
1992	3.05	2.06	2.74	0.84	1.89	1.98	42.12	158.53	71.12	50.35	14.93	6.34
1993	2.71	1.31	0.70	0.91	2.13	10.37	85.92	140.17	100.44	37.68	11.71	4.74
1994	2.38	1.31	0.61	0.35	1.01	19.35	84.88	194.35	122.47	19.99	7.02	4.14
1995	2.16	1.67	1.48	1.40	1.56	4.99	61.61	148.57	98.55	24.95	17.02	12.74
1996	7.46	3.59	3.37	3.40	7.99	56.43	179.08	200.47	101.51	36.94	22.11	15.25
1997	10.78	7.99	6.63	4.97	7.35	48.03	141.98	150.53	79.62	58.90	54.58	16.69
1998	-	-	-	-	1.91	10.80	67.38	138.08	92.61	28.14	8.82	8.70
1999	6.79	1.72	0.75	0.56	0.74	5.00	71.48	97.54	52.79	59.75	13.01	-

There are missing stream flow data in 1998 and 1999 E.C. years. Regression method is selected to fill the missed data.

Table 3. 8: Filled stream flow data of Gumara River based on E.C.

	Jan	Feb	Mar	Apr	May	Jun	Jul	Aug	Sep	Oct	Nov	Dec
1990	2.39	0.91	0.61	0.40	0.54	1.31	52.81	180.36	109.28	19.82	4.14	1.93
1991	1.01	0.53	0.38	0.44	0.81	14.22	83.22	168.09	76.81	23.43	4.76	4.79
1992	3.05	2.06	2.74	0.84	1.89	1.98	42.12	158.53	71.12	50.35	14.93	6.34
1993	2.71	1.31	0.70	0.91	2.13	10.37	85.92	140.17	100.44	37.68	11.71	4.74
1994	2.38	1.31	0.61	0.35	1.01	19.35	84.88	194.35	122.47	19.99	7.02	4.14
1995	2.16	1.67	1.48	1.40	1.56	4.99	61.61	148.57	98.55	24.95	17.02	12.74
1996	7.46	3.59	3.37	3.40	7.99	56.43	179.08	200.47	101.51	36.94	22.11	15.25
1997	10.78	7.99	6.63	4.97	7.35	48.03	141.98	150.53	79.62	58.90	54.58	16.69
1998	17.46	16.84	13.19	8.12	1.91	10.80	67.38	138.08	92.61	28.14	8.82	8.70
1999	6.79	1.72	0.75	0.56	0.74	5.00	71.48	97.54	52.79	59.75	13.01	9.43

By arranging the stream flow discharge in descending order, the percentage of exceedance or equaled are calculated, as shown in Table 3.9.

The exceedance/equaled percent is calculated by using wail bull man formula;

$$\text{exceedance } \% = n/m+1. \quad (3.14)$$

where n = rank and m = 120 observations.

Table 3. 9: Rank and exceedance /equaled percent of Gumara River

Discha.	Rank	excee. %	Discha.	Rank	excee. %	Discha.	Rank	excee. %	Discha.	Rank	excee. %
200.5	1	0.8	54.6	31	25.6	8.8	61	50.4	2.0	91	75.2
194.4	2	1.7	52.8	32	26.4	8.7	62	51.2	1.9	92	76.0
180.4	3	2.5	52.8	33	27.3	8.1	63	52.1	1.9	93	76.9
179.1	4	3.3	50.3	34	28.1	8.0	64	52.9	1.9	94	77.7
168.1	5	4.1	48.0	35	28.9	8.0	65	53.7	1.7	95	78.5
158.5	6	5.0	42.1	36	29.8	7.5	66	54.5	1.7	96	79.3
150.5	7	5.8	37.7	37	30.6	7.4	67	55.4	1.6	97	80.2
148.6	8	6.6	36.9	38	31.4	7.0	68	56.2	1.5	98	81.0
142.0	9	7.4	28.1	39	32.2	6.8	69	57.0	1.4	99	81.8
140.2	10	8.3	24.9	40	33.1	6.6	70	57.9	1.3	100	82.6
138.1	11	9.1	23.4	41	33.9	6.3	71	58.7	1.3	101	83.5
122.5	12	9.9	22.1	42	34.7	5.0	72	59.5	1.3	102	84.3
109.3	13	10.7	20.0	43	35.5	5.0	73	60.3	1.0	103	85.1
101.5	14	11.6	19.8	44	36.4	5.0	74	61.2	1.0	104	86.0
100.4	15	12.4	19.4	45	37.2	4.8	75	62.0	0.9	105	86.8
98.6	16	13.2	17.5	46	38.0	4.8	76	62.8	0.9	106	87.6
97.5	17	14.0	17.0	47	38.8	4.7	77	63.6	0.8	107	88.4
92.6	18	14.9	16.8	48	39.7	4.1	78	64.5	0.8	108	89.3
85.9	19	15.7	16.7	49	40.5	4.1	79	65.3	0.7	109	90.1
84.9	20	16.5	15.2	50	41.3	3.6	80	66.1	0.7	110	90.9
83.2	21	17.4	14.9	51	42.1	3.4	81	66.9	0.7	111	91.7
79.6	22	18.2	14.2	52	43.0	3.4	82	67.8	0.6	112	92.6
76.8	23	19.0	13.2	53	43.8	3.0	83	68.6	0.6	113	93.4
71.5	24	19.8	13.0	54	44.6	2.7	84	69.4	0.6	114	94.2
71.1	25	20.7	12.7	55	45.5	2.7	85	70.2	0.5	115	95.0
67.4	26	21.5	11.7	56	46.3	2.4	86	71.1	0.5	116	95.9
61.6	27	22.3	10.8	57	47.1	2.4	87	71.9	0.4	117	96.7
59.8	28	23.1	10.8	58	47.9	2.2	88	72.7	0.4	118	97.5
58.9	29	24.0	10.4	59	48.8	2.1	89	73.6	0.4	119	98.3
56.4	30	24.8	9.4	60	49.6	2.1	90	74.4	0.3	120	99.2

Based on the discharge and exceedance percent flow, the duration curve will be generated. Flow duration curve shows the percentage of time that certain values of discharges are equaled or exceeded. The energy output of the scheme is derived from the flow duration curve. Where there are no constraints on the scale of developments, the 30% exceedance flow gives a first estimate for the design capacity for the scheme (H.G. Tolland and E.M. Wilson, 1984).

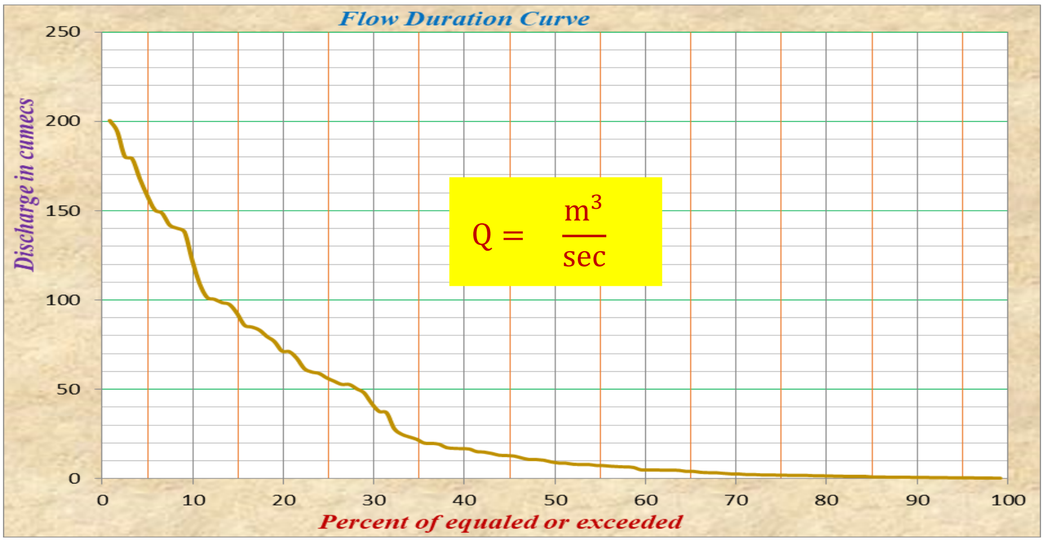

Fig. 3. 9: Flow duration curve of Gumara river

Fig. 3. 10: Watershed of specific project

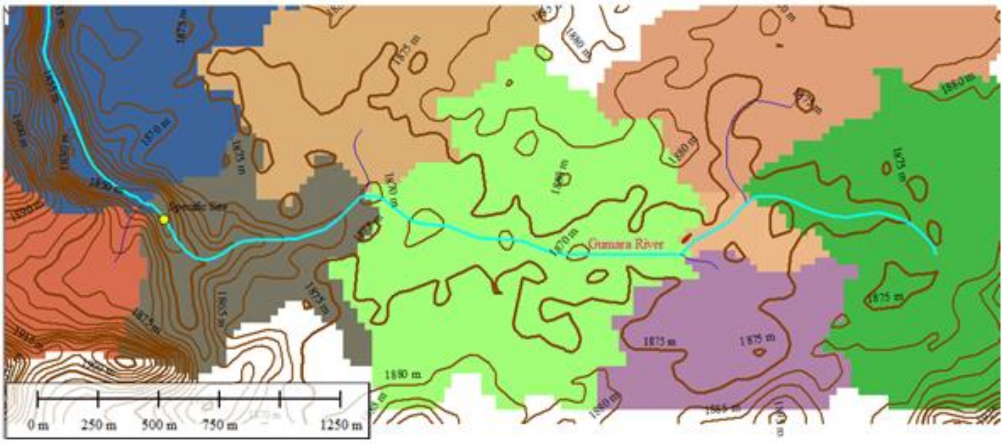

Fig. 3. 11: Contour map of specific project

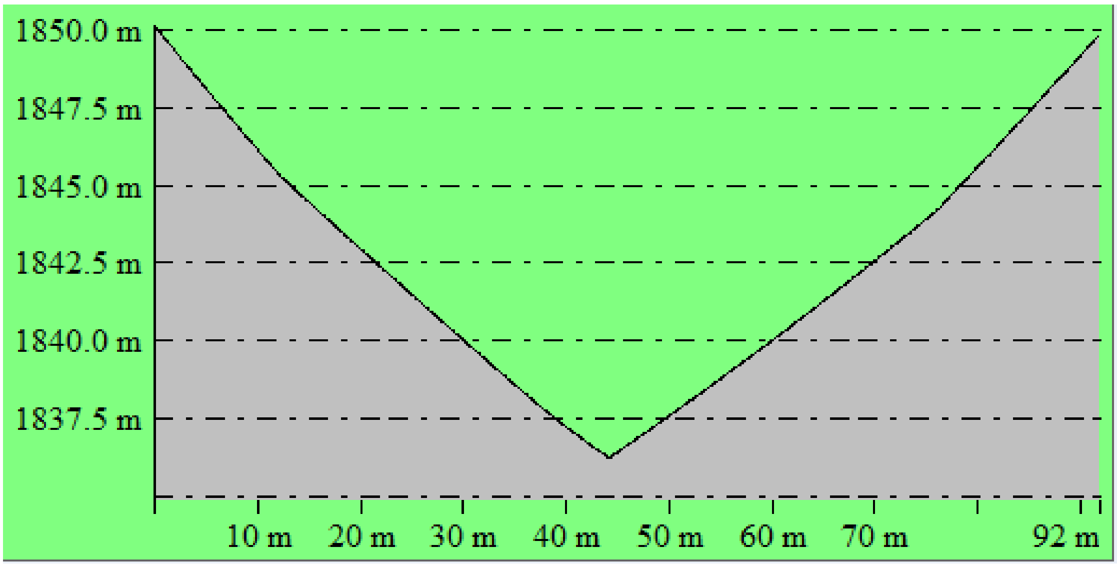

Fig. 3. 12: Path profile of project area

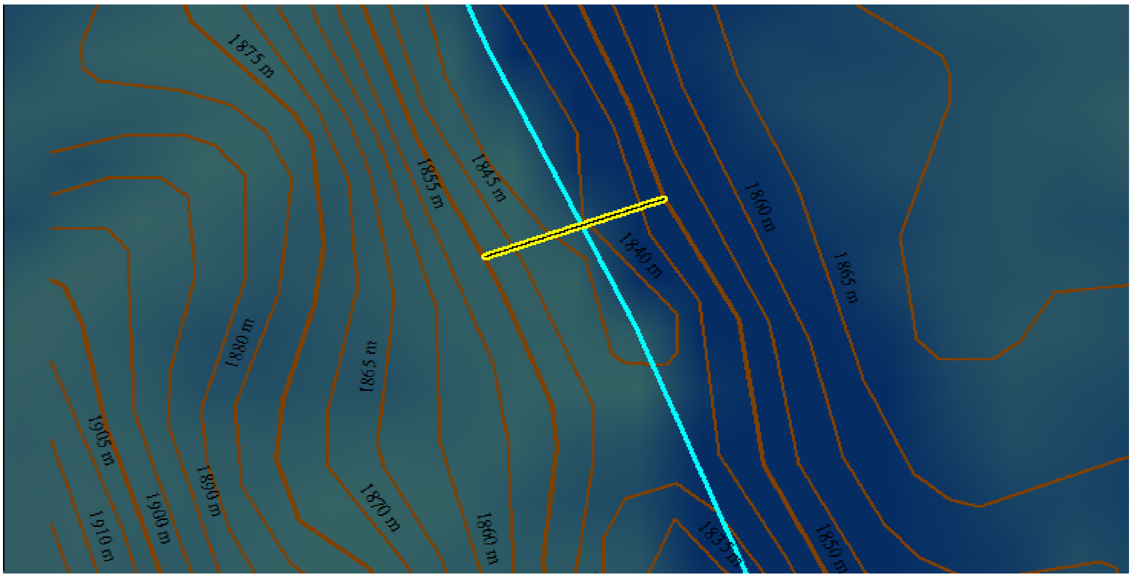

Fig. 3. 13: Specific site

3.4.4. Biomass Energy Resource Assessment

The annual Rice production is shown in Table 3.10 and which was taken from Fogera Wereda Rice Office. Total average annual Rice production of Fogera Wereda after 20 years is 53,3194.36 metric tons per year. If the Rice seed to Rice husk ratio is 75%: 25% 39,895.77metric tons of Rice seed and 13,298.59 metric ton of rice husk has been produced from 53,194.36 metric ton rice green (Rice eshete).

Table 3. 10: Bio-mass energy resource assessment

Year(E.C)	Total production in metric.tons
1990	50660
1991	47805.6
1992	60293.6
1993	61082
1994	73208.32
1995	73768
1996	46744
1997	80876
1998	52052
1999	59114
2000	54465.2
2001	82362.4
2002	62869.2
2003	43061.2
2004	34344
2005	26344
2006	17460
2007	52072
2008	48072
2009	44072
2010	46356
Av. yearly production	53194.36

If 2% of rice husk produced is assumed to be wasted and 8% of rice husk is considered useful for compost and other applications and the rest 90% (11,968.731 metric tons) of the produced husk is dumped (thrown) without any economic environment. Approximately 33.246 metric tons of husk (waste) per day is given to environment. But, the Rice husk (waste) is intended to be used for generating energy rather than polluting the environment.

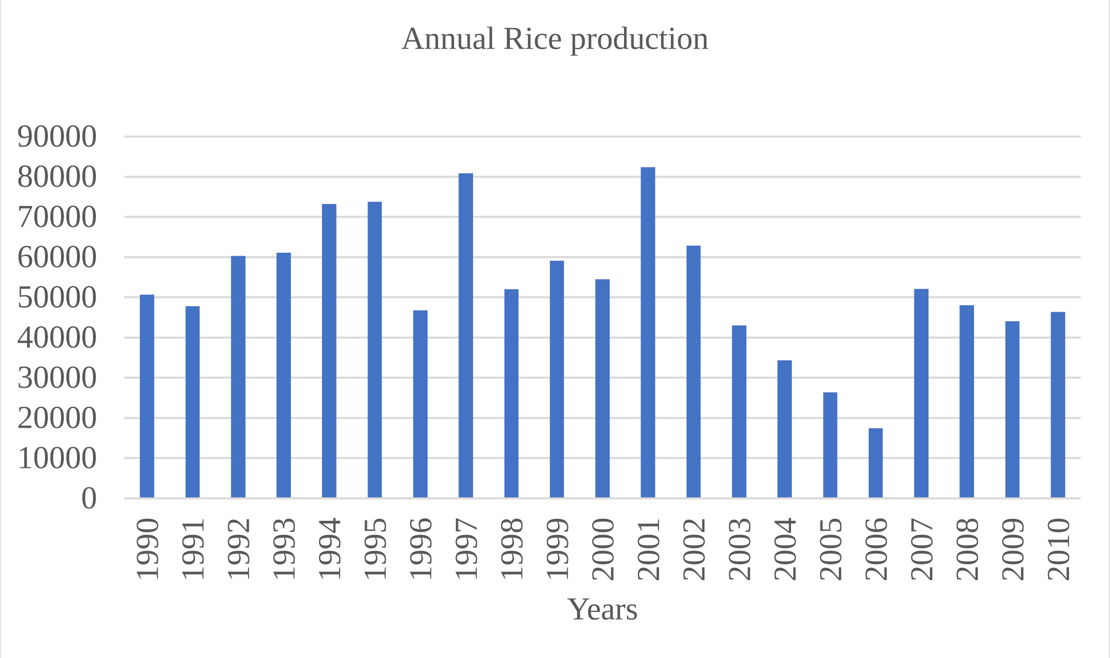

Fig. 3. 14: Average yearly Rice seed production

3.5. Mathematical Cost Model of Energy Systems

This work developed a mathematical model of a system that could deploy the best renewable energy options available at any base station located in any part of a country in the world; where the term Best represents the integral (total sum) of the minimum economic and environmental (health and safety) costs of the considered options.

The Annualized Cost of a Component. - The annualized cost of a component includes annualized capital cost, annualized replacement cost, annual operation and maintenance (O&M) cost and emissions cost. Operation cost is calculated hourly on daily basis. **Annualized Capital Cost. -** The annualized capital cost of a system component is equal to the total initial capital cost multiplied by the capital recovery factor. Annualized capital cost is calculated by using:

$$C_{cap} = C_{cap} \times CRF(i, R_{PROj}) \quad (3.15)$$

where, Cacap – is annualized capital cost, CRF (i, Rproj) – is capital recovery factor, i – is interest rate, Rproj – is project lifetime, Ccap – is initial capital cost of the component

Annualized Replacement Cost. - The annualized replacement cost of a system component is the annualized value of all the replacement costs occurring throughout the lifetime of the project minus the salvage value at the end of the project lifetime. Annualized replacement cost, Carep is calculated by using:

$$C_{arep} = C_{rep} \times f_{rep} \times SFF(i, Rcomp) - S \times SFF(i, Rproj) \quad (3.16)$$

where, Crep – is replacement cost of the component, SFF – is sinking fund factor, Rcomp – is lifetime of the component, S – is salvaged value of the component, frep – is replacement factor, frep, a factor arising because the component lifetime can be different from the project lifetime, is given by:

$$f_{rep=\frac{CRF(i,R_{proj}}{CRF(i,Rrep)}} \left| R_{rep} > 0, R_{rep=0} \right. \quad (3.17)$$

where Rrep-is replacement cost duration which is given as

$$R_{rep} = Rcomp \times INT(\frac{R_{porj}}{Rcomp}) \quad (3.18)$$

where, INT () is the integer function, returning the integer portion of a real value. SFF (), the sinking fund factor is a ratio used to calculate the future value of a series of equal annual cash flows, is given by

$$SFF(i, N) = \frac{i}{(1+i)^{N-1}} \quad (3.19)$$

where, *N* = number of years

The salvaged value of the component at the end of the project lifetime is proportional to its remaining life. Therefore, the salvage value *S* is given by:

$$S = C_{rep} \times \frac{R_{rem}}{R_{comn}} \quad (3.20)$$

where Rrem- is remaining life of the component

The remaining life of the component, Rrem at the end of the project lifetime is given by:

$$R_{rem=R_{Comp}} - (Rproj - Rrep) \quad (3.21)$$

Annualized Operating Cost (Caop**). -** The operating cost is the annualized value of all costs and revenues other than initial capital costs and is calculated by using:

$$\left[Caop = \sum_{t=1}^{365} \{ \ \sum_{t=1}^{24} \left[\left(Coc(t) \right) \ \right] \ \} \quad (3.22)$$

where, Coc(t)- is the cost of operating component. Total cost of component =Economic cost+ Environmental cost

Where, Economic cost=Capital cost+ Replacement cost +O&M cost, Environmental cost =Emission cost=0, Annualized cost of a component is calculated using:

Cann = Cacap + Carep + Caop + Cemissions = Cacap + Carep + Caop (3.23)

Annualized total cost of a component is calculated using:

$$\mathrm{Cann,tot,c} = \sum_{c=1}^{Nc}(\mathrm{Cacap,c} + \mathrm{Carep,c} + \mathrm{Caop,c}) \quad (3.24)$$

where, Cann, tot, c – is Annualized capital cost of a component, Caop, c – is Annualized operating cost of a component, Carep, c – is Annualized replacement cost of a component. From Equation (3.24), the Economic and Environmental cost model through annualized total cost of different configuration of power system were derived as follows: Economic and environmental cost model of running Solar power only is calculated as:

$$\mathrm{Cann,tot,s} = \sum_{S=1}^{Ns}(\mathrm{Cacap,s} + \mathrm{Carep,s} + \mathrm{Caop,s} + \mathrm{Cemissions}) \quad (3.25)$$

where Cacap, s is annualized Capital Cost of solar power, Carep, s -is annualized replacement cost of solar power, Caop, s-is annualized operating cost of solar power. Economic and environmental cost model of running micro-hydropower only is calculated as:

$$\mathrm{Cann,tot,mhp} = (\mathrm{Cacap,mhp} + \mathrm{Carep,mhp} + \mathrm{Caop,mhp} + \mathrm{Cemissions}) \quad (3.26)$$

where, Cacap, mhp- is annualized capital cost of micro hydropower, Carep, mhp -is annualized replacement cost of micro hydro power, Caop, mhp-is annualized operating cost of micro hydro power.

Economic and Environmental cost model of running Bio-mass power only is calculated as:

$$\mathrm{Cann,tot,bio} = \sum_{bio=1}^{Nbio}(\mathrm{Cacap,bio} + \mathrm{Carep,bio} + \mathrm{Caop,bio} + \mathrm{Cemissions}) \quad (3.27)$$

$$\mathrm{Cann,tot,b} = \sum_{b=1}^{Nb}(\mathrm{Cacap,b} + \mathrm{Carep,b} + \mathrm{Caop,b} + \mathrm{Cemissions}) \quad (3.28)$$

where, Cacap, bio- is annualized capital cost of biomass hydropower, Carep, bio -is annualized replacement cost of biomass power, Caop, bio-is annualized operating cost of Biomass power. economic and environmental cost model of running batteries is calculated as:

where, Cacap, b- is annualized capital cost of batteries power, Carep, b -is annualized replacement cost of batteries power, Caop, b-is annualized operating cost of batteries power.

Economic and Environmental cost model of running converter is calculated as:

$$\mathrm{Cann,tot,c} = \sum_{c=1}^{Nc}(\mathrm{Cacap,c} + \mathrm{Carep,c} + \mathrm{Caop,c} + \mathrm{Cemissions}) \quad (3.29)$$

where, Cacap, c- is annualized capital cost of converter power, Carep, c -is annualized replacement cost of converter power, Caop, c-is annualized operating cost of converter power.

Hybridizing the renewable energy generators (PV, Biomass, Micro hydro) results different topologies as:

Economic and environmental cost model of running Solar only + Batteries + Converter is calculated as:

$$\text{Cann, tot, s} + \text{mhp} + \text{Bio} + \text{c} + \text{b} = \sum_{S=1}^{Ns} (\text{cacap, s} + \text{Crep, s} + \text{Cemission}) \qquad (3.30)$$

$$+ = \sum_{c=1}^{Nc} (\text{cacap, c} + \text{Crep, c} + \text{Cemission})$$

$$+ = \sum_{b=1}^{Nb} (\text{cacap, b} + \text{Crep, b} + \text{Cemissions})$$

Economic and environmental cost model of running Hybrid (Micro hydro, biomass and Solar) +Batteries+ Converter calculated as:

$$\text{Cann, tot, s} + \text{mhp} + \text{Bio} + \text{c} + \text{b} \qquad (3.31)$$

$$= \sum_{S=1}^{Ns} (\text{cacap, s} + \text{Crep, s} + \text{Cemission})$$

$$+ \sum\nolimits_{M=1}^{Mhp} (\text{Cacap, mhp} + \text{Carep, mhp} + \text{Caop, mhp} + \text{Cemissions})$$

$$+ = \sum\nolimits_{bio=1}^{Nbio} (\text{Cacap, bio} + \text{Carep, bio} + \text{Caop, bio} + \text{Cemissions})$$

$$+ \sum\nolimits_{b=1}^{Nb} (\text{Cacap, b} + \text{Carep, b} + \text{Caop, b} + \text{Cemissions})$$

$$+ \sum\nolimits_{c=1}^{Nc} (\text{Cacap, c} + \text{Carep, c} + \text{Caop, c} + \text{Cemissions})$$

The mathematical model derived estimates the life-cycle cost of the system, which is the total cost of installing and operating the system over its lifetime.

3.6. The Energy Optimization Model

The process of optimization had been of concern for man for many ages. Previously there were no defined and scientific rules for optimum conditions. But with the passage of time and advancement in science and technology, everything was considered to be based on certain reasons or logics. Mathematical calculations involving process of optimization have become more famous in recent years. True meaning of optimization is to find the best answer for a particular problem. For example, problems dealing with the cost will require the best cost to be as less as possible. On the other hand, problems dealing with profit will see the maximum value as the best answer. So ‘Optimum’ is the word which is used to demonstrate the meaning of best, and the process of finding the best solution to a particular problem is known as the process of optimization. To solve an optimization problem, we require an optimization algorithm. An optimization algorithm is the algorithm which is used to define an optimized solution for a particular function. Thus, for the stand-alone Micro hydro, solar and Bio-mass hybrid system with constraints under study, we have the following optimization algorithm.

Minimize

$$\text{Cost} = \sum_{i} C_{mhpi} N_{mhpi} + \sum_{j} C_{pvi} N_{pvi} + \sum_{m} C_{bioi} N_{g} + \sum_{n} C_{cn} N_{cn} \tag{3.32}$$

Subject to the constraints

$$\text{Load} \leq \sum_{i} E_{mhpi} N_{mhpi} + \sum_{j} E_{pvi} N_{pvi} + \sum_{m} E_{bioi} V_{g} \tag{3.33}$$

$$\text{Maximum power Wattage} \leq \sum_{n} P_{cn} N_{cn}$$

where, C_{mhpi} – is Cost of hydro turbine, C_{pvi} – is Cost of aPV module, C_{Bm} – is Cost of a generator, C_{Cn} – is Cost of a converter, NPVi – is Number of PV modules, NMhp i – is Number of hydro turbines, NBim-is Number of generators, N_{Cn} – is Number of converters, E_{PVj} – is kWh generated by PV module j, E_{mhpj} – is kWh generated by hydro turbine i, P_{Cn} – is maximum output power of converter.

3.7. Load Sharing of the Hybrid Components

Due to production costs, Energy optimization model, potential availability and other associated advantages Micro hydro power production is preferable to solar power production.

Hybrid Micro hydro, solar, and bio-mass is an efficient system of producing energy especially in Benti village. In this thesis work it is considered 50% of the power demand which is around 60 kW is to be produced from micro hydro, and 30% of the load demand which is around 36 kW is to be produced from solar panels, and the rest 20% of the load demand which is around 24 kW is to be produced from Biomass technology illustrated Fig. 3.15.

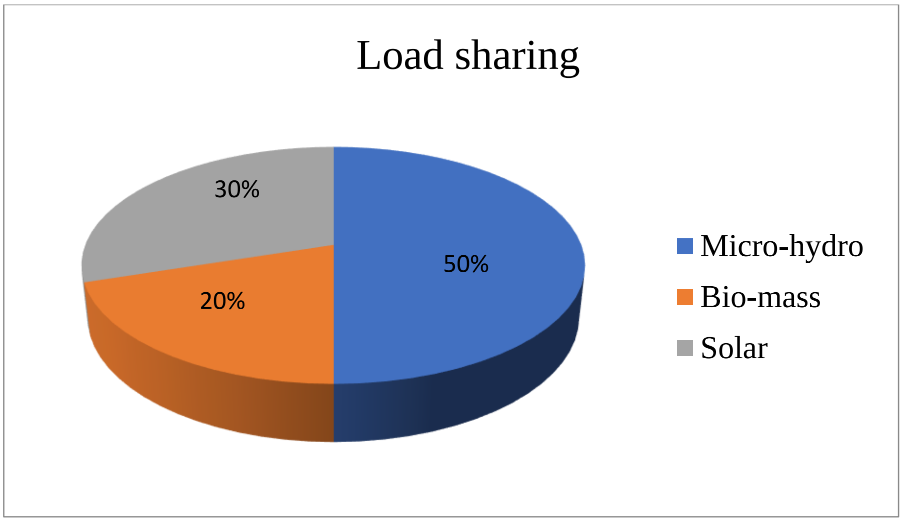

Fig. 3. 15: Load sharing among the hybrid components

The first step in designing a solar PV after analyzing the availability of solar energy resource is to find out the total power and energy consumption of all loads that need to be supplied by the solar PV system, and the next step is size of the PV modules, because different size of PV modules will produce different amount of power to find out sizing of PV module, the total peak power to be produced is needed, and this depends on the size of the PV module and climate of the site location, and in this selected site the power demand to be produced from the solar PV module is around 36 kW (considering 10% of system loss), the last step is to decide the number of PV modules, area of the total panels, and to determine the capacity of power converters. The power to be generated from the biomass technology is about 24 kW considering 10% loss, also the power to be generated from the Micro hydro system is about 60 kW considering 10% loss.

Table 3. 11: Shows the five years average daily sunshine hours in each month for the site under study.

Year	Jan	Feb	Mar	Apr	May	Jun	Jul	Aug	Sep	Oct	Nov	Dec
2018	9	9.4	8.1	8.9.2	8.6	6.2	4.3	3.4	7.5	7.5	7.8	8.5
2017	8.9	9.6	8.2	8.9	8.5	6.4	4.5	5.4	6.2	8.7	6.7	8.5
2016	8	10.2	6.3	7.9	5.8	6.7	4.8	4.6	6.2	8.2	7.5	9.1
2015	7.9	8.7	7.2	6.1	6.4	6.1	3	2.9	6.2	7.8	7.5	8.1
2014	9.6	7.9	7.2	8.5	7.9	6.3	3.4	4.6	6.4	6.5	8	7.8
Daily Average hrs. (S)	8.68	9.16	7.4	8.12	7.44	6.34	4	4.18	6.5	7.74	7.5	8.4

The most common solar energy resource data collected in many of the meteorological stations (NMSA) throughout the country is the average daily sunshine hours. The available sunshine hour data from the National Meteorological Agency of Ethiopia (Debretabor branch) was used to estimate the solar radiation energy of the sites.

As it is seen on the Table 3.11 the maximum average sunshine hour is occurred during November, December, January, February and the minimum average sunshine hour occurred during June, July, August and September.

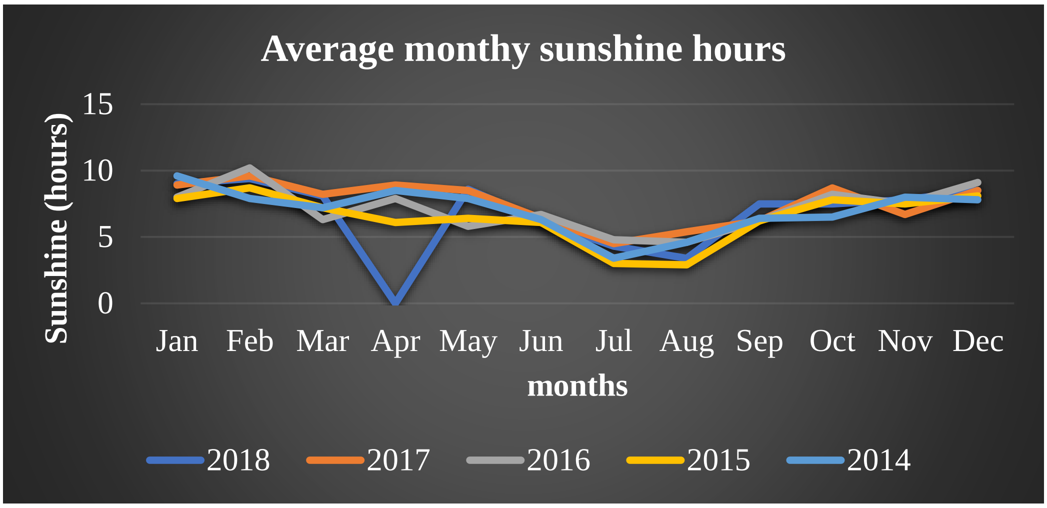

Fig. 3. 16: Average sunshine hours

3.8. Sizing of the Hybrid System Components

3.8.1. PV System Designing

Solar PV system includes different components that should be selected according to the system type, site location and applications. The major components for solar PV system are PV module, inverter, and loads (appliances) with off-grid. The first step in designing a solar PV system is to find out the total power or energy consumption of all loads that need to be supplied by the solar PV system [62].

The total electrical power demand of Benti Village for the year 2030G.c was 120 kW. 30% of the total power demand was covered by, (0.3 x 120 kW= 36 kW), solar PV system. Assuming the system power loss was 10%, system loss= 36*0.1=3.6 kW. The total power generation capacity of the solar PV system is 40 kW. The second step is sizing the solar PV system components, the number of PV module, area of total panels, and determining capacity of power converter or inverter. To calculate number of parallel strings assumed (system voltage is 12V (V_m), a string with 4 modules (N_s), rated solar power is 325W(P_m) module). The following empirical formula can be used [62].

Average daily solar radiation= 4 kW/m^2/day [62].

Step 1: Calculation of radiation

PSH: Peak solar hours (hours @1 kW/m^2 = kW/m^2/day)

Worst month: PSH = 4h/day

Step 2: Calculation of installed power

$$\text{POWER} \times \text{TIME} = 40\text{kW} \times 4\text{kW} / \text{M}^2 / \text{Day} = 160\text{kWh} \tag{3.34}$$

$$P_{pv} = \frac{\text{Load}}{\text{Efficiency}} = \frac{160}{0.69}\text{kW} / \text{day} = 231.88\text{kWh} / \text{day} \tag{3.35}$$

$$P_{peak} = \frac{231.88\text{kWh} / \text{day}}{\text{PSH}(4\text{kW} / \text{m}^2 / \text{day}} = 57.97\text{kWp} \tag{3.36}$$

Step 2: Calculation of string length, from the module voltage, V_m (assume 12V: string with 4 modules) used higher standard voltage for reducing losses.

$$\frac{V_{DC}}{V_m} = N_s = \frac{48}{12} = 4 \tag{3.37}$$

Step 3: Calculation number of strings (assume 325Wp module)

$$N_p = \frac{P_{peak}}{P_m \times N_s} = \frac{57.97\text{kW}}{325 \times 4} \tag{3.38}$$

Step 4: Calculation total number of modules,

$$\text{Total Module} = N_s * N_p = 45*4 = 180 \tag{3.39}$$

Assume a single solar module having 0.4m^2 cross sectional area, the total area required for solar panel is can be calculated as follows [62].

$$A_p = N * A_m = 180*0.4\text{m}^2 = 72\text{m}^2 \tag{3.40}$$

3.8.1.1. Sizing of the Inverter

The size of the inverter is determined by the AC load and consideration for surge power. Inverter size should be 25-30% bigger than the total watts of the loads. Maximum AC load is 40 kW, inverter constant is 1.25. Therefore, Inverter rating is AC x 1.25 = 40 kW*1.25 = 50 kW. Available inverter size was 100, 150, 200, 250kW. The chosen converter size for this thesis was a capacity of 100kW and the full load efficiency were greater than 90% [10].

3.8.1.2. PV Subsystem Model

The equivalent circuit for the solar module arranged in NP parallel and NS series is shown in Fig. 3.17.

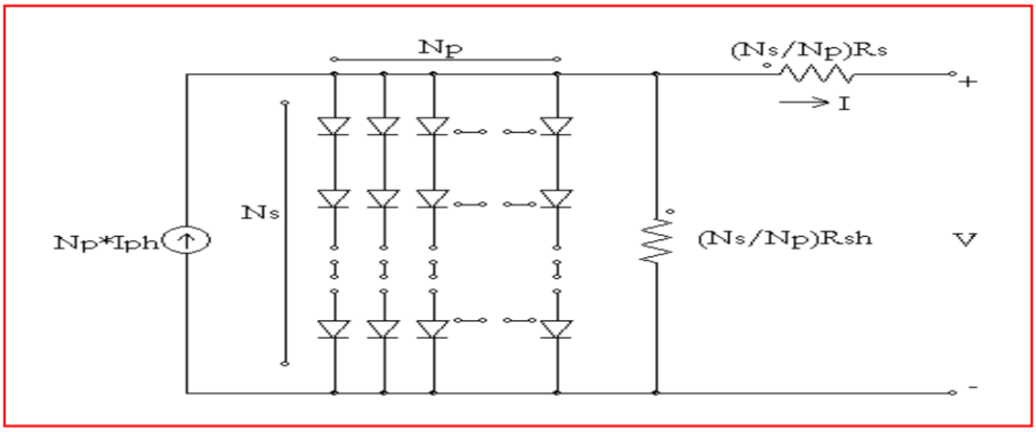

Fig. 3. 17 : Circuit model of a generalized PV array [9]

The terminal equation for the current and voltage of the array becomes expressed in Equation (3.20) as stated in [46], [47], and [48].

$$I = NpI_{PH-}N_pI_S[\exp[q[\frac{V}{N_s}+\frac{IR_s}{N_p}]/KT_ca-1]-\frac{N_PV}{N_S}+IR_s/R_{sh} \qquad (3.41)$$

where: I_{PH} is a light generated current or photocurrent, Is the cell saturation of dark current, q (= 1.6 $\times 10^{-19}$C) is an electron charge, K (= 1.38 $\times 10^{-23}$J/K) is a Boltzmann's constant, T_C is the cell's working temperature, a is an ideal factor, R_{SH} is a shunt resistance, and R_S is a series resistance. The photocurrent mainly depends on the solar insolation and cell's working temperature, which is described as:

$$I_{PH} = (I_{sc} + k_I(T_C - T_{Ref}))\lambda \qquad (3.42)$$

Where: I_{SC} is the modules short-circuit current at a 25°C (T_{Ref}) and 1kW/m^2, K_I is the cells short-circuit current temperature coefficient, T_{Ref} is the cell's reference temperature, and λ is the solar insolation in kW/m^2.

$$T_c = T_{air} + \frac{NoCT-20}{80}s \qquad (3.43)$$

S = insolation in mW/cm^2. (With T_{air} = 20.1^{o}C, NOCT = 47^{o}C and S =80 mW/cm^2), T_c is calculated as 47.1^{o}C. S = insolation in MW/cm^2. (With T_{air} = 20.1^{o}C, NOCT = 47.9^{o}C and

S =80 mW/cm^2), Tc is calculated as 49.1^{o}C. In order to know the values of N_p and N_s, the solar module has been selected. For a typical module cell, R_S = 0.05 to 0.10 ohm and R_{SH} = 200 to 300 ohms [48]. Therefore, for this study the average value of each, that is, R_S = 0.075 and R_{SH} = 250 is used.

The MATLAB Simulink model of PV system is shown in Fig. 3. 18

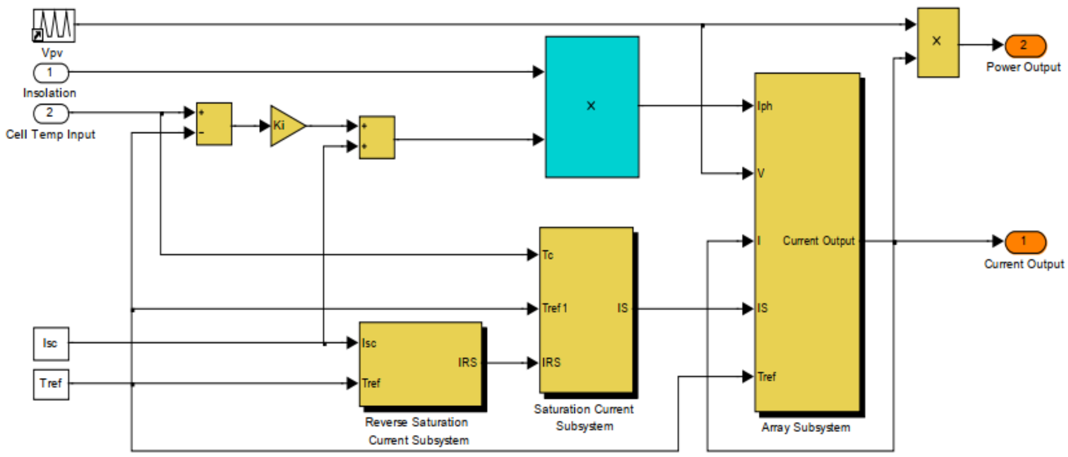

Fig. 3. 18: Model of PV system

On the other hand, the cell's saturation current varies with the cell temperature, which is described as [50]:

$$I_s = I_{RS}(\frac{T_C}{T_{Ref}})^3 \exp[qE_g(\frac{1}{T_{Ref}} - \frac{1}{T_c})/k_a] \qquad (3.44)$$

Where: I_{RS} is the cell's reverse saturation current at a reference temperature and a solar radiation and E_g is the band gap energy (an energy range in a solid where no electron states can exist and itis equal to 1.11 for Silicon semiconductor [48]) of the semiconductor used in the cell. The ideal factor a is dependent on PV technology and 1.3 is used for multi crystal solar module in this study from [48]. The MATLAB Simulink model of saturation current subsystem is shown in Fig. 3. 19

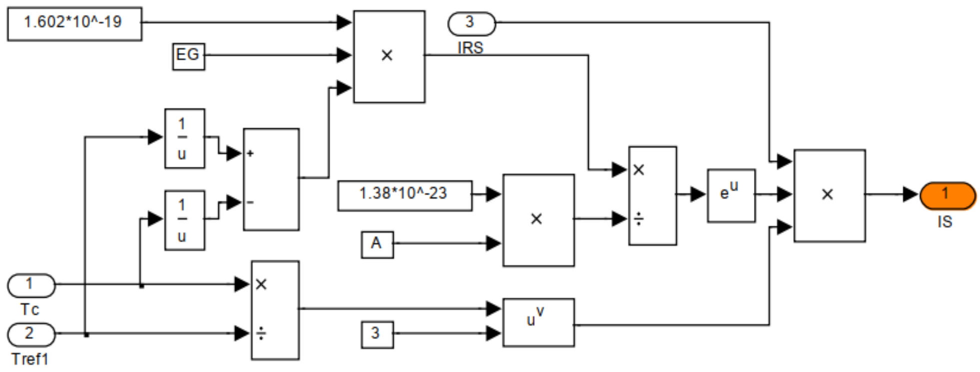

Fig. 3. 19: Expanded view of saturation current subsystem

Given the PV open-circuit voltage, V_{OC}, at reference temperature and ignoring the shunt leakage current, the reverse saturation current at reference temperature can be approximately obtained as [48]

$$I_{RS}=I_{sc} / [\exp(\frac{I_{sc}}{qV_{oc} / N_{ska} T_{Ref}}) - 1] \tag{3.45}$$

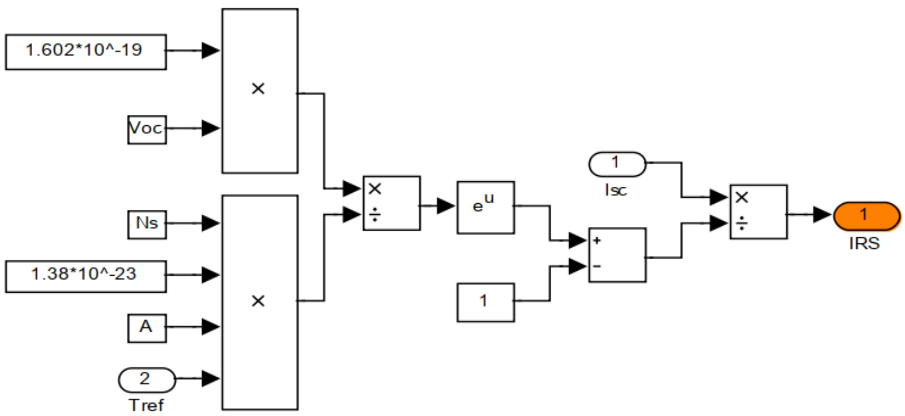

Fig. 3. 20: Expanded view of reverse saturation current mode

The detail of the array subsystem model in the Simulink is given in the Fig.3.21

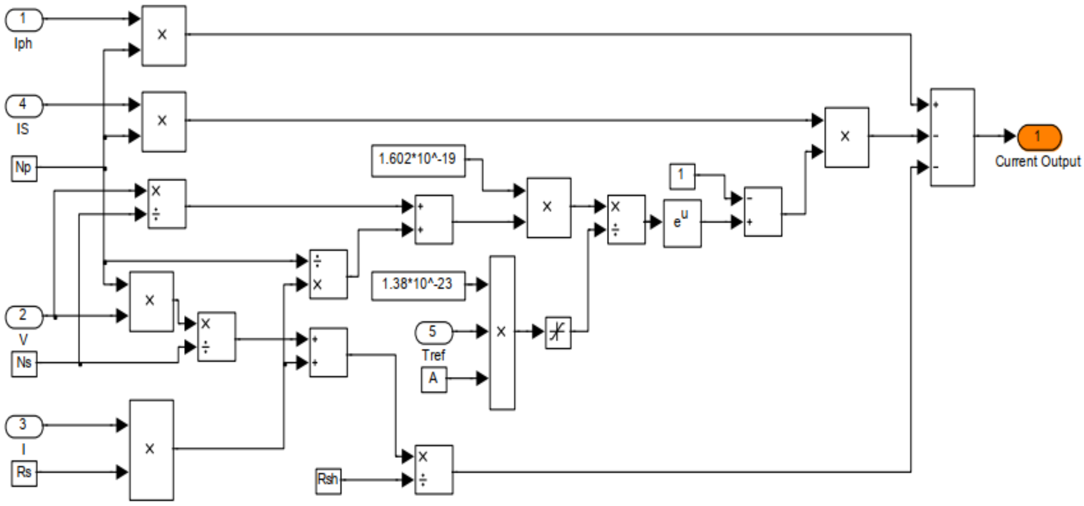

Fig. 3. 21: Expanded view of the array subsystem

For easy simulation, the solar radiation intensity for a sample day is assumed to be of a Gaussian function which is defined as [48]:

$$\lambda(t) = \lambda_{max} \mathrm{Exp}[-\frac{(t - t_c)^2}{2\delta^2})] \quad (3.46)$$

where: λ_{max} is the maximal radiation intensity at a given time, t_c is the center time, and σ is the standard deviation of Gaussian function. Fig. 3.22 shows a plot of the Gaussian function for the solar radiation intensity of a sample day for different months generated from the given monthly average radiation data (in $kWh/m^2/d$) inputs by HOMER. As the figure clearly shows, the maximum average value of the Gaussian function is 0.8. Hence, with the conditions: λ_{max} = 0.8 kW/m^2, t_c = 12, and σ = 2. A MATLAB/ Simulink model has been developed for simulation as indicated in Fig. 3.24. The output from this model is also indicated in Fig. 3.22 and it is the same as HOMER estimates.

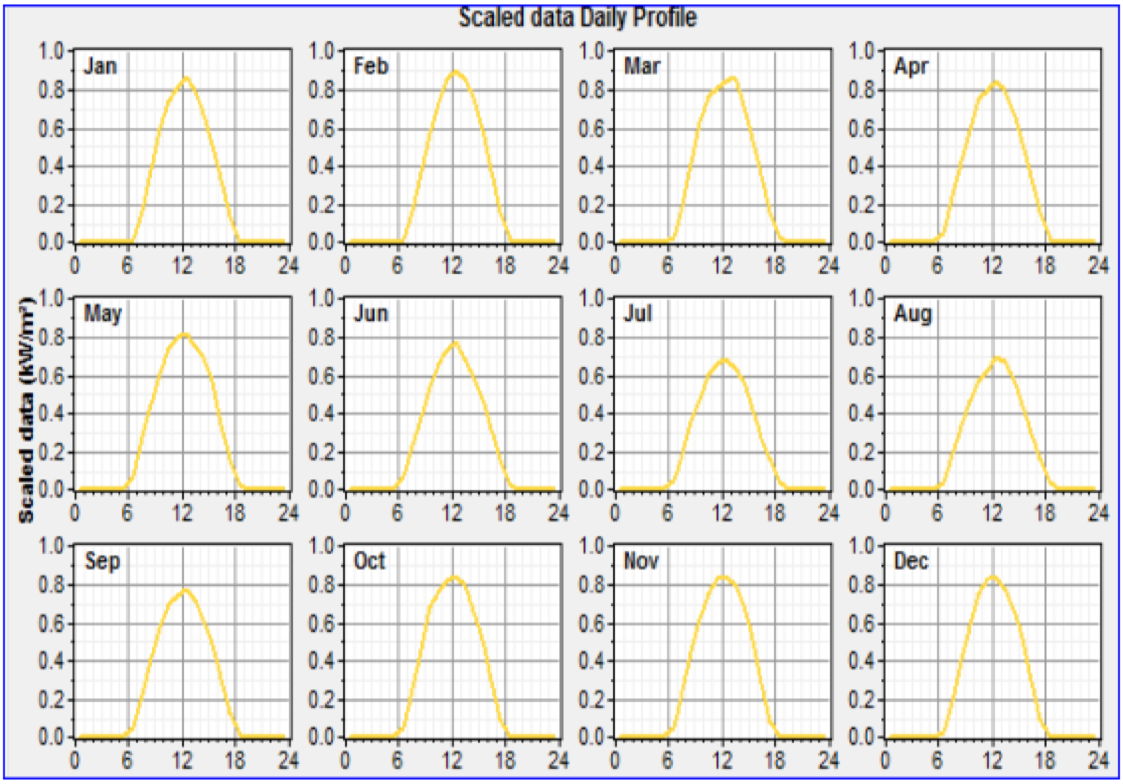

Fig. 3. 22: Scaled data solar insulation's in kW/m^2 in HOMER

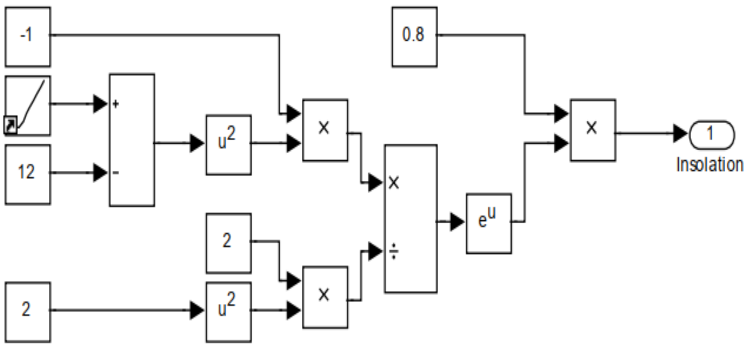

Fig. 3. 23: Expanded view of insolation subsystem model

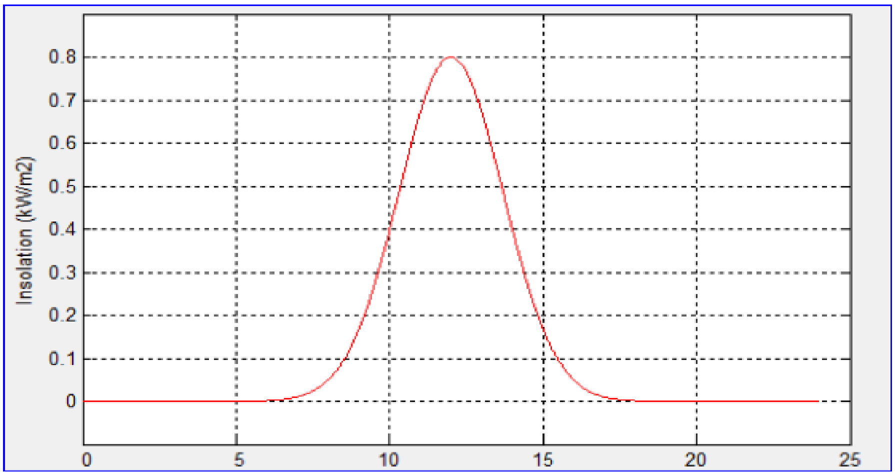

Fig. 3. 24: Insolation input signal generated by the model indicated in Fig. 3.24 (the reader is advised to see the similarity of this and the one indicated in Fig. 3.22)

3.8.2. Micro-Hydro System Designing and Sizing

The total electrical power demand of Benti Village for the year 2030 G.c was calculated as 120 kW. In designing the hybrid power system 50% (60 kW) of the power demand of the village was assumed to be covered by Micro-hydropower system. Assume 10% system loss, 60*0.1=6 kW, Generator capacity = 60+6= 66 kW. It was advisable to take 66 kW. The generating capacity of the Micro-hydro can obtain from equation shown below. Designed parameters were indicated as per hydrological data. H=14 m, assumed 10% head loss, h=0.1*14=12.6 m (The rate is given from hydrological data) designed flow rate =0.9 m^3/s, Efficiency of small turbine = 0.6 [10].

$$P = \eta g Q h = 0.6*9.81*0.9*12.6=66.74KW \tag{3.47}$$

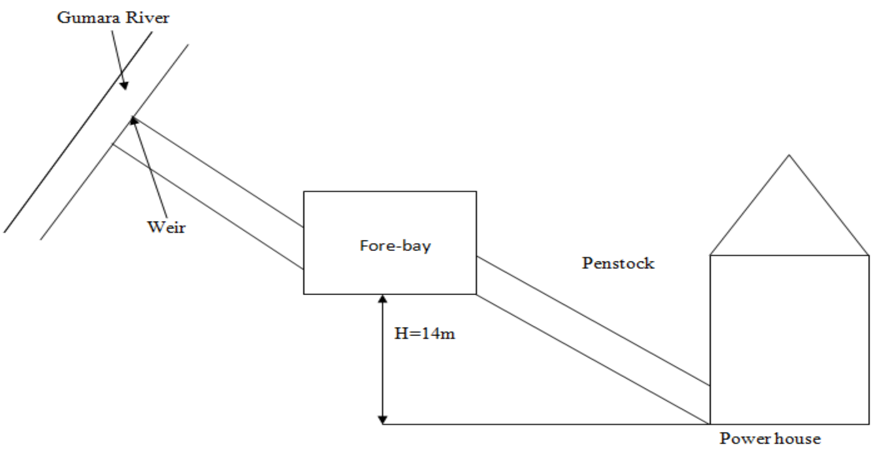

Fig. 3. 25: Micro-hydro structure

1. Weir: - Generally a weir with the crest at a lower level and with some controlling devices is preferred to weirs with high crest level. The reason is that the latter causes excessive afflux when the river is in floods. It's another advantage is that when flood comes, controlling device lower the gates and makes extra space available to discharge the flood quickly.

The Top Width of Weir Wall

Bligh's formula can be used to approximately estimate the top and bottom width of a broad crest weir. However, the dimension values obtained by using the formula should be checked structurally.

$$\text{Top width T in m, } T = \frac{H_e}{\rho - 1} \tag{3.48}$$

Where T is top width of weir wall, H_e is head of water over the weir wall at the minimum flood, ρ is specific gravity of floor material (2.35 for cyclopean concrete, 2.3 for masonry and 2.4 for reinforced concrete). First calculate as what will be the head over the weir when low flood discharge is passing.

$$q = 1.7H^{3\backslash 2} \tag{3.49}$$

where q is the discharge intensity in meter cube per second per meter = $\frac{L}{Q}$,Q = minimum discharge in $\frac{m^3}{s}$ =2.139, L= length of weirs = 92m.

$$q = \frac{2.139\frac{M^3}{S}}{92m} = 0.02325\frac{m^2}{s} \tag{3.50}$$

$$q = 1.7H^{3\backslash 2} \times 0.02325 = H = (\frac{0.03592}{1.7})^{2/3} = 0.057m$$

Now calculating the top width of the weir

$$T' = \frac{H}{\sqrt{\rho - 1}} = \frac{0.057}{\sqrt{2.4 - 1}} = 0.048m$$

2. Canal Sizing

Step 1: calculating the velocity

$$V = (\frac{Qf\,2}{140})^{1/6} \tag{3.51}$$

where Q in $\frac{m^3}{s} = 0.9\frac{m^3}{s}$, V is in m/s, f is silt factor is given by, d_{mm} average particle size in mm, for Benti site the types of soil is sandy, so the average grain size in mm d_{mm} is 0.51mm

$$f = 1.76\sqrt{d_{mm}} = 1.76\sqrt{0.51} = 1.257mm \tag{3.52}$$

$$V = (\frac{Qf^2}{140})^{1/6} = \frac{(0.9 \times 1.257^2)^{1/6}}{140} = 0.465m/s$$

Step 2: Area of canal section

$$A = \frac{Q}{V} = \frac{0.9m^3}{0.465m/s} = 1.93m^2 \tag{3.53}$$

Step 3: The hydraulic mean depth (R),

$$R = \frac{5}{2}\frac{v^2}{f} = \frac{5}{2} \times \frac{0.465^2}{1.257} = 0.43m \tag{3.54}$$

Step 4: Computing the wetted perimeter (P)

$$P = 4.75\sqrt{Q} = 4.75\sqrt{0.9} = 4.5m \tag{3.55}$$

Step 5: Knowing the above values, the canal section is known and finally the bed slope S is determined by the equation.

where, f is the silt factor, Q is the discharge in $\frac{m^3}{s}$

$$S = \frac{f^{5/3}}{3340Q^{1/6}} \tag{3.56}$$

$$S = \frac{1.257^{5/3}}{3340Q^{1/6}} = \frac{1}{3006}$$

So, the bed slope is 1 in 3006

3. Sizing of Penstock

Step 1: Steel penstock diameter is calculated as follows $D_p = 0.72Q^{0.5}$ where Q is flow rate $\frac{m^3}{s}$.

$$D_p = 0.72Q^{0.5} = 0.80 \tag{3.57}$$

$$Q = \frac{0.9m^3}{s}$$

Step 2: Determining the length of penstock, assuming there is only head loss due to friction in penstock (applying the manning formula).

where n is manning coefficient = 0.012. In this thesis work the head loss is assumed = 0.1(10%) x 14m= 1.4m.

$$\text{Head loss} = [10.29n^2 2Q^2 / D^{5.333}p] \times L_p \tag{3.58}$$

$$1.4 = [10.29 \times 0.012^2 \times 0.9^2 / 0.80] \times L_p$$

$$L_p = 154m$$

3.8.2.1. Turbine and Generator Selection

A turbine converts energy in the form of falling water in a rotating shaft power. The selection of best turbine for a particular micro hydro site depends on the site characteristics, the dominant factor is the head available and the power required. Selection also depends on the speed at which it is desired to run the generator or other devices loading the generator. According to the available data propeller turbine was selected from Table (2.3) and (2.5). Propeller turbines are axial-flow reaction turbine, generally used for low heads (usually under 16 m). Three phase synchronous generator was used.

3.8.2.2. Hydro Power Subsystem Model

To determine the hydropower output of a particular site requires two key parameters. These are the stream flow rate and head or vertical distance that the water drops. And also, the magnitude of the hydropower delivered depends mainly on the flow rate and head. The theoretical power output is expressed in the following Equation (3.39).

$$p_{theo} = YQhg \tag{3.59}$$

where, Y=ρg, Ptheo=theoretical power(W), ρ=density of water (kg/m^3), Q=flow rate (m^3/s) and h_g = gross head (m).

Effective Head (h_{ef})

When water flows from the upper elevation to the lower one through medium channels and pipes, there is loss of energy as fractional drag and turbulence. As a result, the gross head

(h_g) will be higher than the net head or effective head (h_{ef}) and the effective Head (h_{ef}) is the difference between the gross head (h_g) and the head loss (h_{loss}).

$$h_{ef} = h_g - h_{loss} \tag{3.60}$$

3.8.2.3. Modelling of Controller

The error in speed is fed as input to the controller and PID controller attempts to reduce the difference between the actual speed and the reference speed by adjusting the constants of the controller. The name derives from three functions involved in calculating the corrections and is accordingly sometimes called three term control: P stands for proportional; I stand for integrator and D stands for derivative [49] controls. These values can be interpreted in terms of time: P depends on the present error, I on the accumulation of past errors, and D is a prediction of future errors, based on current rate of change. The output signal of the PID controller can be written in terms of the error signal.

$$\theta(t) = kpe(t) + ki\int e(t)dt + kd\frac{d\theta(t)}{dt} \tag{3.61}$$

Taking Laplace transform on both sides

$$\theta(s) = kpE(t) + ki\frac{E(s)}{S} + kdsE(s) \tag{3.62}$$

The transfer function of the PID controller is

$$C(s) = \frac{E(s)}{q(s)} = kp + \frac{ki}{s} + k_{ds} \tag{3.63}$$

Here, $\theta(s)$ *is* the output of the PID controller represents position signal

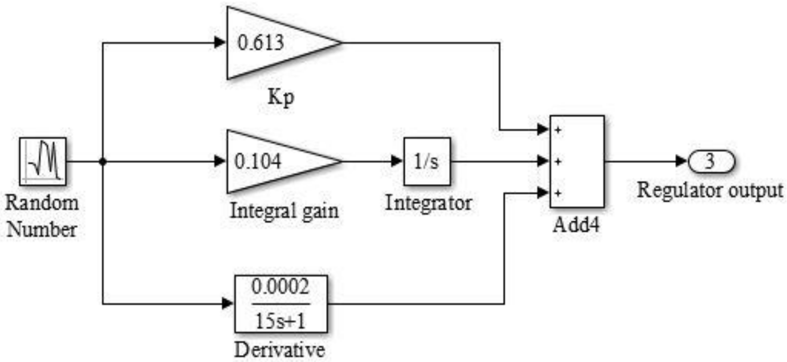

Fig. 3. 26: Simulink model of a controller

3.8.2.4. Modelling of Electro Hydro Servo System

In the model of hydro turbine governor servo motor is used to control the gate valve according to the signal of the controller. The controller nullifies the error in speed signal by sending a signal to the servo motor to control the valve. The torque of the motor is the function of speed and error signal.

$$T_m = f(\theta, e) \tag{3.64}$$

$$T_m = K_e(t) - f\theta(t) \tag{3.65}$$

where

$$K = \frac{dTm}{de} \text{ and } f = \frac{dTm}{d\theta} \tag{3.66}$$

We know the mechanical relations for the motor is,

$$T_m = J\theta'' + Be' \tag{3.67}$$

where, J and B are friction coefficient and moment of inertia respectively. From Equations (3.61) and (3.63) above

$$K_e(t) - f\theta'(t) = J\theta'' + Be' \tag{3.68}$$

Taking Laplace transformation on both sides, we have

$$\frac{e(s)}{E(s)} = \frac{k}{Js^2 + (B+f)s} = \frac{k}{s(Js + B + f)} = \frac{k}{s(t_{as} + 1)} \tag{3.69}$$

where $ka = \frac{k}{B+f}$ and $t_a = \frac{J}{B+F}$ are gain and time constant respectively.

A servo motor controls the gate opening position according to change in speed at shaft of the generator to maintain the constant speed/frequency [50]. Here, the change in speed of the generator acts as the control signal [51]. Equation (3.65) is the required transfer function to develop the complete block diagram of the hydro-electric servo system (Fig. 3.27).

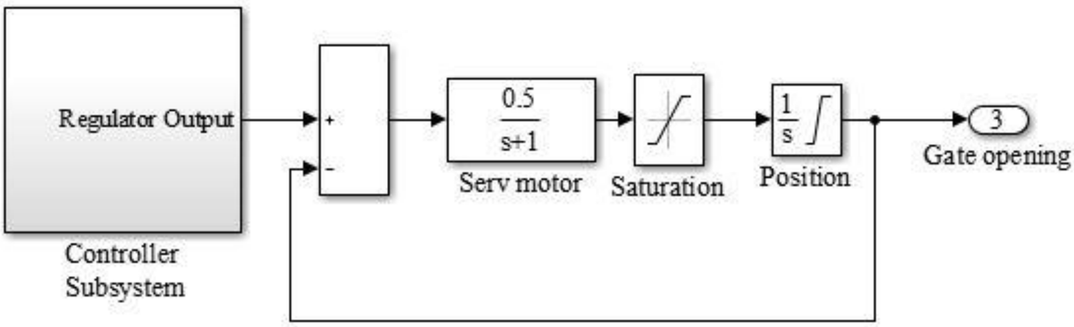

Fig. 3. 27: Model of hydro-electric servo system

3.8.2.5. Modelling of Hydraulic Turbine

This section deals with the equations describing variation in flow and developed mechanical power with respect to the turbine speed, gate opening, and runner blade movement of hydro turbine. The output power of turbine is reduced due to fall of pressure across the turbine. As the developed power in the turbine varies with the flow rate, so the system operates or gains the steady state when the flow through the penstock gets constant. The equations related to the transient performance of the hydraulic turbines are based on the following assumptions [51].

- The hydraulic turbine`s blade is considered as smooth i.e. its frictional resistance is neglected. The water hammer on penstock is neglected.
- The fluid is considered as incompressible.
- The velocity of water in penstock varies directly with gate opening.
- The developed output power of turbine is proportional to the product of head and velocity of flow.

Equation (3.66) and (3.67) represents the flow rate and the developed mechanical power at the shaft respectively in terms gate opening of the system and the net head [51].

$$Q = G\sqrt{H} \tag{3.70}$$

where Q is flow rate in m^3/sec, G is gate opening in rad, H is net head in meter. The developed power, P_m in turbine can be written as

$$P_m = A_t H(Q - Q_{nl} \tag{3.71}$$

where A_t turbine gain, $A_t = \frac{1}{g_{f1} - g_{nl}} Q_{nl}$ is the no load flow rate g_{fl} and g_{nl} are the full load and no-load gate opening. Equation (3.61) is modified to describe the motion of the water in penstock by Equation (3.67).

$$U = KuG\sqrt{H} \tag{3.72}$$

where, U is the velocity of the water in penstock and K is proportional constant. Once the velocity of the water in penstock is determined, the relation of flow rate, head could be established in Equations (3.68) and (3.69).

$$Q = Au \tag{3.73}$$

The acceleration of the fluid in the penstock is described by Equation (3.69) [50].

$$\frac{du}{dt} = \frac{a_g}{L}(H - H_o) \tag{3.74}$$

where, α is the acceleration due gravity, L is the length of penstock. The mechanical power output is given by

$$P_m = p - P_L \tag{3.75}$$

where, P_L is the fixed power loss in turbine due to friction.

$$p_L = U_{NL} H \tag{3.76}$$

where, U_{NL} stands for no load speed. The hydraulic characteristics and mechanical power output of the turbine is modelled here. The nonlinear characteristics of hydraulic turbine are neglected in this model. The complete hydro turbine model is shown in Fig. 3.28. The actuator's (hydro-electric servo motor) output is the gate opening and it controls the valve to maintain a uniform speed by regulating the rate of water flow. The transfer function represented by Equation relates the flow rate Q and net head H. Here (H-H_O) is entered as an input and the flow rate is the output signal of the transfer function. H_O has been assumed a static head with reference value of 1pu.

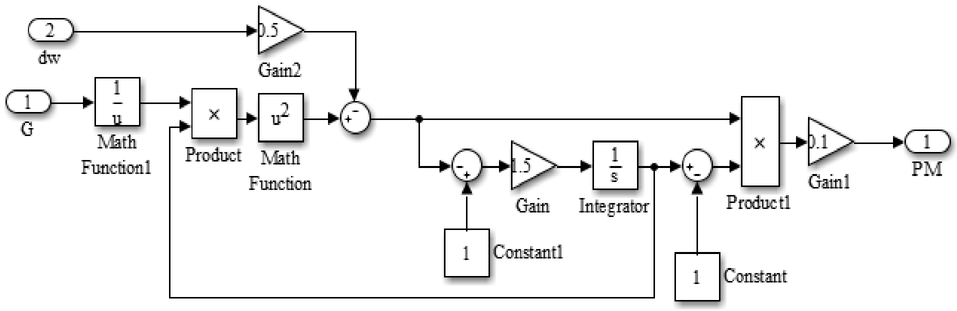

Fig. 3. 28: MATLAB/Simulink model of hydro turbine

3.8.2.6. MATLAB/Simulink Model of Hydro Turbine Governor

Hydro turbine governor is a major part of hydro power plant. It is basically used for two purposes firstly; it develops mechanical power at the shaft of the generator which is fed to the generator for production of electricity. And secondly, it controls the variation of speed of the generator such that the generated frequency remains constant. The PID controller, hydroelectric servo system and hydraulic turbine are the main components of the hydro turbine governor. The mathematical modeling and block formation have been done in the previous section of this chapter. These block model of components are connected in such a manner that the generated frequency remains constant. The block diagram of hydro turbine governor is shown in Fig. 3. 29. Its first element is the PID controller. The error in speed and deviation of power is entire dainty to the controller, which generate the position signal at the input of the hydro-electric servo motor. Further the servo motor response by controlling the valve according to input signal to the servo mechanism. The valve is used to control the flow rate such that the generated frequency of the system remains constant.

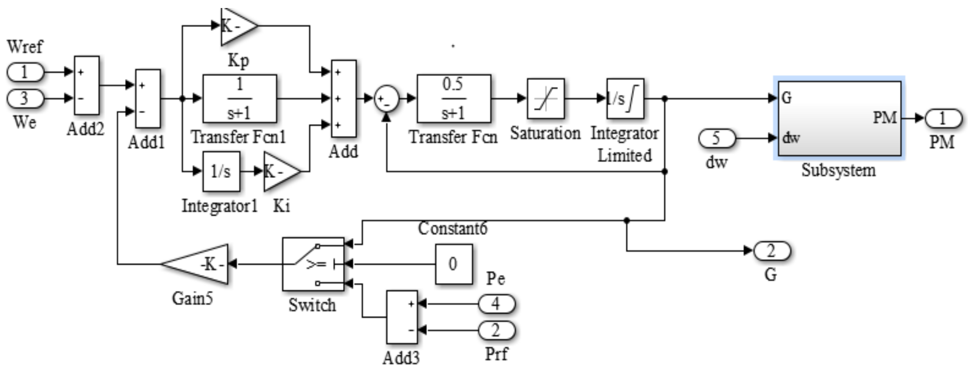

Fig. 3. 29: MATLAB/Simulink model of hydro turbine governor

The mathematical model of a synchronous machine uses Park's equations for the electrical dynamics [52]. Equations (3.72) to (3.76) are here used to model the electrical dynamic soft the synchronous generator [54].

$$T''do\frac{dE''_q}{dt} = E'_q - E''_q + (X'_d - X''_d)I_d \tag{3.77}$$

$$T''qo\frac{dE''_d}{dt} = E'_d - E''_d + (X'_q - X''_q)I_q \tag{3.78}$$

$$T''do\frac{dE''_q}{dt} = E'_f - E''_q + (X_d - X'_d)I_d \tag{3.79}$$

$$T''qo\frac{dE''_q}{dt} = E'_d - E''_q + (X'_q - X''_q)I_q \tag{3.80}$$

$$T''do\frac{dE''_q}{dt} = E'_f - E''_q + (X_d - X''_d)I_d \tag{3.81}$$

$$T''qo\frac{dE''_q}{dt} = E'_d - E''_q + (X'_q - X''_q)I_q \tag{3.82}$$

On the basis of these generalized equations, the synchronous machine model is simulated in MATLAB/Simulink.

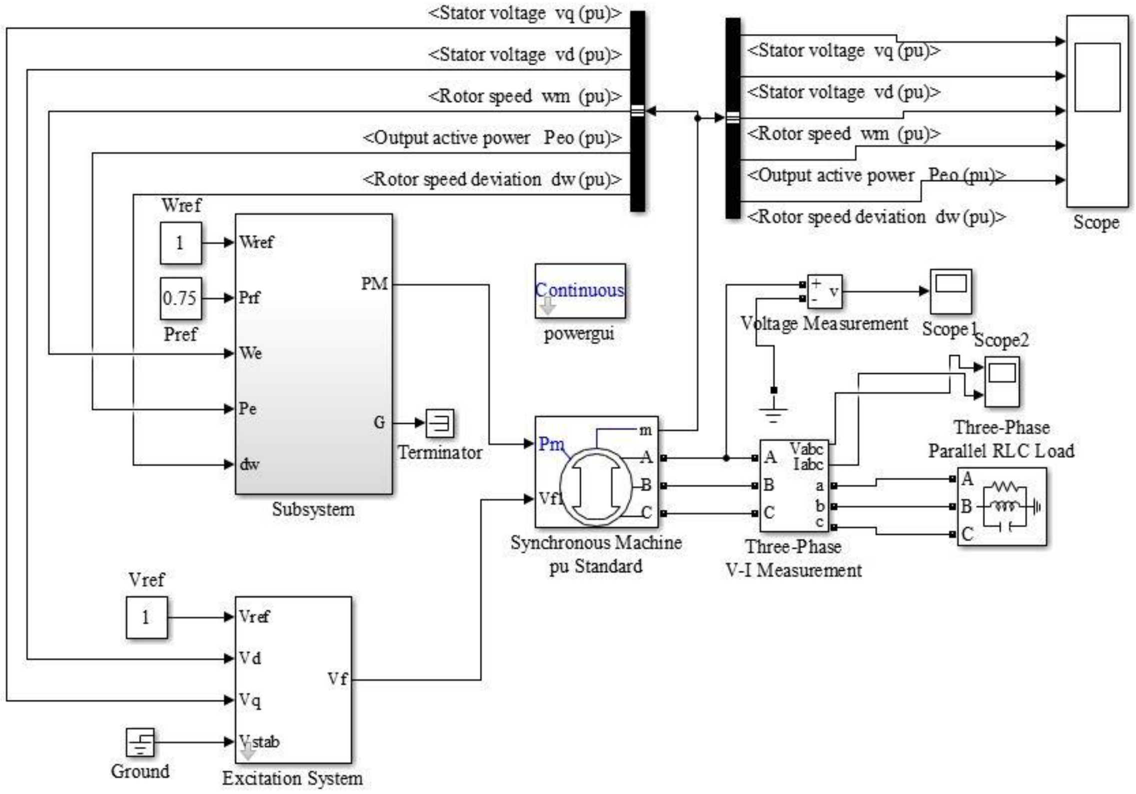

Fig. 3. 30: MATLAB/Simulink model of a hydro power

This model is available as a single block (Fig. 3.30) with various terminals in MATLAB/Simulink library. The model takes into account the dynamics of the stator, field, and damper windings. The individual sub-models like hydro turbine governor, synchronous generator, excitation system and 3-phase RLC load are now connected together to form the complete block diagram of micro hydro power plant.

3.8.3. Bio-Mass System Designing and Sizing

The total Electrical power demand of Benti Village for the year 2030 G.C was calculated as 120KW. In designing the hybrid power system 20% (24 kW) of the power demand of the village was assumed to be covered by Bio-mass power system. 10% of system loss which was 24*0.1=2.4 kW, Generator capacity = 24+2.4= 26.4 kW. Approximately 27 kW. The electrical power generating capacity of the available Rice husk in Benti Wereda was estimated by the following empirical formula [10].

$$p_{\text{Biomass}} = \frac{\text{Efficiency} \times \text{Annual rice husk usge} \dfrac{(\text{metric Tons})}{\text{year}} \times 1000\text{kgs}}{2.5\text{kgs husk / kwh} \times \text{operation hour per day} \times \text{opertion days per year}} \qquad (3.83)$$

The total Rice husk production of Fogera Wereda is 11,968.731 MT/year. Assumed gasification efficiency is 25% [56] and 10% of annual rice husk production, 16 working hours per day, 275 days per year and 2.5 kgs of husk is needed in an hour to produce 1 kW of power [1 Metric tons = 1000kgs]. So, the power generated from Bio-mass is calculated using the following empirical equation.

$$p_{\text{Biomass}} = \frac{10\% \times 11,968.731 \frac{T}{y} \times 1000\text{kgs}}{2.5\text{kgs husk / kWh} \times 16 \times 275} = 27.2\text{kW}$$

3.8.3.1. Gasification Parameters

Knoef et al., (2005) describe gasification parameters, which are the basic and relevant parameters regarding biomass gasification operation, performance, and biomass gasification design.

3.8.3.2. Gas Flow Rate and Gas Production

The power output from the gasification process based on each individual agricultural feedstock is then obtained as: The gasifier's required power output, P (kW), is an important input parameter in which the designer makes a preliminary estimation of the amount of fuel to be fed into the gasifier and the amount of gasifying medium [56]. The volume flow rate of the product gas V_g (Nm^3/s) from its desired lower heating value LHVg (MJ/Nm^3) is found by

$$\text{Gas flow rate } (V_g) = \frac{P}{LHV_g} \text{ Nm}^3/\text{s} \tag{3.84}$$

The composition may be predicted by the equilibrium calculations, or by sophisticated kinetic modelling of the gasifier. The average lower heating value of rice husk varied between 4 and 6 MJ/Nm^3 [21], in here 5 MJ/Nm^3 was chosen. The total MWh energy demand of Benti was estimated as 1015.3 MWh, but 20% of this demand was assumed to generate from Bio-mass and considered 10% system loss. Total MWh capacity of Bio-mass system was = 1015.3*0.2+0.1*203.06 = 223.4 MWh.

$$\text{Gas flow rate } (V_{g)} = \frac{223.4\text{MWh}}{5\text{MJ / NM}^3} = 44.67\text{NM}^3/\text{h} = 0.012\text{ NM}^3/\text{s} \tag{3.85}$$

3.8.3.3. Fuel Feed Rate

To find the biomass feed rate M_f, the required power output is divided by the LHV of the biomass (LHVg) and by the gasifier efficiency, η_{gef}. To find the biomass (rice husk) feed rate, M_f, the required power output (kW) is divided by the lower heating value of the biomass coffee husk (LHV) and by the gasifier efficiency, (η_g =0.25).

$$M_f = \frac{27}{5 \times 0.25} = 21.6 \text{kg} / \text{h} \quad (3.86)$$

Flow rate of gasifiying medium has a major influence on yield and composition of the product gas. For an air-blown gasifier operating, the amount of air required, Ma, for gasification of unit mass of biomass is found by multiplying it by another parameter ER [56].

$$M_a = M_{th} \times ER \quad (3.87)$$

Here, ER is the equivalence ratio. For a fuel feed rate of M_f, the air requirement of the gasifier, M_{fa}, is given by

$$M_{fa} = M_{th} \times ER \times M_f \quad (3.88)$$

$$M_{fa} = Vg \times \rho g \quad (3.89)$$

pg is the density of the medium at the gasifier's operating temperature and pressure. For a biomass gasifier, 0.25 may be taken as a first-guess value for the equivalence ratio, ER. The volume of gas at the operating temperature and pressure, Vg, is estimated from the mass of air (or other medium), M_{fa}, required for gasification as well as for fluidization. Thus, Vg is necessarily the gas passing through the grate and the bed. Take gas density of air 1.225kg/m^3.

$$M_{fa} = V_g \times \rho_g = 0.012 \times 1.225 = 14 \text{g} / \text{s} \quad (3.90)$$

3.8.3.4. Equivalence Ratio, φ

The equivalence ratio is an important gasifier design parameter. It is the ratio of the actual air–fuel ratio to the stoichiometric air–fuel ratio. This term is generally used for air-deficient situations, such as those found in a gasifier [56].

$$\varphi < (1)\,\text{Gasification} = \frac{\text{Actual air}}{\text{Stoichiometric air}} = \frac{(A / F)}{(A / F)s} > (1)\,\text{combustion} \quad (3.91)$$

Where, the equivalence ratio φ, dictates the performance of the gasifier. For example, pyrolysis takes place in the absence of air and hence the φ is zero; for gasification of biomass, it lies between 0.2 and 0.3. In this research thesis the average which is 0.25 was taken.

3.8.3.5. Fluidization Velocity

The range of fluidizing velocity, U_g, in a bubbling bed depends on the mean particle size of the bed materials. The range should be within the minimum fluidization and terminal velocities of the mean bed particles. The particle size may be within group B or group D of Geladart's powder classification (Basu, 2006). The fluidization velocity for silica sand of about 1mm mean diameter is between 1.0 and 2.0 m/s. The range of fluidizing velocity, U_g, in a bubbling bed depends on the mean particle size of the bed materials. The particle size is be within group B or group D of Geladart's powder classification (Basu, 2006. The typical fluidization velocity for 0.67mm mean diameter is varying between 0.5 and 1.0 m/s. In this thesis U_g was taken as 0.5 m/s.

3.8.3.6. Cross-Sectional Area

The inside cross-sectional area of the fluidized-bed gasifier, A_b, is found by dividing the volumetric flow rate of the product gas flow, V_g, by the chosen superficial gas or fluidization velocity through it, U_g, at the operating temperature and pressure. The volume of gas at the operating temperature and pressure, V_g, is estimated from the mass of air (or other medium), M_{fa}, required for gasification as well as for fluidization [56] [57]. Thus, V_g is necessarily the gas passing through the grate and the bed.

$$A_b = \frac{V_g}{U_g} = \frac{0.012}{0.5} = 0.024 \qquad (3.92)$$

The volume of gas at the operating temperature and pressure, Vg, is estimated from the mass of air (or other medium), M_{fa}, required for gasification as well as for fluidization. Thus, Vg is necessarily the gas passing through the grate and the bed.

3.8.3.7. Gasifier Height

1. Fluidized-Bed Height: - The bed height (or depth) of a bubbling fluidized-bed gasifier is an important design parameter. Gas–solid gasification reactions are slower than combustion reactions, so a bubbling bed gasifier is necessarily deeper than a bubbling-bed combustor, which is typically 1.0- to 1.5-m deep for units larger than 1 m in diameter.

2. Freeboard Height: - The empty space above the bed, the freeboard, allows entrained particles to drop back into it. A bubbling, turbulent bed must have such a freeboard section to help avoid excessive loss of bed materials through entrainment and to provide room for conversion of finer entrained char particles. The total height of the gasifier is made up of the height of the fluidized bed and that of the freeboard above it. Total gasifier height = bubbling bed height (depth) + freeboard height = 2.1m.

3.8.3.8. Gas Production Rate

The gas flow rate (m^3/s) can be calculated from the primary air flow if the Nitrogen content in the producer gas is known. The gas flow rate can be measured by orifice plates, venturis, pilot tubes or rota meters placed in the gas flow [Knoef et al., 2005]. Specific gas production rate is the volumetric flow rate of gas per unit area based on the reactor diameter. The gas volume is measured at normal conditions (1 atm, 0^oC).

$$\text{Gas production rate} = \frac{\text{Air flow rate}\left(\frac{3.76}{4.76}\right)}{\text{Nitrogen mole fraction of dry producer gas}} \qquad (3.93)$$

CHAPTER 4

4. RESULT AND DISCUSSIONS

4.1. Introduction

The power generated from the hybrid components, and the fuzzy logic controller are simulated and discussed in the section below. First the solar power system model is modeled and simulated to give an output of around 40kW, according to the designed system model, and next single micro hydro system model. Finally, the intelligent fuzzy logic controller is designed and simulated.

4.2. Solar Power Generation System

The power to be generated from the solar panels is around 40kW, and in order to achieve this a solar panel with short circuit current of 8.6A and an open circuit voltage of 45.74V is selected by considering the solar data radiation of the selected site, and from these technical specifications of the proposed solar panels a string of 4 arrays each containing 45 solar cells connected in series is Required to generate a power of around 40kW. Since the village doesn’t have a large flat area because geographically it is up and down to install the solar panels. The panels are to be installed at different places of the village. Due to this the solar panels will not get the same solar radiation. To consider this effect some of the solar panels are allowed to receive a solar radiation of 1000 kWh/m^2/day, some to get a solar radiation of 800 kWh/m^2/day, and some of the solar panels are allowed to receive a solar radiation of 600 kWh/m^2/day.

4.2.1. Solar Panel Simulation Results

The MATLAB simulation power generated from the proposed solar array is around 40 kW, and this is shown in the current versus voltage curve and also in the power versus voltage curve as shown in Fig. 4.1

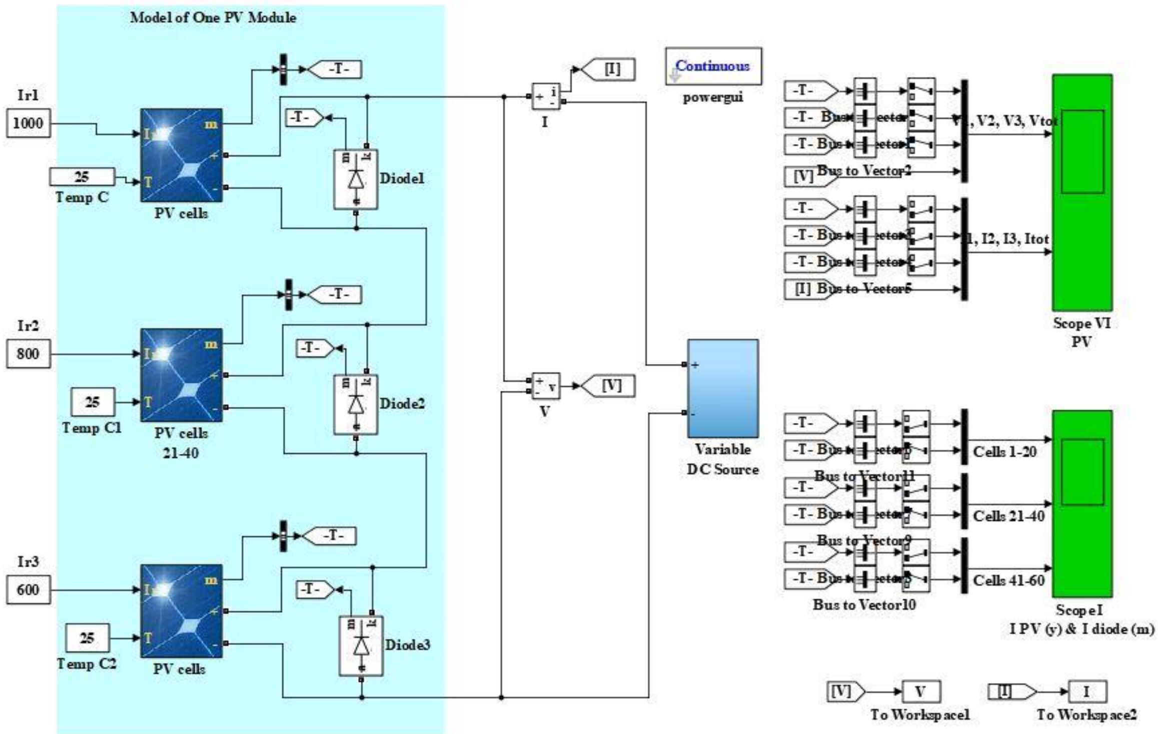

Fig. 4. 1: Simulink realization of the solar panels

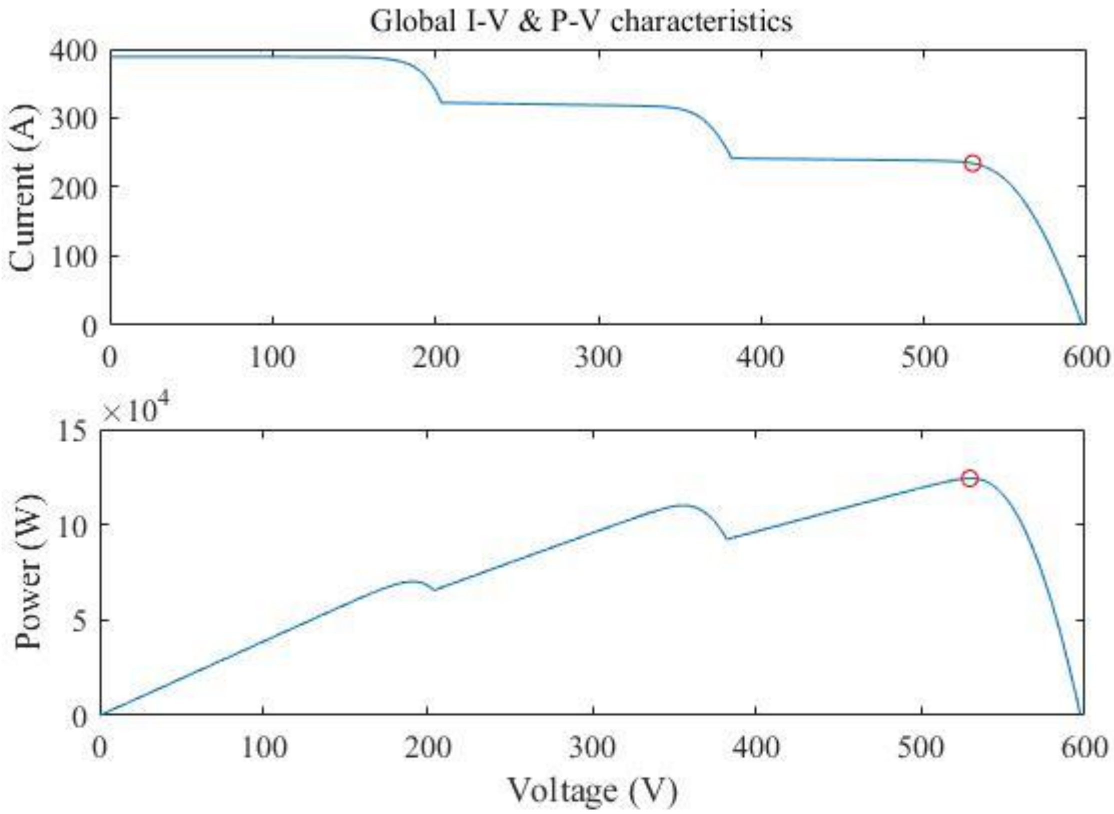

Fig. 4. 2 I-V and P-V characteristics curve of the solar generated power

4.3. Micro hydro Power Generation System

The modelling of micro hydro power plant is done in this thesis by using MALAB/Simulink. Introduction of micro hydro power plant reduces a lot of burden without any adverse effect on environment while meeting the localized power requirement. The simulation results show that with proper choice of governing system for micro hydro power plant leads to proper load sharing, constant voltage output and constant speed with variation of load values. This leads to an economical operation of the system.

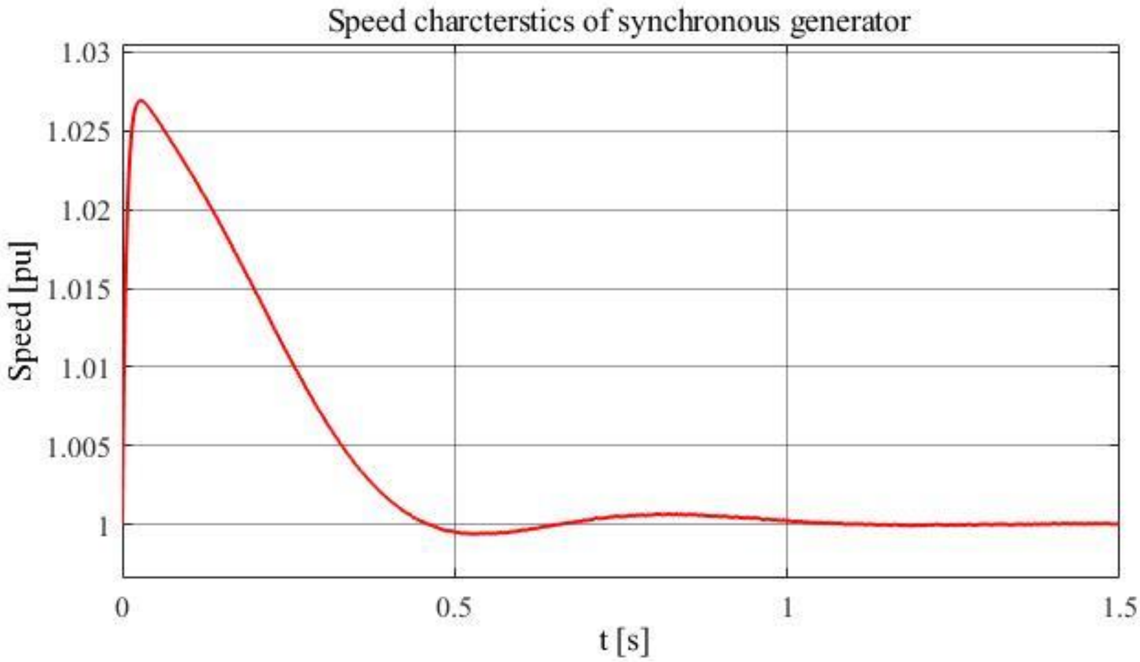

Fig. 4. 3 Synchronous Generator Speed Characteristics

The under damped rotor speed characteristic of hydro (synchronous) generator is shown in Fig. 4.3. From the characteristics, it is observed that the transient time is 40s. After a few seconds its speed reaches steady state at synchronous speed. With sudden application of mechanical torque input to the shaft of alternator, the load angle settles to a steady state value after few oscillations owing to system damping following the swing equation and power angle characteristics. Moreover, the governor setting *kp*= 0.613 *ki*= 0.104 and *kd*= .0002 chosen by trial and error method helps to keep the speed near synchronous speed.

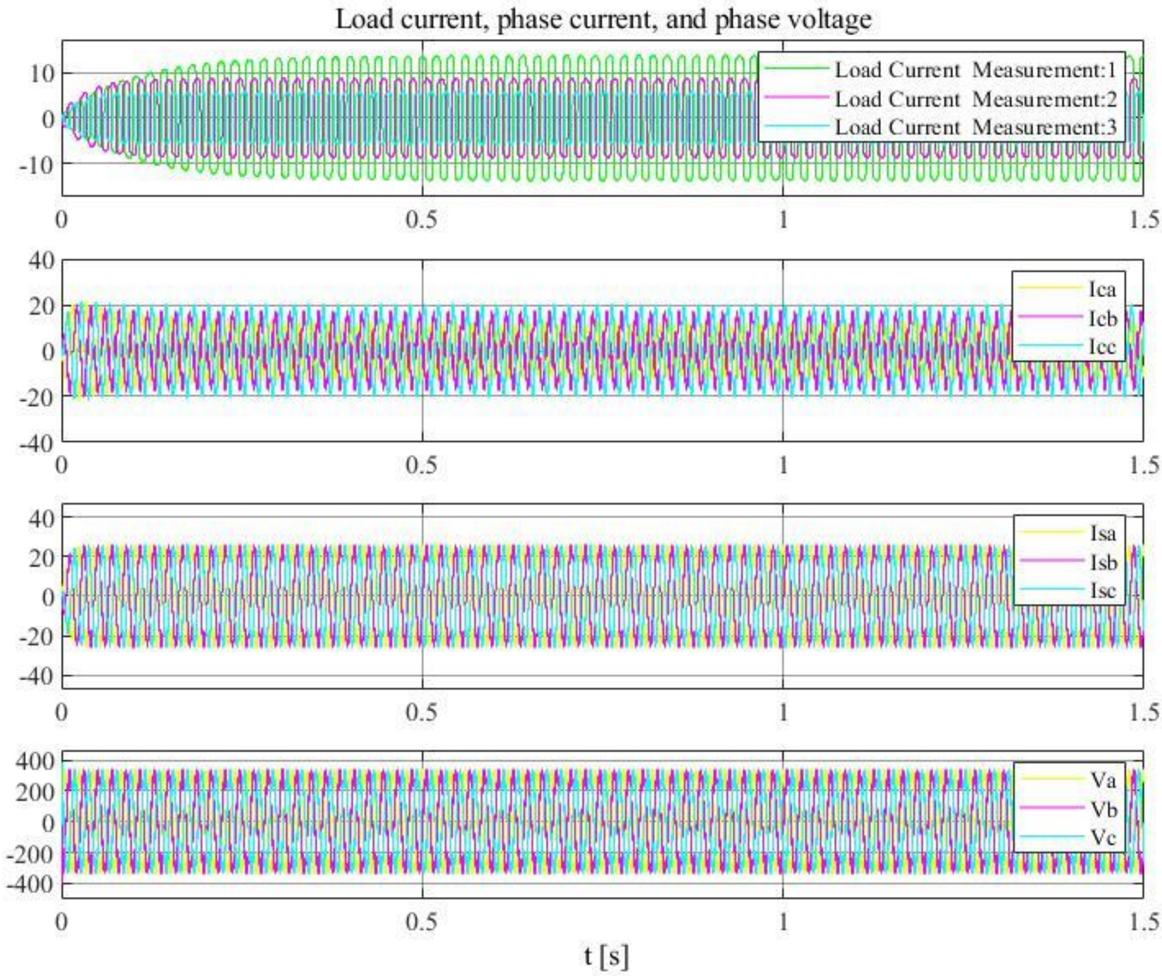

Fig. 4. 4 Three phase current characteristics of a hydro power plant

Fig.4.4 shows the stator current characteristics of the generator. When the load is changed, due to the presence of the transient and sub-transient reactance, envelop of three phase current shows under damped response at initial stage. After that it gains the steady state characteristics. It is observed from the plot that the transient period is 15s for three phase stators current.

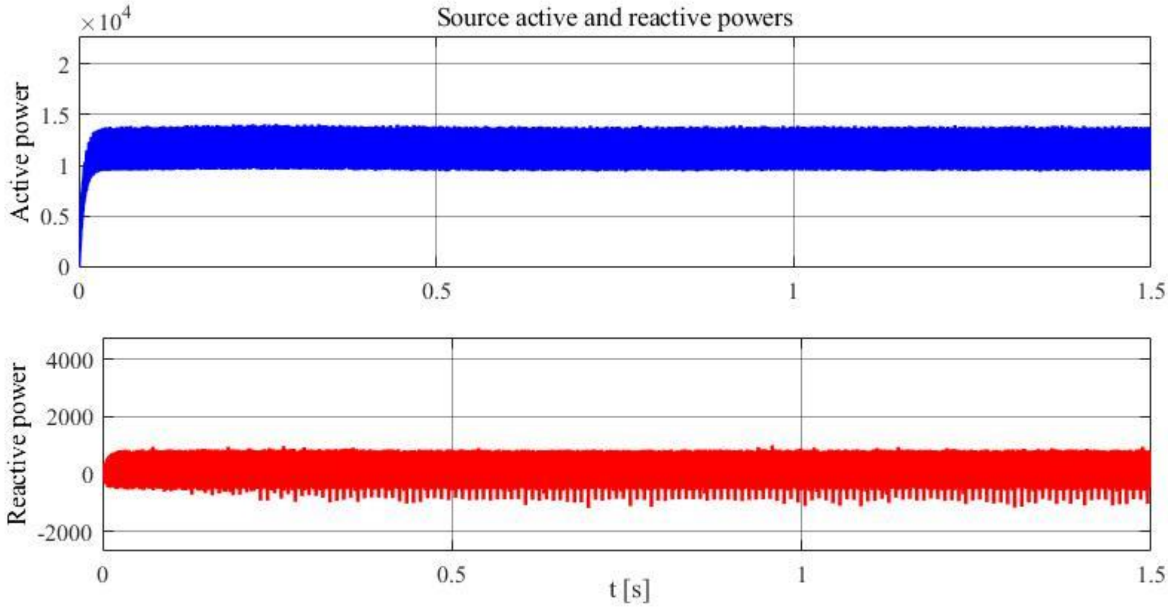

Fig. 4. 5 Source active and reactive powers characteristics

Active power characteristics (Fig 4.5) of synchronous generator, which shows a steady state value of 0.6 pu is nothing but the actual load connected to the plant. It is observed that the steady state is obtained around 27 sec. To reach the stable operating point on power - angle characteristics, few oscillations around this point occurs. This leads to initial overshoots and undershoots of the power characteristics.

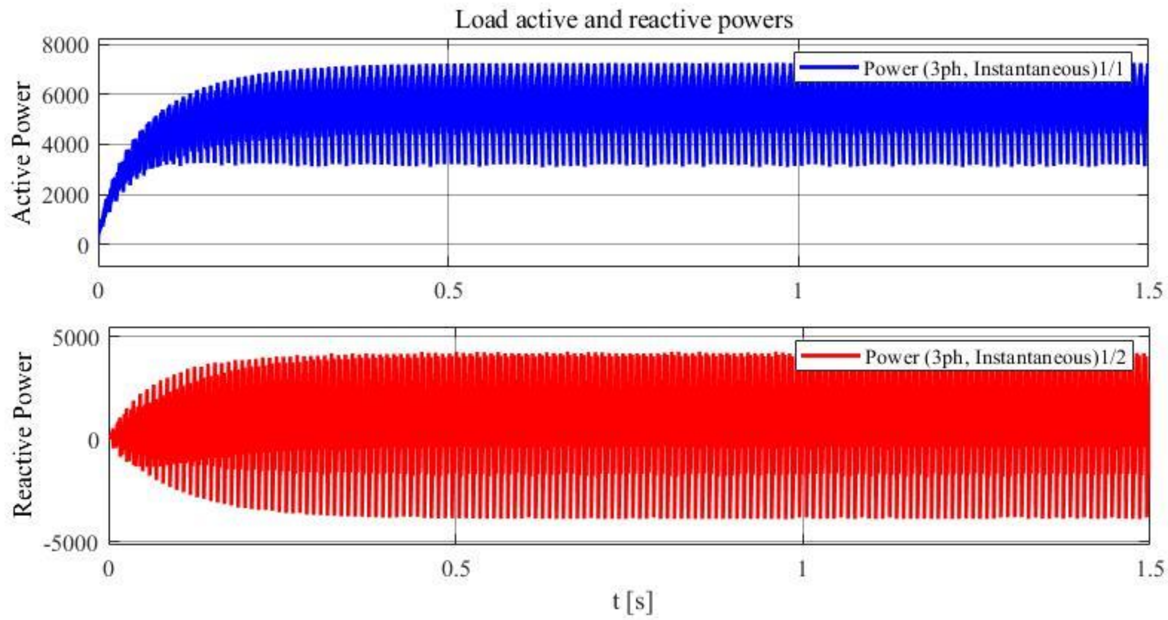

Fig. 4. 6 Load active and reactive powers characteristics

Fig 4.6 shows that the reactive power characteristics complete its transient period in a few seconds and steady state value achieved is obtained which matches the actual reactive load connected.

4.4. Proposed Model Using Fuzzy Logic Controller for the Hybrid System

4.4.1. Modelling of Fuzzy Logic Controller for the Hybrid System

Generation of electrical energy is complex, costly, need resource, requires experts and it is also time taking. But generating of electrical energy by itself is not enough rather the generated electrical power has to be used efficiently and economically. In this thesis the FLC was used to control the generated power from hybrid systems to electrify Benti village.

The proposed hybrid system consists solar, micro-hydro and Biomass renewable energies. The capacity of electric generation in hybrid system is to satisfy the power demand. Fuzzy logic controller is used to control the power efficiently and to serve the power demand of the costumer. The controller looks first at the load and switches the appropriate sources to meet the demand from the costumer side. Comprehensive controller is essential to efficiently manage the energy balance between the total generation and the total demand. The important requirements of the standalone hybrid system are the availability of renewable energy resources.

4.4.2. Fuzzy Logic Controller Algorithm

Fuzzy logic controller is an intelligent tool to manage the integrated energy sources in such a way that it meets the load requirement under varying load conditions. The procedures in making the controller designs are setting the constraints, assigning the linguistic variables and setting the rules for the controller. In this thesis work the fuzzy logic controller has four inputs and one output. The input linguistic variables of FLC are Solar power (Sp), Micro-hydro power (Mhp), Biomass power (Bp) and Power demand (PD) and the single Output linguistic variable is out power (Po). Each input linguistic variable has three linguistic values called Low, Medium and Large and the output linguistic variable has Mhp only, Mhp+Sp, Mhp+Bp, Mhp+Sp+Bp linguistic values. Triangular membership function for Justification, Mamdani inference system for rule processing and center of gravity for De-fuzzy analysis and process by fuzzy logic is used. A typical fuzzy system consists of a membership functions, rule base, inference procedure and rule viewer which were explained in the following sections. After giving membership function for each input output linguistic values and generating the possible operational rules then the next step is to evaluate the rules of the controller for the input values if the output is appropriate or not. To see the overall performance the hybrid system, components are assumed to produce random signal.

A) Fuzzy Interface Model

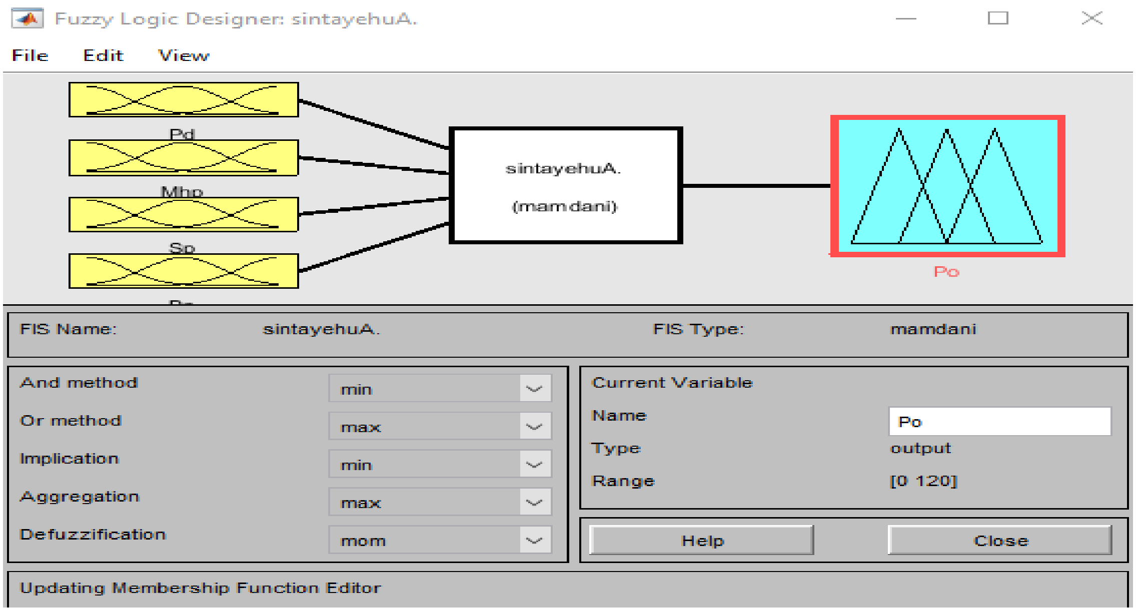

Fig. 4. 7: Fuzzy interface model

B) Membership Function of Power Demand (PD)

The power demand (PD) is one of the input linguistic variables having three linguistic values, Low (0 22.5 45), Medium (30 60 90) and Large (60 90 120).

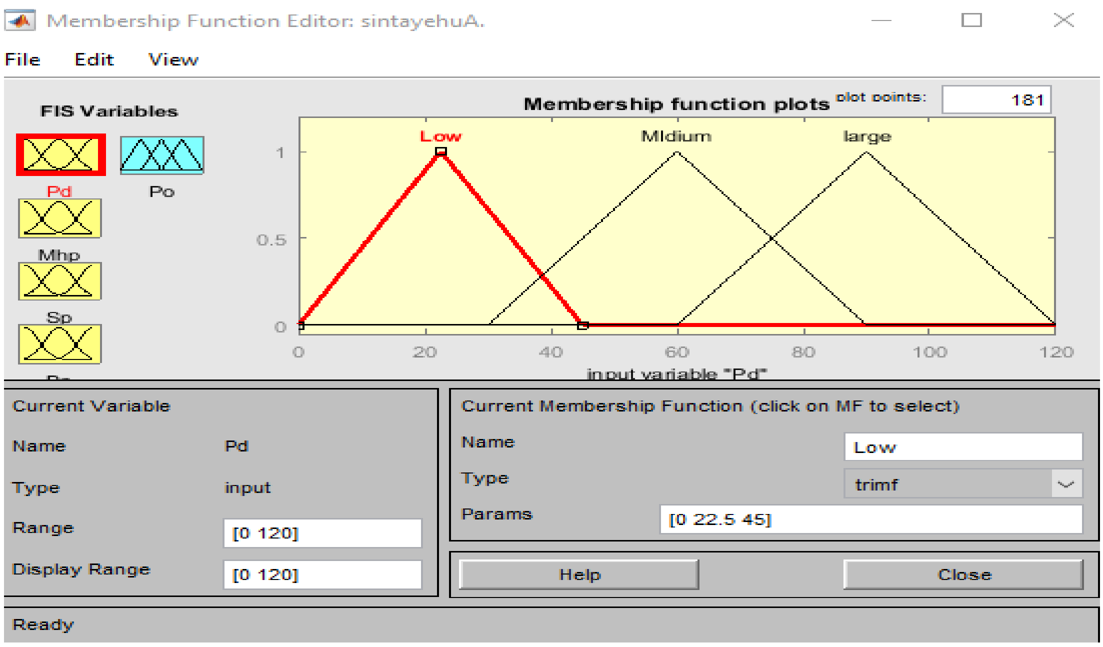

Fig. 4. 8: Membership function of power demand

C) Membership Function of Micro-Hydropower (Mhp)

Micro-hydropower is the second input linguistic variables having three linguistic values, Low (0 13.5 27.5), Medium (18.3 32.08 45.83), Large (36.6 51.3 66).

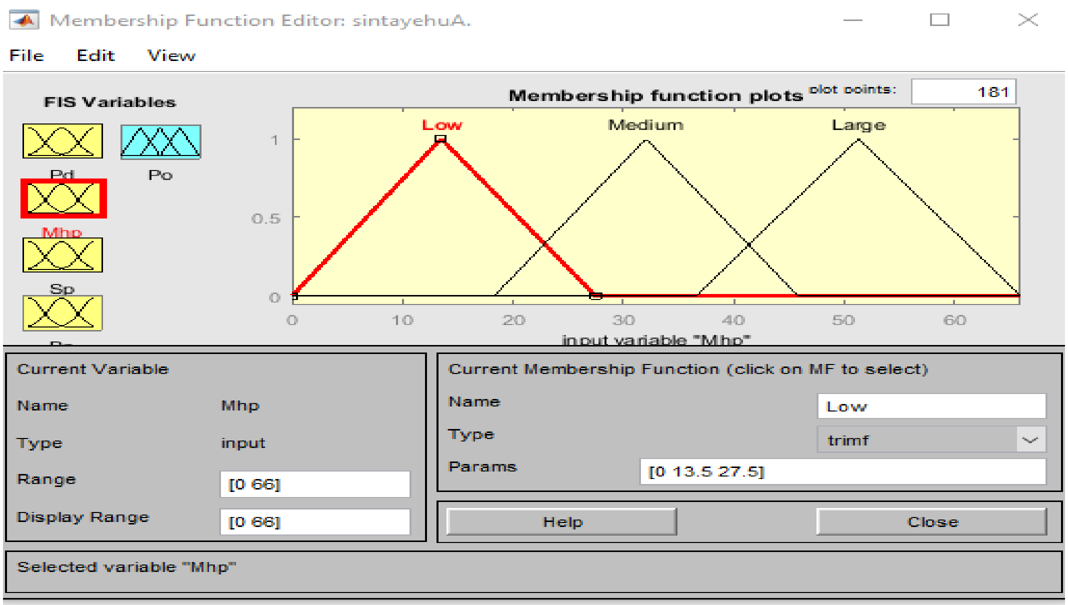

Fig. 4. 9: Membership function of micro-hydro power

D) Membership Function of Solar Power (SP)

Solar power is the third input linguistic variables having three linguistic values, Low (0 6.66 13.33), Medium (6.66 16.67 26.67), Large (20 28 40).

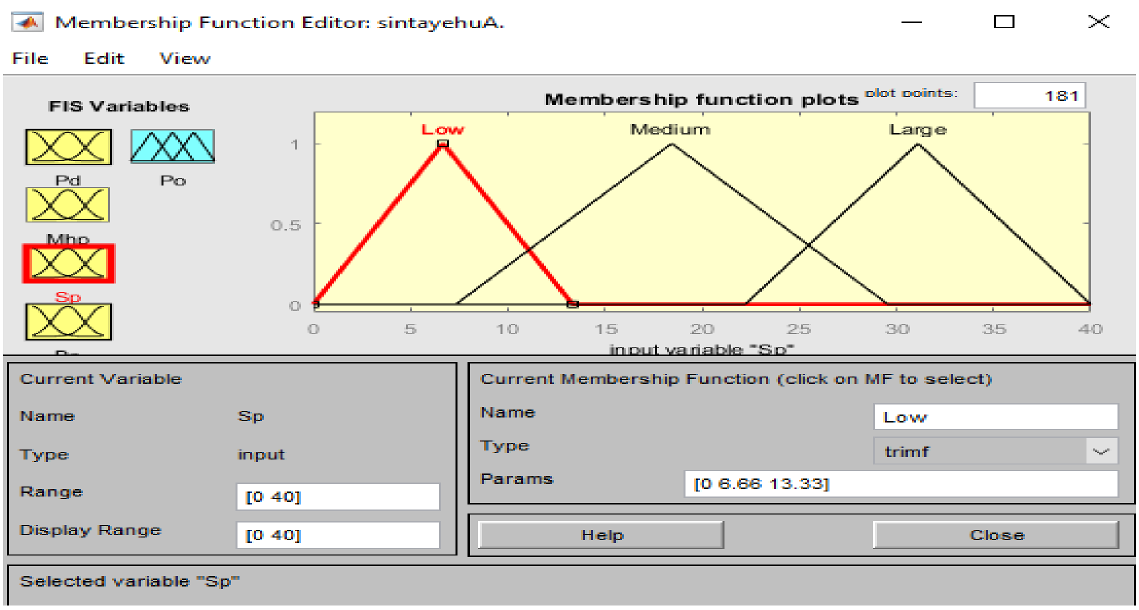

Fig. 4. 10: Membership function of solar power

E) Membership Function of Biomass Power (BP)

Biomass power is the fourth input linguistic variables having three linguistic values, Low (0 5 9.99), Medium (5 12.5 20), Large (15 21 27).

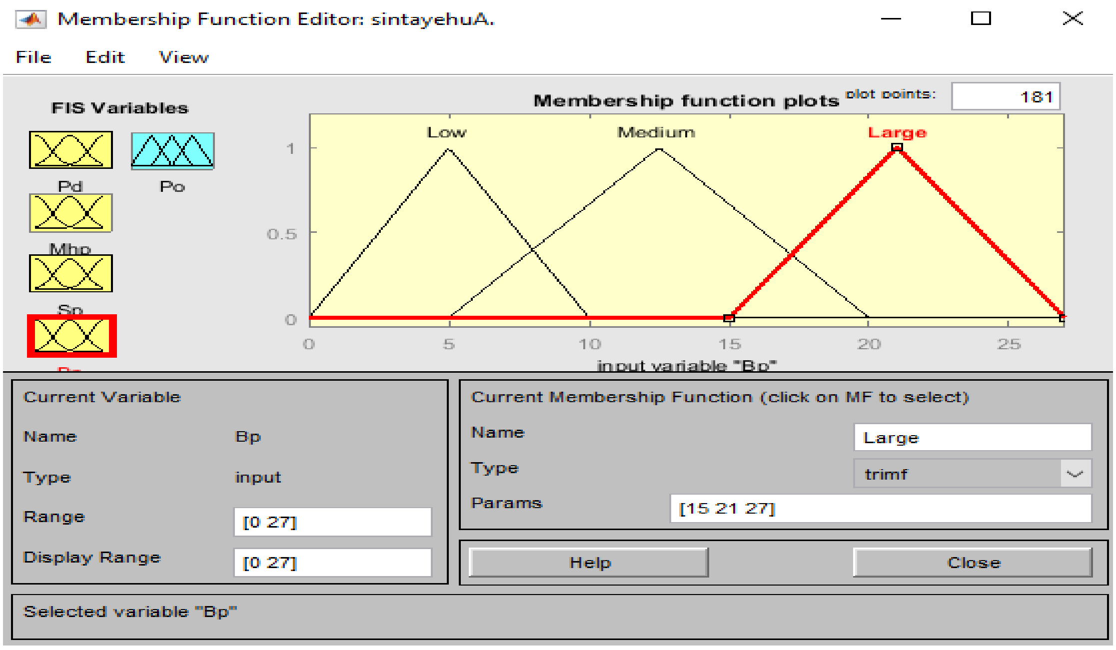

Fig. 4. 11: Membership function of Biomass power (BP)

F) Membership Function of Output Power (Po)

Output power is the only output linguistic variables having three linguistic values, Mhp-only (0 18.75 37.5), Mhp+Sp (30 45 60), Mhp+Bp (45 67.5 90), Mhp+Sp+Bp (75 97.5 120).

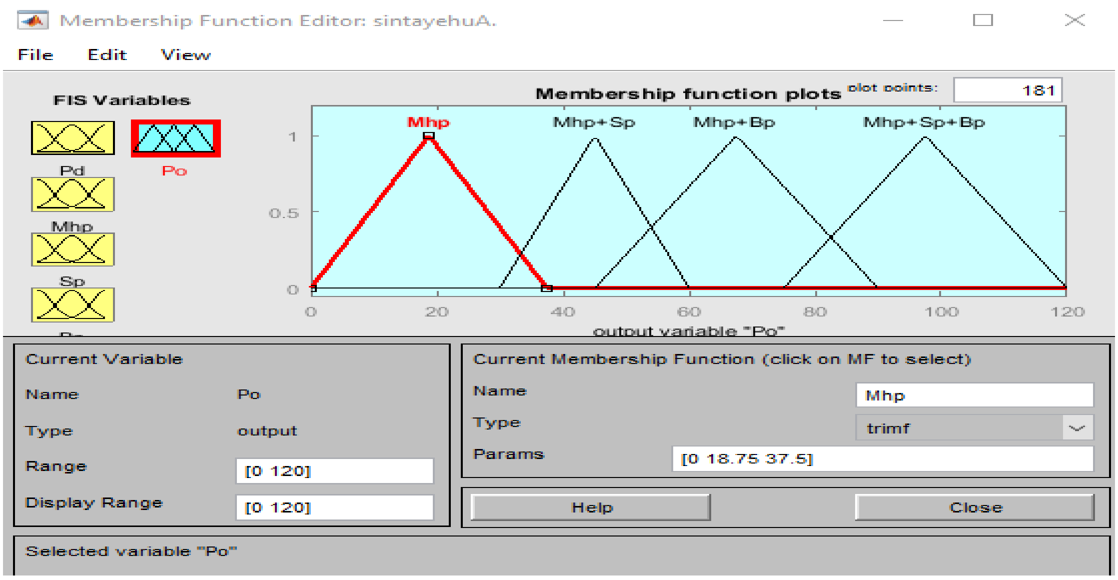

Fig. 4. 12: Membership function of output power (Po)

G) Real Time Modeling of Fuzzy Logic Rules

Here is the model of fuzzy logic controller having four inputs and one output. In control box, a set of rules have been written. The system was operated in accordance to the rules set.

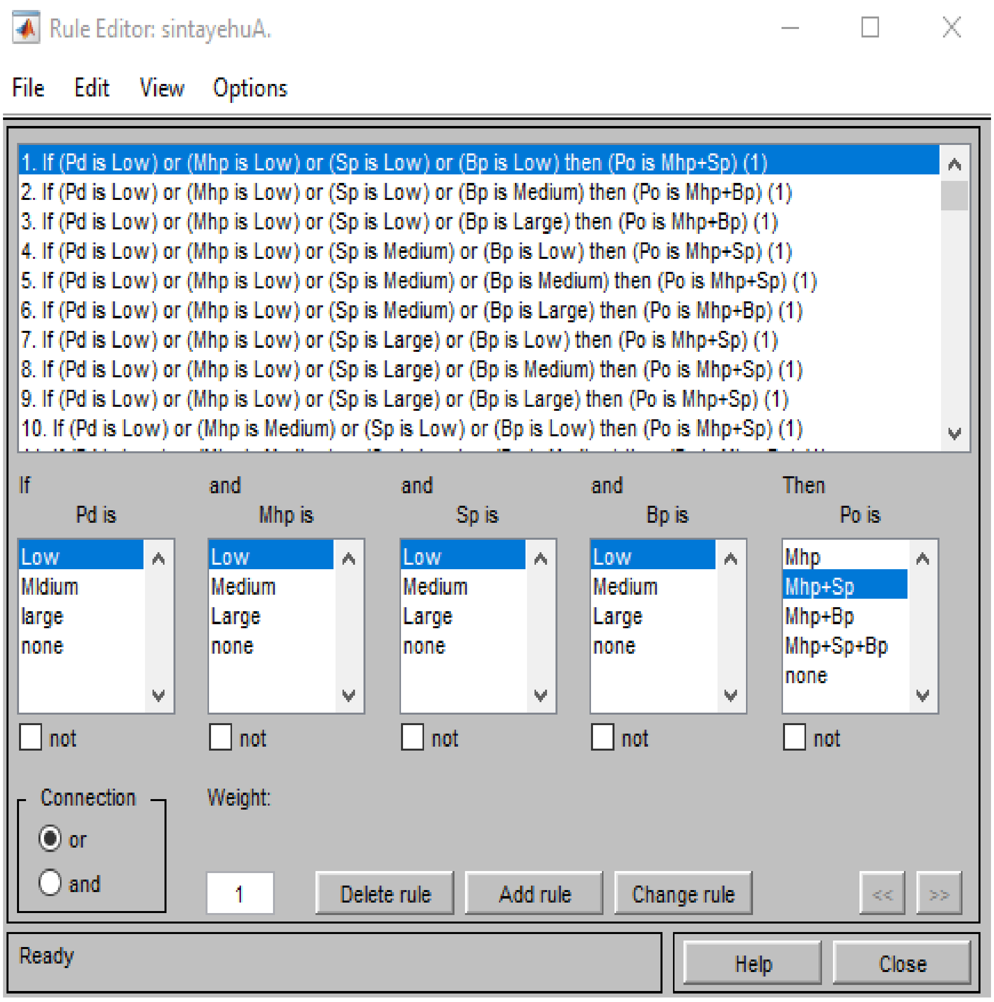

Fig. 4. 13: Real time modeling of fuzzy logic rules

In MATLAB there is an opportunity to view if the system is operating in accordance the written rules, and below a typical example is given by deliberately making all the three renewable energy resources, namely solar power, Micro hydro power, and biomass according ,the decision is to supply the demand power which is around 60 kW and the output power is also 60.2 kW, which shows the fuzzy rule is correctly working for this typical case. The rules are evaluated through the Fig. 4.14.

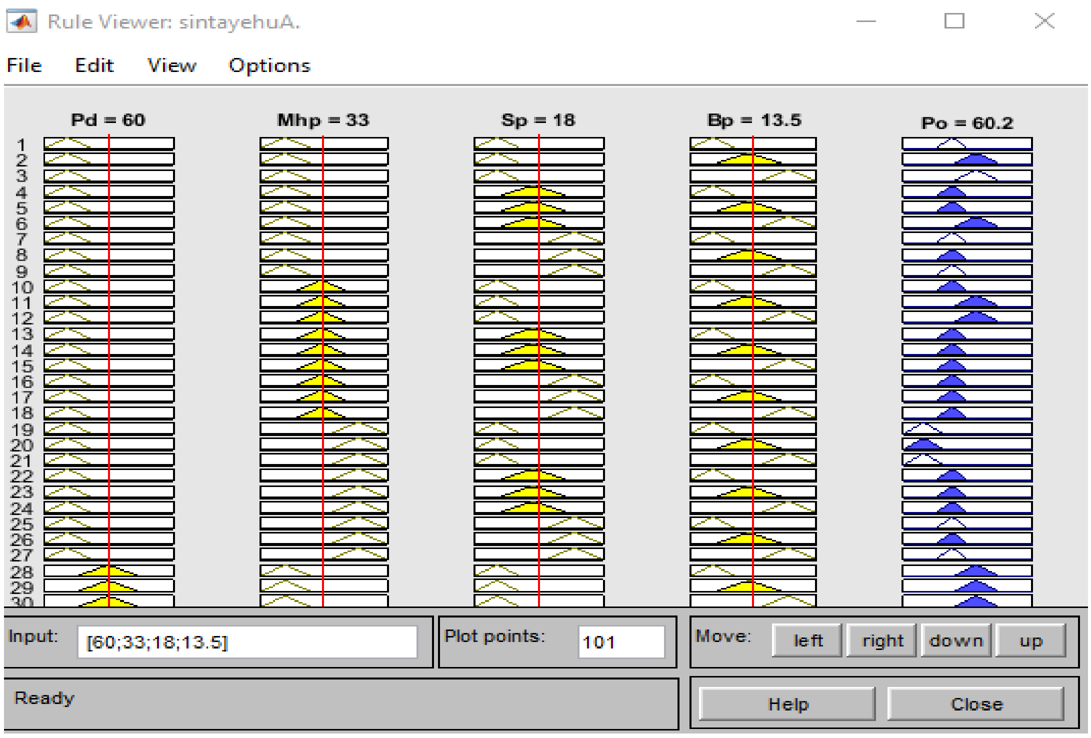

Fig. 4. 14: Rule evaluating one

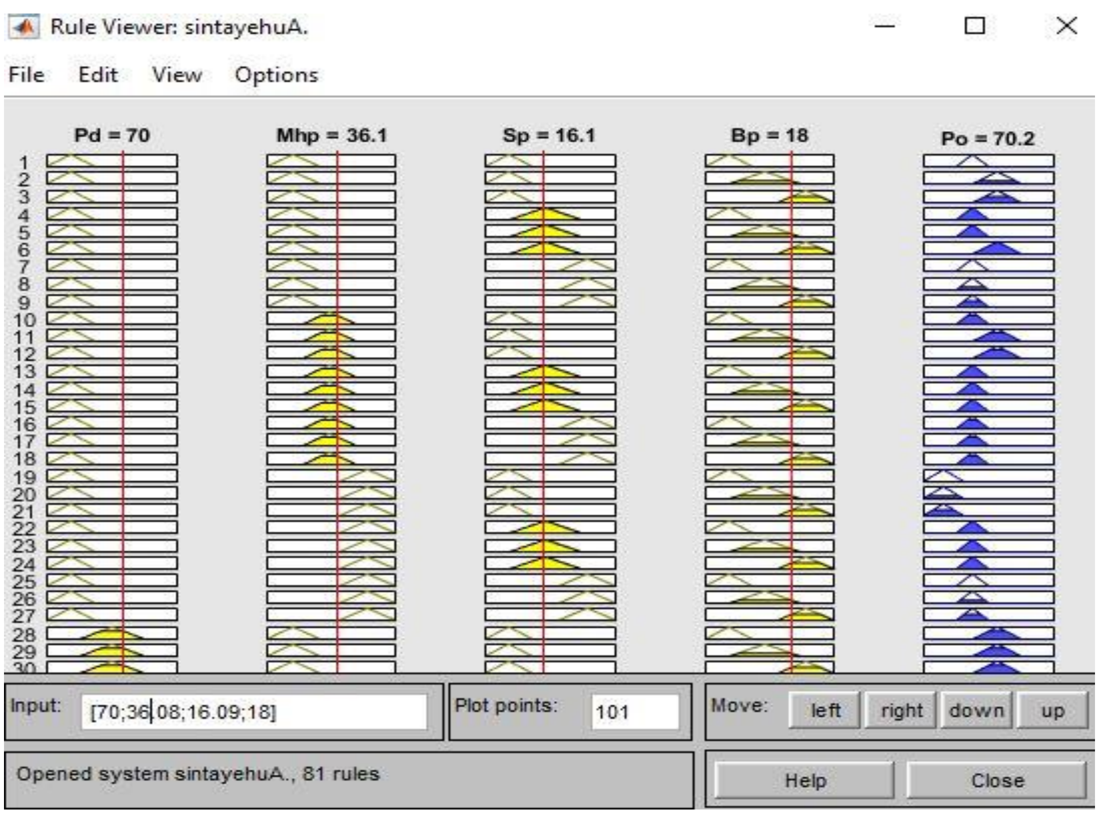

Fig. 4. 15: Rule evaluating two

After modeling fuzzy logic controller, it is possible to evaluate the rules that has been written in rule editor using the rule viewer. Accordingly, for example for the PD 70 kW, the appropriate output power of the controller Po was 70.2 kW [Fig. 4.15]. This indicates the controller helps to use the available resources appropriately for the available power demand.

4.4.3. Overall Fuzzy Logic Controller System

The solar power, micro-hydro power, biomass power and power demand are the input parameters of the controller. Pd, Mhp, Sp and Bp indicates the demand power from the customer side, power from micro-hydro, power from solar system and power from biomass power respectively. The power coming from each component power sources is assumed to be Gaussian random signal generator. The multiport conditional switch will take an action according to the rules written in fuzzy logic controller.

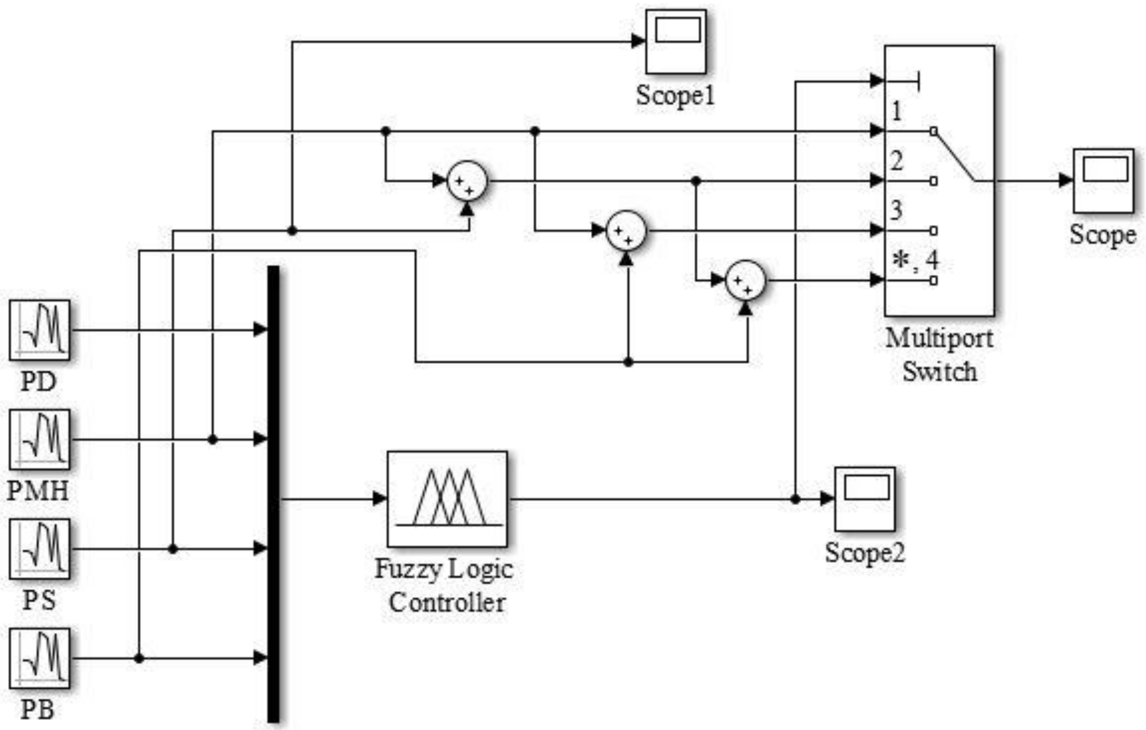

Fig. 4. 16: Overall hybrid system

Because of the intermittent nature of renewable energy resources, all these input sources will vary from time to time, and in order to check if the controller notices this variation, and making a correct final decision to the multiport switch, a Gaussian random number generator is selected as an input for all these five variables (demand power, micro hydro power, solar power, and biomass power), and different cases are taken to check the functionality of this intelligent controller, which are given below.

4.4.4. Case Studies

To evaluate the designed fuzzy logic controller, it was possible to think different operating conditions, such as if the sun shine is low ,flow rate is high and Rice husk is Medium and other conditions But in this case random numbers were given to the controller to evaluate the controller whether it works or not. The scopes show the of the output power. This means the output power which will supply the demand power can vary from 0-120kW,

4.4.4.1. Case Study One

If the demand power PD is 100 kW, Mhp is 60 kW, Sp is 20 kW, and Bp is 20 kW then the output power of fuzzy logic controller is indicated in Fig. 4.17.

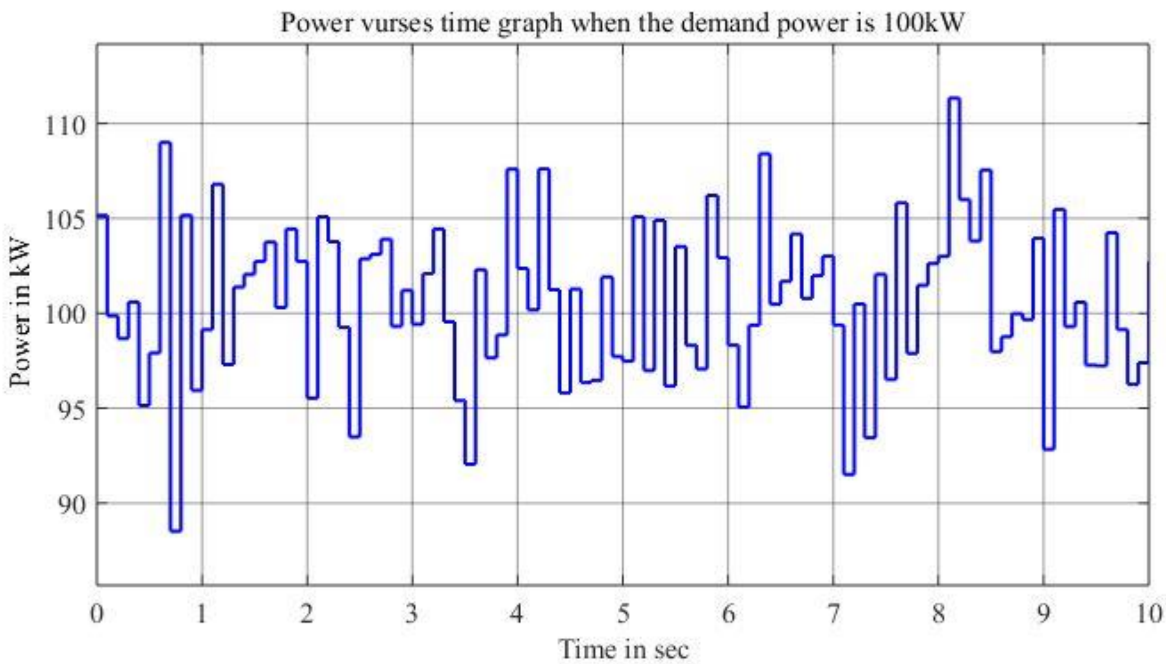

Fig. 4. 17: Simulation result of fuzzy logic controller case one

The controller is helps to use the power efficiently and to serve the power demand of customer. That means the power demand needed about 100kW. The available resource's that is MhP=60kW, Sp=20kW, and Bp=20kW and the output power is 100kW that meet the power demand illustrated in Fig. 4.17

4.4.4.2. Case Study Two

If for example the demand power PD is 40 kW, Mhp = 25 kW, Sp = 15 kW, and Bp = 0 kW, then the output power of fuzzy logic controller will be indicated as in the Fig. 4.18below.

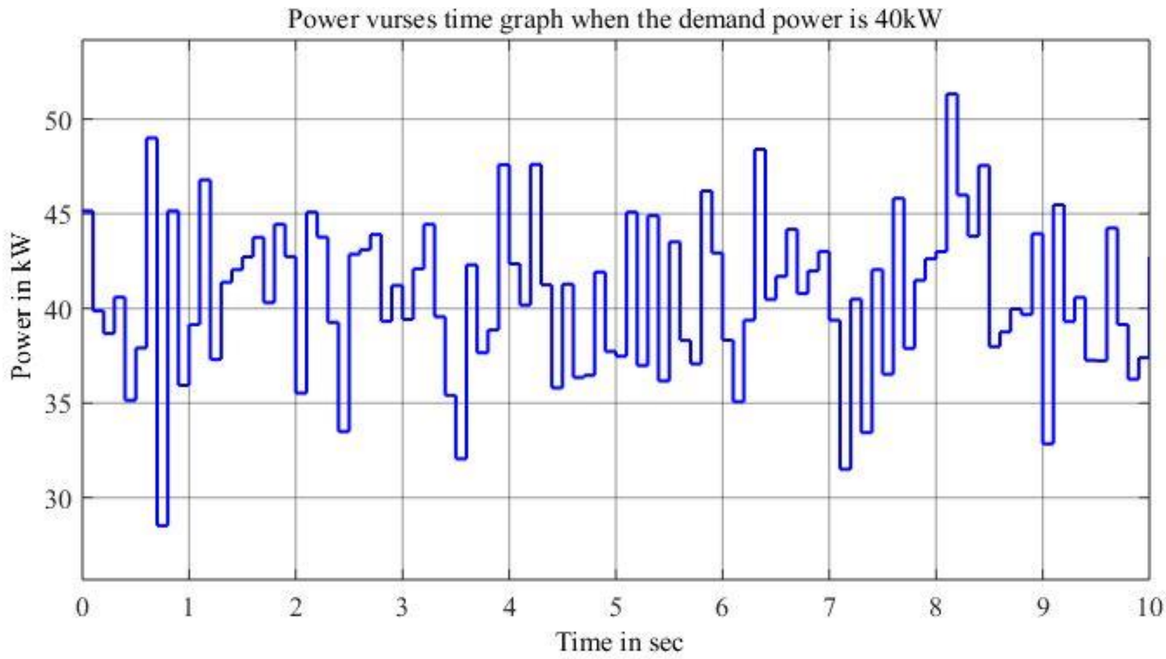

Fig. 4. 18: Simulation result of fuzzy logic controller case two

4.4.4.3. Case Study Three

If for example the demand power PD is 80 kW, Mhp = 55 kW, Sp = 10 kW and Bp = 15kW, then the output power of Fuzzy Logic Controller will be indicated as in the Fig 4.19 bellow.

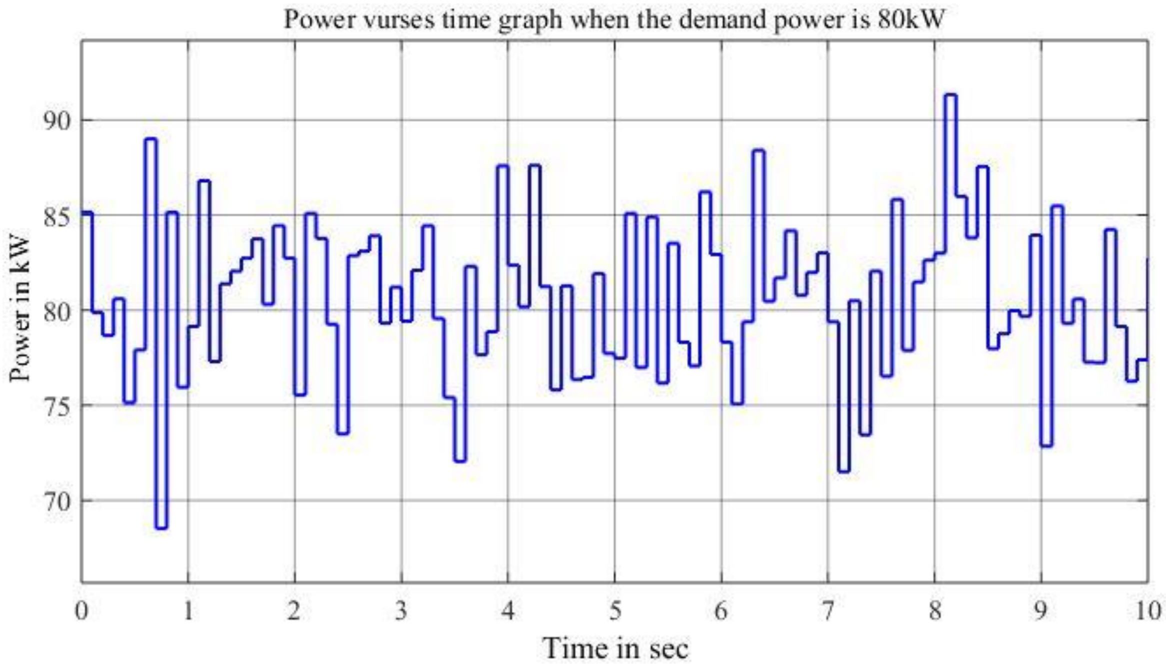

Fig. 4. 19: Simulation result of fuzzy logic controller case three

4.4.4.4. Case Study Four

If for example the demand power PD is 60 kW, Mhp = 25 kW, Sp = 30 kW and Bp = 5kW, then the output power of fuzzy logic controller will be indicated as in the Fig 4.20 bellow.

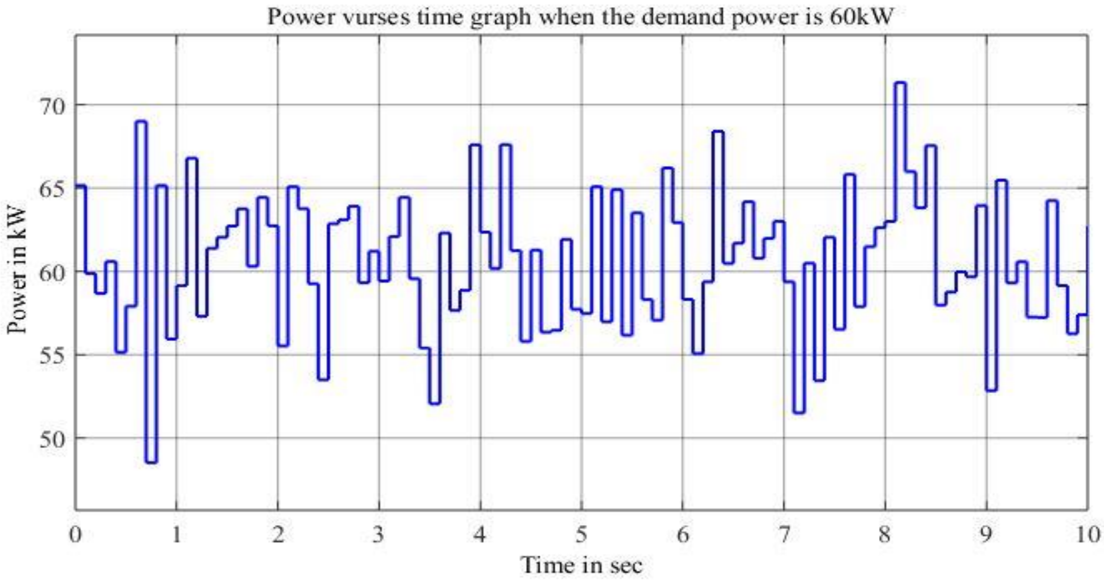

Fig. 4. 20: Simulation result of fuzzy logic controller case three

Practically the controller or power management system should be implemented in real time microcontrollers. Accordingly, the Simulink system is converted to MATLAB programing using mat functions as shown in Appendix. The controller senses the power availability have six combinations that are Pmh, Ps, Pmh+Ps, Pmh+Pbio, Pmh+Ps+Pbio as shown in Table 4.1.

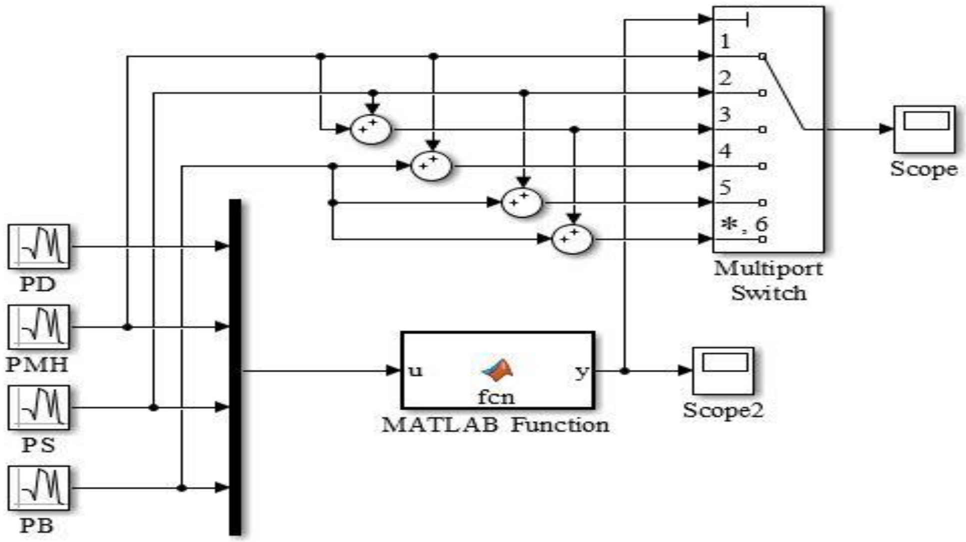

Fig. 4. 21: Overall of the system

The controller is used to use the power efficiently and to serve the power demand of customer. The controller looks first at the load and switches the appropriate source to meet the demand from the customer side as shown Fig. 4. 21.

Table 4. 1: Power combination and switch port

Power combination	Switch port (Index)
Pmh (power of micro hydro)	1
Psolar (power of solar)	2
Pmh+Psolar (combination of two)	3
Pmh+Pbio (power of microhydro+power of biomass)	4
Psolar+Pbio (combination of two)	5
Pmh+Psolar+Pbio (combination of three)	6

4.4.5. Case Study MATLAB Function

To evaluate the designed fuzzy logic controller, it was possible to think different operating conditions, such as if the sunshine is low, flow rate is high and Rice husk is medium and other conditions. But in this case random numbers were given to the controller to evaluate the controller whether it works or not as it was assumed at the beginning.

4.4.5.1. Case Study One

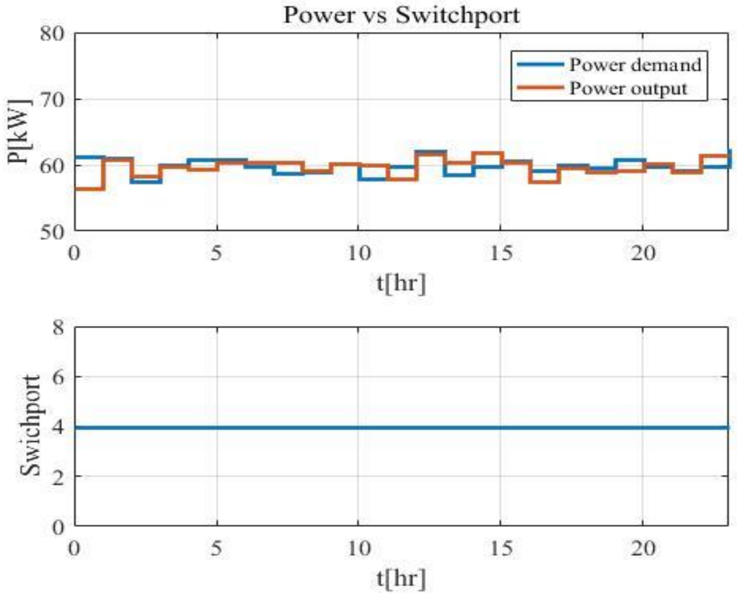

Fig. 4. 22: Simulation result of programmed in MATLAB function case one

If for example the demand power PD is 60 kW, Mhp = 40 kW, Sp = 0 kW and Bp = 20 kW, then the output power of controller is indicated as shown in Fig. 4. 22. The Pd 60 kW and the available sources have only two that is Pmh and Pb then the microcontroller set switch port at four that is the combination of Pmh+Pbio. Because the controller senses the availability of resources.

4.4.5.2. Case Study Two

If for example the demand power PD is 80kW, Mhp = 45 kW, Sp = 20 kW and Bp = 15kW, then the output power of controller will be indicated as in the Fig 4.23 bellow.

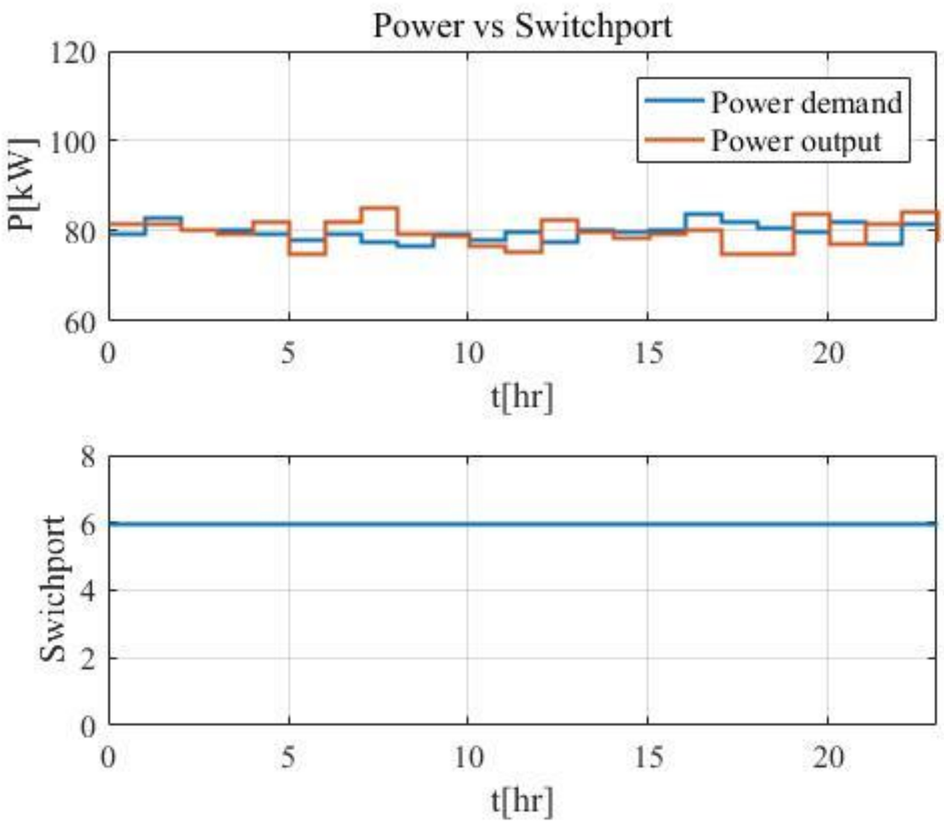

Fig. 4. 23: Simulation result of programmed in MATLAB function case two

Form the Fig. 4.23 the Pd 80 kW and the available resources have switch ports automatically on six that is the power combinations Pmh+Pb+Pbio.

4.4.5.1. Case Study Three

If for example the demand power PD is 100 kW, Mhp = 60 kW, Sp = 25 kW and Bp = 15kW, then the output power of controller will be indicated as in the Fig 4.24 bellow.

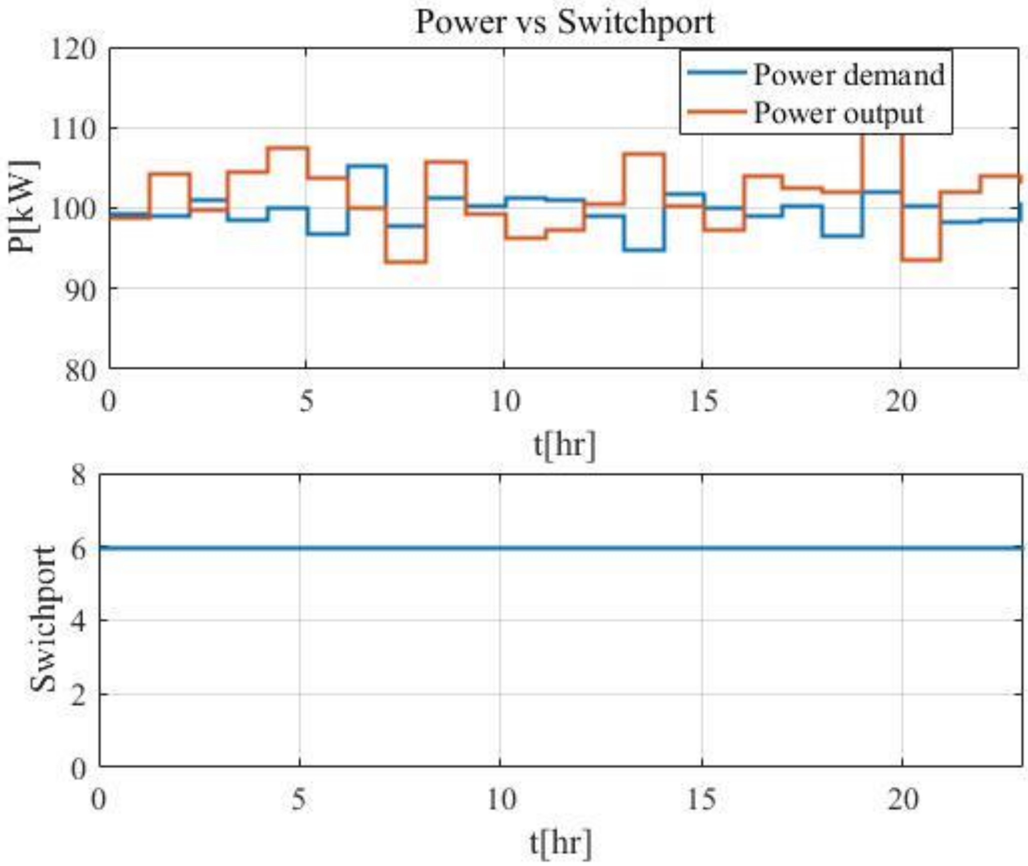

Fig. 4. 24: Simulation result of programmed in MATLAB function case three

4.5. Discussions

A hybrid power system which consists of hydro, PV-arrays and biomass with energy and power electronic devices has been presented to achieve an efficient and cost competitive system configuration so that hybrid power sources could improve the life of people especially in rural areas where electricity from the main grid has not reached yet. After data collection and community load estimated, a hybrid power system containing PV, hydro and biomass power units are studied. Then, with the optimized hybrid system, MATLAB/ Simulink model is developed to examine the dynamic responses of the designed power system over 24 hours of typical day. The result of the dynamic responses of the dynamic model that contains the optimal hybrid system shows that the overall power management strategy is effective and the load demand is balanced successfully. Fuzzy logic controller is used to select the appropriate power source for the load depending on the resource available.

To use the produced power efficiently and economically fuzzy logic controller has been used. This intelligent control system was used to decide intelligent decision by sensing the type and amount of resource available, and then it selects the appropriate alternative source.

To perform this fuzzy rule have been written in fuzzy rule editor and each components of the hybrid system has been modeled using MATLAB/Simulink.

Generally, study area was found potentially blessed of solar power, Micro-hydro power and Bio-mass power therefore it was possible to produce hybrid power from these sources and fuzzy logic controller was used to the generated power appropriately. The simulation results have been observed that the designed fuzzy logic controller and MATLAB function of the hybrid power for Benti village was able to supply the intended power demand in different cases. Hence the designed peak power demand was 120kW.

CHAPTER 5

5. CONCLUSIONS AND RECOMMENDATIONS

5.1. Conclusions

In this study a fuzzy logic controller-based hybrid solar/Micro-hydro/Bio-mass power system for Benti village was designed. To come up finally to the main objective the specific objectives were critically seen step by step. As it was discussed in chapter two this study was conducted in Fogera Wereda, benti village which is located 34km from werta at 1828m elevation having latitude of 11.9167N and longitude of 37.70E.

The sunshine hour data of the solar system was taken from NMSA Debrtabor branch of five year. The study area has on average 7.12 sunshine hrs. per day. The incoming solar energy was converted into kWh/m^2/d using Angstrom estimation (Duffie and Beckman, 1980) model and finally the kWh/m^2/d average 5.4. The NMSA (5.2889) data was compared with NASA (5.4975) and the difference is 0.2086kWh/m^2/d. The flow rate of Gumara river was found 2.139 m^3/s. But the designed value was taken 0.9 m^3/s. As the data from Fogera Wereda Rice production office, the average annual Rice husk production of the study wereda was 11,968.731mT which is around 33.246 MT per day.

Load profile of the village (426 household) was assessed as 1199.616kWh, 12.453kWh, 38 kWh per day for households' applications, Commercial loads and public loads respectively. During the calculation for lighting (100% of household), Radio (70% of household), TV (70% of house hold), refrigerator (25% of house hold), Stove (10% of population), Injera Mitad (7% of population) was assumed. Elementary school, health clinic, commercial loads, and water pumping motors was considered. Total energy consumption of the Benti village per day was 1250.069 kWh per year. During designing the energy consumption of the village was forecasted for 10 years using appropriate formula from 4398.275MWh per year (86.6kW) to 1015.3MWh per year(120kW) from the base year. According to the load assessment conducted, the total electric demand of Benti village was 120kW. To satisfy this demand Solar, Micro-hydro and Bio-mass, 30% of 120kW (36kW), 50% of 120kW (60kW) and 30% of 120kW (24kW) was contributed. During designing 10% system loss was considered. To produce 36kW from Solar system 180 modules, 325W panels having 72m^2 area and 4.0kWh/m^2/d solar insolation was required. For the Micro-hydro to produce 60kW, 0.9 m^3/s flow rate, 12.6 m head, 60% efficiency and 0.048m weir length, 1.93m^2 canal area,154m penstock length was calculated. Propeller reaction turbine and three phase synchronous motor generators was taken. To produce 27kW from Bio-mass system only 10% of the annual Rice husk was used. The fluidizing velocity, Rice husk feed rate, gas flow rate, gasifier height and gasifier cross-sectional area was calculated as 0.5m/s, 21.6kg/h, 0.012Nm^3/s, 2.1m and 0.24m^2 respectively.

To use the produced power efficiently and economically fuzzy logic controller has been used. This intelligent control system was used to decide intelligent decision by sensing the type and amount of resource available, then it selects the appropriate alternative source. To perform these fuzzy rules have been written in fuzzy rule editor and each components of the hybrid system has been modeled using MATLAB/Simulink

Generally, study area was found potentially blessed of solar power, micro-hydro power and Bio-mass power therefore it was possible to produce hybrid power from these sources and fuzzy logic controller was used to the generated power appropriately. The simulation results have been observed that the designed fuzzy logic controller of the hybrid power for Benti village was able to supply the intended power demand in different cases. Hence the designed peak power demand was 120kW.

5.2. Recommendations

In Ethiopia there are Bio-mass such as coffee husk, rice husk, wheat husk and other agricultural residues which can produce electricity, so the gasification technology must be the future issue because of the by-products of agricultural activities are the more pollutants of the environment. And also, most of the time data handling in our country is very weak, this makes finding relevant data very difficult. So, I recommend the concerned governmental body to give a due attention for such research works. It is known that Ethiopia has huge renewable energy (Photovoltaic, Geothermal, Wind Energy, Biomass and Micro-Hydro) resources and if these resources are effectively used by using an intelligent controllers, the livelihood of its population can be improved, anybody who is interested in such works can use one of the different intelligent controllers and can contribute his/her own contribution in improving intelligent energy control mechanisms. Interested researcher can take other residues (Mazie husk, wheat husk) and controllers (Neural network, Nero-fuzzy) for different study area and different hybrid systems.

Reference

[1] Frank, Yebah, Dazie, Design of a grid connected photovoltaic system for KNUST and Economic and environmental Analysis of the design system available, p. 6, 2010).

[2] Federal Democratic Republic of Ethiopia Ministry of Water and Energy, 2012, “Scaling - Up Renewable Energy Program Ethiopia Investment Plan

[3] S. Kumaravel a & S. Ashok, 2012, “An Optimal Stand-Alone Biomass/Solar-PV/PicoHydel Hybrid Energy System for Remote Rural Area Electrification of Isolated Village in Western-Ghats Region of India”, Department of Electrical Engineering, National Institute of Technology Calicut, Calicut, Kerala, India

[4] Abatcha H.G., Ahmad M.Y., Ladan M., 2011, Design and simulation of a hybrid PV/Fuel Cell Energy System, ISSN: 2141-4068.

[5] Linn Solheim, Scaling an Optimized PV-cluster as part of a Micro grid in Wawa Shang, Nicaragua, 2013.

[6] Punyashree Pattanayak,2015 Overcome of Energy crisis using hybrid Renewable Energy resources in India: HOMER Application.

[7] A Shezan SK.,et al .,2016 “ Fuzzy Logic Implementation with MATLAB for Solar-Wind Battery-Diesel Hybrid Energy System” Department of Electrical and Electronic Engineering, Faculty of Engineering, Uttara University, Dhaka, Bangladesh. Vol-2

[8] Lau, K. Y., MFM Yousof, SNM Arshad, M. Anwari and AHM Yatim, 2010, Performance analysis of hybrid photovoltaic/ diesel energy system under Malaysian conditions, Energy, 35(8), pp. 3245-55.

[9] Siddhartha Gobina Deb,2012, *Optimal Sizing of a Stand-alone Solar-Wind-Battery DG/Biomass Hybrid Power System to Meet the Load Demand of a Typical Village at Sagar Island Using Genetic Algorithm*. Master thesis, Jadavpur University

[10] Melaku.M, 2014, Fuzzy logic controller-based hybrid renewable power generation for Barsoma village.

[11] Zelalem Girma and Martin Braun ,2013, *Techno Economic Assessment and Optimization Study of Hybrid Power System Using Homer Software for Electrification of Rural District in Ethiopia*. International journal of renewable energy research Institute of Wind Energy and Technology, Vol.3, No.3.

[12] J.P.Sharma, Oct, 2015, A Standalone Hybrid Energy system modelling for Academic institution

[13] Martin Galad, Pavol Spanik, 2014, Design of Photovoltaic Solar Cell Module for Stand- alone Renewable System.

[14] Adisu Teshale, 2012, Modelling and simulation of fuzzy logic based hybrid power for irrigation system in case of wonji-shoa villages.

[15] Getachew Bekele, Bjorn Palm, "Feasibility study for a standalone solar-wind-based hybrid energy system for application in Ethiopia", Applied Energy, vol 87, pp487-495, 2010.

[16] Abebe Wolie, 2013, Assessment of Renewable Energy Resources Potential and Design of Hybrid Power System for Selected Sites in Eastern Amhara Region of Ethiopia. Master thesis, Arba Minch University.

[17] Berihun G. (2013) modeling and simulating of a micro hydro wind hybrid power generation system for rural area of Ethiopia. Mater thesis in Addis Ababa University

[18] Shezan, S.A., et al., *Feasibility analysis of a hybrid off-grid wind–DG-battery energy system for the eco-tourism remote areas.* Clean Technologies and Environmental Policy, 2015. **17**(8): p. 2417-2430.

[19] Bekele G., 2009, The Study In to the Potential and Feasibility of Standalone SolarWind Hybrid Electric Energy Supply System for Application in Ethiopia, KTH Royal Institute of Technology Doctoral Thesis, ISSN: 1102-0245, ISBN: 978-917415-329.

[20] Wang C., 2006, Modeling and Control of Hybrid Wind/Photovoltaic/Fuel Cell Distributed Generation Systems, Montana State University Doctoral Thesis, Bozeman, Montana

[21] Tom Markvart and Luis Castaner, 2012, Principles of solar Cell Operation

[22] RETScreen: *text book on clean energy project analysis, PV project analysis chapter,* [Online] htp//www.retscreen.net

[23] Harvey, A., Brown, A., Hettiarachi, P., A (1998): *Micro Hydro design manual, a guide to small – scale water power schemes,* Intermediate Technology Publications

[24] http://en.wikipedia.org/wiki/World_energy_resources_and_consumption

[25] Florida Solar Energy Center, May 1999, Handbook for Solar Photovoltaic (PV) Systems

[26] EEU, Universal Electric Access Program (UEAP). Electric Power Distribution Network Design and Construction Training Manual.

[27] Luque, A. and Hegedus, S., (Ed) (2003) Handbook of Photovoltaic Science and Engineering. West Sussex, England: John Wiley & Sons Ltd.

[28] Nigussie, A. (2010). Development of a dual mode frequency controller for standalone, micro and mini hydropower systems (A thesis Submitted to the Addis Ababa Institute of Technology, in partial fulfillment of the requirement for the degree of Master of Science in Electrical Power Engineering).

[29] Dominik Schmitz, 2006,'' *Developing a methodology for assessing the Sustainable Development impact of Small Scale CDM hydropower projects*'' Hamburg Institute of International Economic.

[30] Jorde, K., Hartmann, E., & Unger, H. (2009). Good & Bad of Mini Hydro Power. R. Ritter (Ed.).

[31] *C. C.* Warnick," Hydropower *engineering ''* University of Idaho Moscow.

[32] Santarelli, M., Calì, M., & Macagno, S. (2004). Design and Analysis of Stand-alone Hydrogen Energy Systems with Different Renewable Sources. International Journal of Hydrogen Energy, 29(15), 1571-1586.

[33] Dan New, Canyon Hydro, 5500 Blue Heron Ln., Deming, WA 98244 • 360-592-5552.

[34] D. New, Intro to Hydropower, Part 1: System overview, Home power 103/October & November 2004

[35] Penche, C. (1998). Layman's Guidebook on how to develop a small hydro site.

[36] Range of Specific speed, available from: http://www.intechopen.com/source/html/40550/media/image14_w.jpg.

[37] Inversin, A. R. (1986). Micro-hydropower Source book; a practical guide to design and implementation in developing countries.

[38] Sharma, H., & Singh, J. (2013). Run off river plant: Status and prospects. International Journal of Innovative Technology and Exploring Engineering (IJITEE), ISSN, 2278-3075.

[39] Selection of Generator Type, available from http://waterturbines. wikidot. com/system:join

[40] Federal Democratic Republic of Ethiopia Ministry of Water and Energy "Scaling – up Renewable Energy program Ethiopia Investment Plan" January 2012 for Rural Village Electrification" Master Thesis.

[41] Micro hydro power resource assessment handbook Asian and Pacific Centre for transfer of technology of the United Nations-Economic and social commission for Asia and Pacific (ESCAP), September 2009]

[42] 500Assessment of Hydropower Potential of Selected Rivers in North Shoa Zone, Amhara Regional State, Ethiopia

[43] De Souza-Santos, M. L. 2010. Solid Fuels Combustion and Gasification - Modeling, Simulation, and Equipment Operations. 2nd edition. CRC Press, Taylor & Francis Group. New York, USA. ISBN 978-1-4200-4749-3. 482 pages.

[44] Eriksson, Timo. 2003. The gasification solution. [e-document] [Retrieved June 29, 2011]from:http://www.powergenworldwide.com/index/display/articledisplay/193156/articles/power-engineering-international/volume-11/issue-10/features/the-gasificationsolution. html.

[45] Basu, P. 2010. Biomass Gasification Design Handbook. Elsevier Inc. DO1: 10.1016/B978 -0- 12-374988-8.00005-2. 323 pages

[46] Alemayehu Tenaw, 2011, *design and simulation of photovoltaic thermal system for improving pvmodule efficiency*. Master thesis, Bahir Dar University.

[47] Becherif M., Paire D., Miraoui A., 2007, Energy Management of Solar Panel and Battery System with Passive Control, *International Conference on Clean Electrical Power*, pp. 14-19

[48] Tsai H.L., Tu C.S., and Su Y.J., 2008, Development of Generalized Photovoltaic Model Using Matlab/Simulink, *Proceedings of the World Congress on Engineering and Computer Science* (WCECS), San Francisco, USA

[49] http://wwwdsa.uqac.ca/~rbeguena/Systemes_Asservis/PID.pdf

[50] D. E. Hesmondhalgh and E. R. Laithwaite, Method of analysing the properties of 2-phase servo-motors and AC tachometers, Volume 70, 1987-1993.

[51] X. Zhang, M. Zhang, An adaptive fuzzy PID control of hydro-turbine governor, *International Conference on Publication Year: 2008*, 4139 – 4143(2002)

[52] A. Kaabeche, M. Belhamel and R. Ibtiouen, Optimal sizing method for stand-alone hybrid PV/wind powergeneration system, *Revue des Energies Renouvelables SMEE'10 BouIsmail Tipaza*, 205 – 213 (2010).

[53] G. Singh and D. S. Chauhan et al., Simulation and modeling of hydro power plant to study time response during different gate states, *International Journal of Advanced Engineering Sciences and Technologies*, Volume 10 (1), 042 – 047 (2011).

[54] P. Drtinaand and M. Sallaberger, Hydraulic turbines—basic principles and state-of-the art computational fluid dynamics applications, *ProcInstnMechEngrs*, Volume 213 (C), 1999.

[55] http://www.files.harc.edu/Documents/EBS/CEDP/HydropowerPart2.pdf

[56] Michael Lubwama, 2010, Technical *Assessment of the functional and operational performance fixed bed biomass gasifier using agricultural residues*. Master thesis, Stockholm University.

[57] Guo, Feiqiang; Dong, Yuping; Dong, Lei; Guo, Chenlong. (2014). "Effect of design and operating parameterson the gasification process of biomass in a downdraft fixed bed: An experimental study", International Journalof Hydrogen Energy; 39; pp. 5625-5633.

[58] Alhassan, M and Alhaji M. M. "Utilization of Rice Husk Ash for Improvement of Deficient Soils in Nigeria: A Review" Nigerian Journal of Technology, Vol. 36, No. 2, pp. 389 – 394, 2016.

[59] Phyllis. "Database for Biomass and Waste." 4 August 2011. http://www.ecn.nl/phyllis/. Accessed September 8, 2011.

[60] PowerConversionTable,RetrievedonNovember24fromhttps://www.aquacalc.com/convert/power/megajoule-per-hour-to-kilowatt, 2017.

[61] Bimrew Tamrat, "Comparative Analysis of Feasibility of Solar PV, Wind and Micro Hydro Power Generation for Rural Electrification in the Selected Sites of Ethiopia", A thesis submitted to the School of Graduate Studies of AAIT, Thermal Engineering Stream, July2007

[62] MC Brito, *Energia Solar Photovoltaics PV system sizing*. Mestrado Integrado Engenhariada Energia e do Ambiente, Faculdade Ciências da Universidade de Lisboa.

Appendix

Appendix A: MATLAB codes

```
% written by Sintayehu Alemnew, June 2020.
% Adama Institute of Technonlogy
% power mangement
function [Pout,idx]= PMS_m(Pd,Pmh,Ps,Pb)
if Pmh ~= 0
if Pd < Pmh
    Pout= Pmh;
    idx= 1;
elseif Ps ~= 0
if Pd-Pmh <= Ps
      Pout= Pmh+Ps; idx= 3;
else
      Pout= Pmh+Ps+Pb; idx= 6;
end
else
      Pout= Pmh+Pb; idx= 4;
end
else
if Pd < Ps
    Pout= Ps; idx= 2;
else
    Pout= Ps+Pb; idx= 5;
end
```

```
end
avePd=50;avePmh=30;avePb=0;avePs=20;
devPd=2 ;devPmh=2;devPb=2;devPs=2;
b= [];
for i=0:23
    Pd= 50+devPd*randn;
    Pmh= 30+devPmh*randn;
    Ps= 20+devPs*randn;
    Pb= 0+devPb*randn;
    [Pout,idx]= PMS_m(Pd,Pmh,Ps,Pb);
    b= [b; i Pd Pout idx];
end
subplot 211
stairs(b(:,1),b(:,2:3),'linewidth',1)
axis([0 23 40 120])
legend('Power demand', 'Power output')
xlabel('t[hr]')
ylabel('P[kW]')
grid on
subplot 212
stairs(b(:,1),b(:,4),'linewidth',1)
axis([0 23 0 8 ])
xlabel('t[hr]')
ylabel('swichport')
```

```
grid on
avePd=50;avePmh=30;avePb=0;avePs=20;
devPd=2 ;devPmh=2;devPb=2;devPs=2;
b= [];
for i=0:23
    Pd= avePd+devPd*randn;
    Pmh= avePmh+devPmh*randn;
    Ps= avePs+devPs*randn;
    Pb= avePb+devPb*randn;
    [Pout,idx]= PMS_m(Pd,Pmh,Ps,Pb);
    b= [b; i Pd Pout idx];
end
subplot 211
stairs(b(:,1),b(:,2:3),'linewidth',2)
axis([0 23 60 120])
legend('Power demand', 'Power output')
xlabel('t[hr]')
ylabel('P[kW]')
subplot 212
stairs(b(:,1),b(:,4),'linewidth',2)
axis([0 23 0 8 ])
xlabel('t[hr]')
ylabel('swichport')
```

```
% SECTION TITLE
% DESCRIPTIVE TEXTSECTION TITLE
% DESCRIPTIVE TEXT
devPd=1;
devPmh=1;
devPb=1;
devPs=0;
b= [];
for i=0:23
    Pd= 50+devPd*randn;
    Pmh= 40+devPmh*randn;
    Ps= 0+devPs*randn;
    Pb= 10+devPb*randn;
    [Pout,idx]= PMS_m(Pd,Pmh,Ps,Pb);
    b= [b; i Pd Pout idx];
end
subplot 211
stairs(b(:,1),b(:,2:3),'linewidth',2)
axis([0 23 50 70])
legend('Power demand', 'Power output')
xlabel('t[hr]')
ylabel('P[kW]')
subplot 212
stairs(b(:,1),b(:,4),'linewidth',2)
```

```
axis([0 23 0 8 ])

xlabel('t[hr]')

ylabel('swichport')
```

Appendix B: Data of power demand of benti village

Time	Church room Lighting (4)*13 (52w)	Fluorescent lamp berenda(2)*13 (26w)	Microphone (2)*15 (30w)	Tape recorder (1)*50 (50w)	Energy (KWh/day)
0:0-1:0	-	26	-	-	0.026
1:0-2:0	-	-	-	-	-
2:0-3:0	-	-	-	-	-
3:0-4:0	-	-	-	-	-
4:0-5:0	-	-	-	-	-
5:0-6:0	104	-	30	-	0.134
6:0-7:0	104	-	30	-	0.134
7:0-8:0	-	-	-	-	-
8:0-9:0	-	-	-	-	-
9:0-10:0	-	-	-	-	-
10:0-11:0	-	-	-	-	-
11:0-12:0	-	-	-	-	-
12:0-13:0	-	-	-	-	-
13:0-14:0	-	-	-	-	-
14:0-15:0	-	-	-	-	-
15:0-16:0	-	-	-	-	-
16:0-17:0	-	-	-	-	-
17:0-18:0	-	-	30	50	0.080
18:0-19:0	104	-	30	50	0.184
19:0-20:0	104	26	30	-	0.160
20:0-21:0	-	26	-	-	0.026
21:0-22:0	-	-	-	-	-
22:0-23:0	-		-	-	-
23:0-24:0	-		-	-	-
Total daily load	416	78	150	100	0.744

Time			Clinic					
	room Lighting (8) (104W)	HO office (2) (26W)	Fluorescent lamp berenda (2) (26W)	Vaccine refrigerator (1) (100W)	Microscope (1) (15W)	Water heater (1) (1000W)	Computer (1) (300W)	Energy (kWh per day)
0:0-1:0	-	-	26	100	-	-	-	0.126
1:0-2:0	-	-	-	100	-	-	-	0.1
2:0-3:0	-	-	-	100	-	-	-	0.1
3:0-4:0	-	-	-	100	-	-	-	0.1
4:0-5:0	-	-	-	100	-	-	-	0.1
5:0-6:0	-	-	-	100	-	-	-	0.1
6:0-7:0	-	-	-	100	-	-	-	0.1
7:0-8:0	-	-	-	100	-	-	-	0.1
8:0-9:0	-	-	-	100	15	1000	-	1.115
9:0-10:0	-	-	-	100	15	1000	300	1.415
10:0-11:0	-	-	-	100	-	-	300	0.4
11:0-12:0	-	-	-	100	-	-	-	0.1
12:0-13:0	-	-	-	100	-	-	-	0.1
13:0-14:0	-	-	-	100	-	-	-	0.1
14:0-15:0	-	-	-	100	15	1000	-	1.115
15:0-16:0	-	-	-	100	15	1000	300	1.415
16:0-17:0	-	-	-	100	-	-	300	0.4
17:0-18:0	-	-	-	100	-	-	-	0.1
18:0-19:0	104	-	-	100	-	-	-	0.204
19:0-20:0	104	-	-	100	-	-	-	0.204
20:0-21:0	-	52	-	100	-	-	-	0.152
21:0-22:0	-	52	-	100	-	-	-	0.152
22:0-23:0	-	-	26	100	-	-	-	0.126
23:0-24:0	-	-	26	100	-	-	-	0.126
Total daily load	208	104	78	2400	60	4000	1200	8.085

Time	Elementary School					
	Class room Lighting (10) (130W)	Staff cfl (4) (52w)	Fluorescent lamp berenda (4) 52W	Copy machine (1) 900 W	Computer (1) (300W)	Energy (kWh per day)
0:0-1:0	-	-	-	-	-	-
1:0-2:0	-	-	-	-	-	-
2:0-3:0	-	-	-	-	-	-
3:0-4:0	-	-	-	-	-	-
4:0-5:0	-	-	-	-	-	-
5:0-6:0	-	-	-	-	-	-
6:0-7:0	-	-	-	-	-	-
7:0-8:0	-	-	-	-	-	-
8:0-9:0	-	-	-	-	-	-
9:0-10:0	-	-	-	-	-	-
10:0-11:0	-	-	-	900	300	1.2
11:0-12:0	-	-	-	-	300	0.300
12:0-13:0	-	-	-	-	-	-
13:0-14:0	-	-	-	-	-	-
14:0-15:0	-	-	-	-	300	0.3
15:0-16:0	-	-	-	-	300	0.3
16:0-17:0	-	-	-	900	-	0.9
17:0-18:0	-	-	-	-	-	-
18:0-19:0	130	52	-	-	-	0.182
19:0-20:0	130	52	52	-	-	0.234
20:0-21:0	-	52	52	-	-	0.104
21:0-22:0	-	-	52	-	-	0.052
22:0-23:0	-	-	52	-	-	0.052
23:0-24:0	-	-	-	-	-	-
Total daily load	260	156	208	1800	1200	3.624

Total energy consumption of Benti village

Time	Total load (kWh)					
	Energy Household (kWh)	Public loads (pump) (kWh)	Energy in church (kWh)	Energy in clinic (kWh)	Energy in school (kWh)	Total load Energy
0:0-1:0	10.65	-	0.026	0.126	-	10.802
1:0-2:0	10.65	-	-	0.1	-	10.75
2:0-3:0	10.65	-	-	0.1	-	10.75
3:0-4:0	10.65	-	-	0.1	-	10.75
4:0-5:0	16.188	-	-	0.1	-	16.288
5:0-6:0	105.222	-	0.134	0.1	-	106.122
6:0-7:0	108.63	-	0.134	0.1	-	108.864
7:0-8:0	44.73	-	-	0.1	-	44.83
8:0-9:0	44.73	9.5	-	1.115	-	55.345
9:0-10:0	44.73	9.5	-	1.415	-	55.645
10:0-11:0	44.73	-	-	0.4	1.2	46.33
11:0-12:0	44.73	-	-	0.1	0.300	45.13
12:0-13:0	108.63	-	-	0.1	-	108.73
13:0-14:0	44.73	-	-	0.1	-	44.83
14:0-15:0	44.73	9.5	-	1.115	0.3	55.645
15:0-16:0	44.73	9.5	-	1.415	0.3	55.945
16:0-17:0	44.73	-	-	0.4	0.9	46.03
17:0-18:0	44.73	-	0.080	0.1	-	44.91
18:0-19:0	136.32	-	0.184	0.204	0.182	136.89
19:0-20:0	72.42	-	0.160	0.204	0.234	73.018
20:0-21:0	72.42	-	0.026	0.152	0.104	72.702
21:0-22:0	57.51	-	-	0.152	0.052	57.714
22:0-23:0	21.726	-	-	0.126	0.052	21.904
23:0-24:0	10.65	-	-	0.126	-	10.776
Total load Energy	1199.616	38	0.744	8.085	3.624	1250.069

Bio-mass energy resource assessment (taken from Fogera woreda)

Year(E.C)	Total production in metric.tons
1990	50660
1991	47805.6
1992	60293.6
1993	61082
1994	73208.32
1995	73768
1996	46744
1997	80876
1998	52052
1999	59114
2000	54465.2
2001	82362.4
2002	62869.2
2003	43061.2
2004	34344
2005	26344
2006	17460
2007	52072
2008	48072
2009	44072
2010	46356
Av. yearly production	53194.36

Five years average daily sunshine hours for the site NMA deberetabor branch

Year	Jan	Feb	Mar	Apr	May	Jun	Jul	Aug	Sep	Oct	Nov	Dec
2018	9	9.4	8.1	8.9.2	8.6	6.2	4.3	3.4	7.5	7.5	7.8	8.5
2017	8.9	9.6	8.2	8.9	8.5	6.4	4.5	5.4	6.2	8.7	6.7	8.5
2016	8	10.2	6.3	7.9	5.8	6.7	4.8	4.6	6.2	8.2	7.5	9.1
2015	7.9	8.7	7.2	6.1	6.4	6.1	3	2.9	6.2	7.8	7.5	8.1
2014	9.6	7.9	7.2	8.5	7.9	6.3	3.4	4.6	6.4	6.5	8	7.8
Daily Average hrs. (S)	8.68	9.16	7.4	8.12	7.44	6.34	4	4.18	6.5	7.74	7.5	8.4

Appendix C: Parameter of hydro-power

Table 1 synchronous machine parameters

Symbol	Quantity	value in p.m
V_a	stator voltage	1 sin(100*Ω*t)
f	frequency	50 Hz
Xis	inductance of stator coil	0.08
Rs	Resistance stator coils	0.03788
Xmd	mutual inductance on d axis	2.16
Xmq	mutual inductance on q axis	0.94
Xlkd	inductance of damping coils among d axis	0.3085
Xlkq	inductance of damping coils among q axis	0.05281
Rkd	Resistance of damping coils among d axis	0.1463
Rkq	Resistance of damping coils among d axis	0.05754

Table 2 hydro turbine model parameters.

symbol	Quantity	value
k_p	proportional PID gain	0.613
Ki	Integral PID gain	0.104
Kd	Derivative PID gain	0.002
td	Time PID gain constant	0.095sec
ka	Servomotor gain	3.2
ta	Servomotor time	0.069sec
Tw	Hydro turbine time constant	2.7 sec

Table 3 excitation system parameters

symbol	Quantity	value
Tc,Ts	Transient time constant	0
Ka	Regulator gain	275
Ta	Regulator time constant	0.002sec
K_E	Exciter gain	1
T_E	Exciter time constant	0sec
K_F	Damper gain	0.01
T_F	Damper time constant	0.95sec

Solar insulation taken from NASA

-BEGIN HEADER-
NASA/POWER SRB/FLASHFlux/MERRA2/ 0.5 x 0.5 Degree Climatologies
22-year Additional Solar Parameter Monthly & Annual Climatologies (July 1983 - June 2005), 30-year Meteorological and Solar Monthly & Annual Climatologies (January 1984 - December 2013)
Location: Latitude 11.916 Longitude 37.7
Elevation from MERRA-2: Average for 1/2x1/2 degree lat/lon region = 1828 meters Site = na
Climate zone: na (reference Briggs et al: http://www.energycodes.gov)
Value for missing model data cannot be computed or out of model availability range: -999
Parameter(s):
DIFF_MIN SRB/FLASHFlux 1/2x1/2 Minimum Diffuse Radiation On A Horizontal Surface (kW-hr/m^2/day)
DNR_MIN SRB/FLASHFlux 1/2x1/2 Minimum Direct Normal Radiation (kW-hr/m^2/day)
DIFF_MAX SRB/FLASHFlux 1/2x1/2 Maximum Diffuse Radiation On A Horizontal Surface (kW-hr/m^2/day)
KT SRB/FLASHFlux 1/2x1/2 Insolation Clearness Index (dimensionless)
ALLSKY_SFC_LW_DWN SRB/FLASHFlux 1/2x1/2 Downward Thermal Infrared (Longwave) Radiative Flux (kW-hr/m^2/day)
ALLSKY_SFC_SW_DWN SRB/FLASHFlux 1/2x1/2 All Sky Insolation Incident on a Horizontal Surface (kW-hr/m^2/day)
SRF_ALB SRB/FLASHFlux 1/2x1/2 Surface Albedo (dimensionless)
DNR SRB/FLASHFlux 1/2x1/2 Direct Normal Radiation (kW-hr/m^2/day)
DNR_MAX SRB/FLASHFlux 1/2x1/2 Maximum Direct Normal Radiation (kW-hr/m^2/day)
DIFF SRB/FLASHFlux 1/2x1/2 Diffuse Radiation On A Horizontal Surface (kW-hr/m^2/day)
ALLSKY_TOA_SW_DWN SRB/FLASHFlux 1/2x1/2 Top-of-atmosphere Insolation (kW-hr/m^2/day)
PARAMETER JAN FEB MAR APR MAY JUN JUL AUG SEP OCT NOV DEC ANN
-END HEADER-
SRF_ALB 0.18 0.18 0.17 0.17 0.17 0.18 0.19 0.21 0.20 0.18 0.18 0.18 0.18
ALLSKY_SFC_LW_DWN 7.45 7.75 8.29 8.46 8.56 8.48 8.45 8.46 8.33 8.07 7.67 7.44 8.12
ALLSKY_TOA_SW_DWN 8.72 9.49 10.22 10.56 10.52 10.40 10.41 10.45 10.25 9.66 8.88 8.44 9.83
DNR 8.52 8.01 6.91 6.73 6.16 5.21 4.21 4.10 5.37 6.22 7.72 8.34 6.45
DNR_MAX 9.35 9.50 8.58 7.65 7.28 6.27 5.54 5.53 6.17 7.55 8.80 9.38 7.63
DNR_MIN 7.57 6.97 5.99 5.40 4.21 3.94 2.77 2.83 4.63 4.74 6.29 6.58 5.16
DIFF_MAX 1.25 1.55 1.93 2.17 2.27 2.25 2.27 2.32 2.15 1.95 1.53 1.37 1.92

DIFF_MIN 0.88 1.00 1.41 1.75 1.81 1.96 2.08 2.12 1.92 1.48 1.03
0.82 1.52
DIFF 1.07 1.35 1.77 1.94 2.02 2.12 2.23 2.29 2.06 1.74 1.27
1.05 1.74
KT 0.70 0.69 0.64 0.63 0.60 0.55 0.48 0.50 0.56 0.61 0.67
0.70 0.61
ALLSKY_SFC_SW_DWN 5.91 6.18 5.90 6.72 5.62 4.53 4.90 4.14 5.13
5.61 5.35 5.98 5.4975

temperature

-BEGIN HEADER-
NASA/POWER SRB/FLASHFlux/MERRA2/ 0.5 x 0.5 Degree Climatologies
22-year Additional Solar Parameter Monthly & Annual Climatologies (July 1983 - June 2005), 30-year Meteorological and Solar Monthly & Annual Climatologies (January 1984 - December 2013)
Location: Latitude 11.8666 Longitude 37.9954
Elevation from MERRA-2: Average for 1/2x1/2 degree lat/lon region = 2109.8 meters Site = na
Climate zone: na (reference Briggs et al: http://www.energycodes.gov)
Value for missing model data cannot be computed or out of model availability range: -999
Parameter(s):
TS_MIN MERRA2 1/2x1/2 Minimum Earth Skin Temperature (C)
T2M_RANGE MERRA2 1/2x1/2 Temperature Range at 2 Meters (C)
FROST_DAYS MERRA2 1/2x1/2 Frost Days (Days)
HDD0 MERRA2 1/2x1/2 Heating Degree Days Below 0 C (Degree C-d)
T2M MERRA2 1/2x1/2 Temperature at 2 Meters (C)
T2M_MIN MERRA2 1/2x1/2 Minimum Temperature at 2 Meters (C)
TS MERRA2 1/2x1/2 Earth Skin Temperature (C)
TS_MAX MERRA2 1/2x1/2 Maximum Earth Skin Temperature (C)
CDD10 MERRA2 1/2x1/2 Cooling Degree Days Above 10 C (Degree C-d)
TS_RANGE MERRA2 1/2x1/2 Earth Skin Temperature Range (C)
T2MDEW MERRA2 1/2x1/2 Dew/Frost Point at 2 Meters (C)
TS_AMP MERRA2 1/2x1/2 Earth Skin Temperature Amplitude (C)
HDD10 MERRA2 1/2x1/2 Heating Degree Days Below 10 C (Degree C-d)
T2M_MAX MERRA2 1/2x1/2 Maximum Temperature at 2 Meters (C)
CDD18_3 MERRA2 1/2x1/2 Cooling Degree Days Above 18.3 C (Degree C-d)
T2MWET MERRA2 1/2x1/2 Wet Bulb Temperature at 2 Meters (C)
CDD0 MERRA2 1/2x1/2 Cooling Degree Days Above 0 C (Degree C-d)
HDD18_3 MERRA2 1/2x1/2 Heating Degree Days Below 18.3 C (Degree C-d)
PARAMETER JAN FEB MAR APR MAY JUN JUL AUG SEP
OCT NOV DEC ANN
-END HEADER-
TS_MAX 32.00 34.87 36.08 35.31 33.72 29.33 23.64 22.95 24.96 25.92
27.65 29.50 29.66
TS_MIN 12.27 14.00 15.88 16.61 16.64 16.39 15.32 15.03 14.74 13.05
11.92 11.69 14.46
T2M_RANGE 11.87 12.13 11.28 10.43 9.88 8.31 5.69 5.40 6.65 9.00
10.40 11.22 9.36
FROST_DAYS 0.00 0.00 0.00 0.00 0.00 0.00 0.00 0.00 0.00 0.00
0.00 0.00 0.00
CDD0 598.96 587.91 676.69 663.85 684.95 611.36 550.43 548.36 557.21
560.47 544.70 573.48 7158.36
CDD10 288.96 305.17 366.69 363.85 374.95 311.36 240.43 238.36 257.21
250.47 244.70 263.48 3505.62
CDD18_3 33.82 71.05 109.61 115.03 117.98 63.22 7.10 3.92 13.63 7.93
9.99 14.12 567.40
HDD0 0.00 0.00 0.00 0.00 0.00 0.00 0.00 0.00 0.00 0.00 0.00
0.00 0.00
HDD10 0.00 0.00 0.00 0.00 0.00 0.00 0.00 0.00 0.00 0.00 0.00
0.00 0.00
HDD18_3 2.16 0.56 0.22 0.18 0.33 0.86 23.97 22.85 5.42 14.77
14.29 7.94 93.55

TS 20.32 22.47 24.03 24.27 23.77 21.80 18.76 18.42 19.24 18.59 18.53 18.98 20.76
T2MDEW 6.73 6.24 7.61 8.84 9.97 12.53 13.67 14.00 12.92 10.13 8.35 7.31 9.86
T2MWET 6.74 6.25 7.63 8.85 9.98 12.53 13.67 14.00 12.92 10.14 8.35 7.32 9.86
T2M_MAX 25.26 26.86 27.47 27.34 27.04 24.53 20.60 20.39 21.90 22.58 23.36 24.11 24.29
T2M_MIN 13.38 14.73 16.19 16.91 17.15 16.22 14.91 14.99 15.25 13.58 12.96 12.89 14.93
T2M 18.95 20.50 21.55 21.85 21.73 19.91 17.42 17.42 18.36 17.96 17.94 18.15 19.31
TS_RANGE 19.73 20.87 20.20 18.70 17.08 12.93 8.32 7.92 10.22 12.87 15.74 17.81 15.20
TS_AMP 9.87 10.43 10.10 9.35 8.54 6.47 4.16 3.96 5.11 6.43 7.87 8.90 7.60

Stream flow data of Gumara river (taken federal democratic republic of Ethiopia ministry of water irrigation and energy)

E.C	Jan	Feb	Mar	Apr	May	Jun	Jul	Aug	Sep	Oct	Nov	Dec
1990	2.394	0.911	0.606	0.404	0.539	1.312	52.81	180.362	109.281	19.82	4.143	1.931
1991	1.008	0.531	0.379	0.443	0.814	14.216	83.215	168.091	76.814	23.426	4.757	4.788
1992	3.046	2.064	2.738	0.841	1.89	1.976	42.12	158.532	71.115	50.348	14.929	6.339
1993	2.705	1.309	0.697	0.911	2.125	10.371	85.924	140.165	100.436	37.675	11.713	4.738
1994	2.378	1.311	0.609	0.348	1.013	19.354	84.876	194.354	122.469	19.987	7.016	4.14
1995	2.164	1.673	1.481	1.395	1.555	4.987	61.61	148.572	98.553	24.945	17.016	12.738
1996	7.455	3.591	3.371	3.402	7.991	56.43	179.079	200.466	101.512	36.935	22.107	15.246
1997	10.777	7.993	6.631	4.968	7.351	48.026	141.976	150.534	79.622	58.902	54.579	16.692
1998	-	-	-	-	1.908	10.798	67.383	138.082	92.608	28.136	8.815	8.698
1999	6.787	1.719	0.746	0.559	0.742	4.999	71.481	97.537	52.79	59.751	13.005	-

Annex: Photo taken during field survey